

Hydroikos Ltd.

2512 Ninth Street, Ste. 7
Berkeley, CA 94710
Phone: (510) 295-4094
coats@hydroikos.com
www.hydroikos.com



REALIGNING THE LAKE TAHOE INTERAGENCY MONITORING PROGRAM

Vol. I: Main Report

By

Robert Coats and Jack Lewis

August 25, 2014



Table of Contents

Table of Contents.....	1
Acknowledgements	3
List of Figures.....	4
List of Tables.....	7
List of Appendices.....	9
List of Acronyms and Abbreviations.....	11
Glossary.....	14
Abstract	17
Executive Summary.....	18
1 Introduction and Background	27
2 Current Understanding of Water Quality Issues in the Tahoe Basin	35
2.1 Limiting Nutrients.....	36
2.2 The Importance of Fine Sediment.....	37
2.3 Channel Erosion as a Source of Sediment.....	37
2.4 Land Use Influences: Urban Runoff, Fire and Dirt Roads	37
2.5 Implications of Climate Change.....	38
3 Measuring Stream Discharge.....	39
4 Water Quality Constituents: Sampling and Analytic Methods.....	40
4.1 Suspended Sediment	40
4.2 Turbidity	41
4.3 Nitrogen	41
4.3.1 Nitrate-nitrogen.....	42
4.3.2 Ammonium-N.....	42
4.3.3 Total Kjeldahl Nitrogen	43
4.4 Phosphorus	43
4.4.1 Soluble Reactive Phosphorus.....	43
4.4.2 Total Phosphorus	43
4.5 Iron.....	44
4.6 Temperature	44
4.7 Conductivity, pH and Dissolved Oxygen.....	44
5 Sampling Strategy and Methodology	45
6 Calculating Total Loads.....	51



7 Statistical Criteria for a Monitoring Program 54

8 Statistical Tests of Sampling and Load Calculation Methods 57

8.1 Synthetic data sets 57

8.1.1 Sampling from the synthetic records 62

8.2 The worked records 64

8.2.1 Sampling from the worked records 65

8.3 Load estimation methods 68

8.4 Evaluation of optimal handling of low SSC values 71

8.5 Simulation results for daytime sampling 73

8.6 Recalculated annual loads and total annual Q 79

9 Time-of-Sampling bias—methods and results 79

9.1 Simulations 82

9.2 Historical load estimates 85

9.3 Induced trends from eliminating night-time samples 86

10 Bias in standard sediment rating curves and optimal methods 88

11 Time trend analysis on Total Load residuals; Hypotheses to explain observed trends 91

11.1 Trend results 92

12 Statistical power analysis 100

12.1 Power analysis methodology 100

12.2 Power analysis results 101

13 Reducing Bias Through Improved Sampling 103

13.1 Continuous Turbidity Monitoring 103

13.2 Pumping Samplers vs. Grab Sampling 105

14 Sample Size, Accuracy and Confidence Limits 106

14.1 Achieving specified levels of precision in total load 107

14.2 Detecting differences of a specified magnitude 109

15 Summary and Recommendations 111

16 References 114

17 Personal Communications 120



Acknowledgements

We thank Charles Goldman and Geoffrey Schladow for their many years of leadership of the UC Davis Tahoe Research Group and Tahoe Environmental Research Center; Patty Arneson for careful data stewardship and patiently responding to our questions about the LTIMP data, Nancy Alvarez for helpful suggestions, critical review and information about the USGS work in the Basin; John Reuter and Scott Hackley for review and helpful suggestions throughout the project, Nicole Beck, Gary Conley, Mark Grismer, Alan Heyvaert, Andy Stubblefield, and Rick Susfalk, for generously sharing their turbidity and discharge data for basin streams; Dan Nover for sharing his fine sediment data, Bob Thomas for helpful suggestions and critical review of the report, Raphael Townsend for help with cost estimates and advice on station installation issues, Zach Hymanson for review and help with formatting the report, Jim Markle for the use of six photographs illustrating LTIMP sampling methods, Bob Richards for providing the photo for the Appendix title page, and Tiff van Huysen for contract administration. This work was funded by grant no. 13-DG-11272170-009 from USDA Forest Service under the Southern Nevada Public Land Management Act.



List of Figures

Figure ES-1	Trends in NO ₃ -N after accounting for inter-annual variation in total and maximum daily runoff
Figure 1-1	Figure 1-1. LTIMP history of funding levels and station numbers. From U.S. Geological Survey
Figure 1-2	Map of the Tahoe Basin, showing locations of the LTIMP watersheds and sampling sites
Figure 5-1	Mean number of LTIMP water quality samples per station per year.
Figure 5-2	Scott Hackley of TERC collecting samples at Blackwood Creek. (a) Stretching a tape across the creek for EWI sampling; (b) Collecting a sample with the DH81 sampler; (c) Pouring the sample into the churn splitter; (d) Filtering a sample for analysis of dissolved constituents; (e) Collecting an unfiltered sample from the churn splitter for TP and TKN; (f) Labeling a sample bottle. Photos by Jim Markle (http://jimmarkle.smugmug.com/)
Figure 6-1	Summary of load calculation methods used for LTIMP streams, 1980-2012
Figure 7-1	Bias and precision in a sampling program
Figure 8.1-1	Synthetic TP trace with Caspar Creek autoregressive coefficient, 0.5.
Figure 8.1-2	Synthetic TP trace smoothed by increasing autoregressive coefficient to 0.95.
Figure 8.1-3	Illustration of algorithm for sampling synthetic data sets.
Figure 8.1-4	Illustration of mapping the 24-hour day onto a 9am-6pm workday
Figure 8.1-5	Three sampling templates used to sample synthetic data for WC-8 in 2011
Figure 8.2-6	Example of a worked record for nitrate
Figure 8.4-1	Synthetic data for WC-8 WY1999
Figure 8.5-1	The 6 top-ranking methods by RMSE in the simulation of suspended sediment sampling from the synthetic data for station WC-8 in WY 1999



- Figure 8.5-2 The 6 top-ranking methods by RMSE in the simulation of suspended sediment sampling from the synthetic data
- Figure 9-1 Histograms of the distribution of sampling times for the three west-side streams and other streams, for two time periods
- Figure 9-2 Results of 90 simulations at Homewood Creek WY2010 for sediment rating curve load estimates (n=28)
- Figure 9.1-1 Bias of the estimation method rcb2 for SS loads, with and without nighttime samples
- Figure 9.1-2 Bias of the estimation method rcb2 for TP loads, with and without nighttime samples
- Figure 9.1-3 Bias of the estimation method pdmean for TKN loads, with and without nighttime samples
- Figure 9.2-1 Average percent change in load from omitting nighttime samples, for those stations and years where this procedure reduced number of samples by 25% or more
- Figure 9.3-1 Trends in SS load with and without including night samples for the period 1992-2012
- Figure 10-1 Bias in TKN load estimates for standard rating curve and period-weighted estimates, from simulations (24-hr sampling)
- Figure 10-2 Difference between standard rating curve and period-weighted estimates of historic loads, for TKN
- Figure 11.1-1 Trends in SS after accounting for inter-annual variation in total and maximum daily runoff
- Figure 11.1-2 Trends in TP after accounting for inter-annual variation in total and maximum daily runoff
- Figure 11.1-3 Trends in TKN after accounting for inter-annual variation in total and maximum daily runoff.
- Figure 11.1-4 Trends in NO₃ after accounting for inter-annual variation in total and maximum daily runoff.
- Figure 11.1-5 Trends in SRP after accounting for inter-annual variation in total and maximum daily runoff.



- Figure 11.1-6 Trends in SS, TP, TKN, NO₃, and SRP after accounting for inter-annual variation in total and maximum daily runoff. Residuals are pooled from all gaging stations shown in Figures 11.1-1 to 11.1-5
- Figure 12.1-1 Quantile-quantile plots of the residuals for models used in the trend tests (Table 10-1). A linear pattern suggests a normal distribution
- Figure 12.2-1 Power analysis for TP loads, contrasting 3 levels of relative measurement error (CV), for 3 bias levels and slopes, at 0.005 significance level
- Figure 13.1-1 SSC (mg/l) vs. turbidity (NTUs) for a station on Rosewood Creek at State Route 28, for five water years. From Susfalk et al, 2010.
- Figure 13.1-2 TP concentration vs. turbidity during snowmelt, for Ward Creek 2000, and Blackwood Creek, 2001. From Stubblefield et al., 2007
- Figure 14-1 Confidence limits on errors for TKN.
- Figure 14.2-1 Sample sizes required to detect a specified difference in loading at the 95% confidence level, for each of the major LTIMP nutrients.
- Figure 14.2-2 Sample sizes required to detect a specified difference in loading at the 95% confidence level, for SS and TP, with and without the benefit of continuous turbidity measurements.



List of Tables

Table ES-1	Load estimation methods used in simulations
Table ES-2	Selected best estimation methods for all constituents with and without turbidity data
Table 1-1	List of LTIMP stations
Table 1-2	Table 1-2. Site numbers and names of USGS gaging stations used in the LTIMP.
Table 1-3	Constituents analyzed
Table 1-4	303(d) streams listed in the Basin Plan as impaired
Table 8.1-1	Synthetic data sets used for simulations
Table 8.1-2	Models used to generate synthetic data sets
Table 8.2-1	Number of worked records with complete data from Apr 15 to Jul 15
Table 8.2-2	Number of worked records with complete data from Oct 1 to Sep 30
Table 8.2-3	LTIMP sample sizes for each worked record in Table 8.2-1
Table 8.2-4	Percentages of zeroes in each worked record in Table 8.2-1
Table 8.4-1	Sediment loads computed from worked records and estimated from LTIMP samples using regression method rcb2 with various rules for handling small values of SSC.
Table 8.5-1	Best estimation method for suspended sediment according to either RMSE or MAPE from simulated sampling of synthetic data sets
Table 8.5-2	Best estimation method for suspended sediment according to either RMSE or MAPE from simulated sampling of synthetic data sets
Table 8.5-3	Selected best estimation methods for all constituents with and without turbidity data
Table 10.1	Number of samples required to achieve a given level of confidence by the standard rating curve method compared with new recommended methods.
Table 9.3-1	Tests of induced trend at west-side stations BC-1, GC-1, and WC-8 for selected constituents



Table 11-1	Models for constituent loads to account for hydrologic variability
Table 14-1	Number of samples required to achieve a given level of precision at a given level of confidence in estimates of total annual load



List of Appendices

- A-1 Analytical Methods and correction of nitrate-N data
- A-2 Detailed results for all simulations
 - A-2.1 Simulations from synthetic populations
 - A-2.1.1 SS
 - A-2.1.2 FS by mass
 - A-2.1.3 FS by count
 - A-2.1.4 TP
 - A-2.1.5 TKN
 - A-2.2 Simulations from the worked records
 - A-2.2.1 NO₃
 - A-2.2.2 SRP
 - A-2.2.3 SS
 - A-2.2.4 THP
 - A-2.3 Confidence limits as a function of sample size
 - A-2.3.1 Without turbidity
 - A-2.3.2 With Turbidity
- A-3 Time-of-sampling bias
- A-4 Bias in loads estimated from a standard sediment rating curve
 - A-4.1 Simulation results
 - A-4.1.1 Simulations from synthetic populations
 - A-4.1.2 Simulations from the worked records
 - A-4.2 Historic loads
- A-5 Time Trend Analysis
 - A-5.1 Partial regression plots for loads computed from daytime samples



A-5.2 Adjusted Mann-Kendall p-values

A-6 Power analysis methodology and results

A-6.1 Propagation of measurement error

A-6.2 Power analysis methodology

A-6.3 Power analysis results

A-7 Treatment of values less than Method Detection Limit



List of Acronyms and Abbreviations

ac	Acres
ACE	Alternating Conditional Expectations (see Glossary)
AIC	Akaike's Information Criterion (see Glossary)
AVAS	Additivity and Variance Stabilization for regression (see Glossary)
BAP	Biologically Available Phosphorus
BMP	Best Management Practice
C	Concentration, usually in micrograms or milligrams per liter ($\mu\text{g/l}$ or mg/l)
$^{\circ}\text{C}$	Degrees Celsius
cfs	cubic feet per second
CWA	Clean Water Act
D	Days since the start of the water year
DCNR	Nevada Department of Conservation and Natural Resources
DIN	Dissolved Inorganic Nitrogen; nitrate + nitrite + ammonium
DON	Dissolved Organic Nitrogen
DRI	Desert Research Institute
Et	Evapotranspiration
EWI	Equal Width Increment, a stream sampling method
FS	Fine sediment (< 16 or 20 microns) by mass
FSP	number of fine sediment particles per unit volume
GIS	Geographic Information System
GRMSE	Gilroy's estimate of Root Mean Square Error (see Glossary)
HWD	Homewood Creek, a non-LTIMP stream
l	Liters
LRWQCB	Lahontan Regional Water Quality Control Board
LSPC	Loading Simulation Program in C++ (Lake Tahoe Watershed Model)



LTADS	Lake Tahoe Atmospheric Deposition Study
LTBMU	Lake Tahoe Basin Management Unit
LTIMP	Lake Tahoe Interagency Monitoring Program
MAPE	Median absolute percent error
MDQ	Mean daily discharge
MDQ1	Mean daily discharge on the previous day
MT	Metric Tonne
NDEP	Nevada Division of Environmental Protection
NH ₄	Ammonium
NO ₃ -N	Nitrate-Nitrogen; the analytical method includes nitrite-nitrogen, which is usually negligible
NTU	Nephelometric Turbidity Units
<i>n/y</i>	Number of Particles per Year
POM	Particulate Matter
PON	Particulate Organic Nitrogen
PP	Particulate Phosphorus
PSW	The Pacific Southwest Research Station of the US Forest Service
PWE	Period-weighted estimator (see PWS)
PWS	Period-weighted sample method of calculating load
Q	Instantaneous discharge in volume per unit time, i.e. cubic ft per second
Q-wtd	Flow-weighted
RMSE	Root Mean Square Error (see Glossary)
RSE	Residual standard error
s.d.	Standard deviation
SNPLMA	Southern Nevada Public Lands Management Act
SRP	Soluble Reactive Phosphorus
SS	Suspended Sediment
SSC	Suspended Sediment Concentration, usually in mg/l
stn	Station; generally a USGS gaging station used for flow measurement and sampling



SWRCB	State Water Resources Control Board (California)
T	Turbidity
TCR1	Trout Creek Reach 1 (data from Conley, 2013)
TDP	Total Dissolved Phosphorus
TERC	Tahoe Environmental Research Center
THP	Total Acid-Hydrolyzable-Phosphorus
TKN	Total Kjeldahl Nitrogen (all organic nitrogen plus NH ₄ +)
TKN + nitrate	Total Nitrogen
TMDL	Total Maximum Daily Load
TON	Total Organic Nitrogen
TP	Total Phosphorus
TRG	Tahoe Research Group, predecessor to TERC
TRPA	Tahoe Regional Planning Agency
TSS	Total Suspended Sediment; measured by a different method than SSC
UC Davis	University of California Davis
USACE	United States Army Corps of Engineers
USDA	United States Department of Agriculture
USEPA	United States Environmental Protection Agency
USFS	United States Forest Service
USGS	United States Geological Survey
UTR	Upper Truckee River
WY	Water Year, or Hydrologic Year; Oct. 1- Sept.30



Glossary

ACE. An acronym for Alternating Conditional Expectations, which is the name of an algorithm that finds transformations of y and x that maximize the proportion of variation in y explained by x . *ACE* is implemented in package *acepack* of R (Spector et al., 2010). In our implementation of *ACE*, the algorithm was limited to finding monotonic transformations, in which y is an increasing function of x .

AIC. Akaike's Information Criterion, specifically the corrected version, AIC_c recommended by Burnham and Anderson (2002). This criterion incorporates a penalty for including extra variables in the model.

AR. Autoregressive model. A statistical model for time series data, where the response variable depends on its own previous value. In an AR model of order p , the response depends on its values in the previous p time steps. AR models may be used to describe regression residuals that are not independent but serially correlated. An autoregressive coefficient for an order one AR model relates a new value at time $t+1$ to the value at time t .

AVAS. An acronym for Additivity and VAriance Stabilization for regression, an algorithm that estimates transformations of x and y such that the regression of y on x is approximately linear with constant variance. AVAS is also implemented in package *acepack* of R, and we again limited the algorithm to finding monotonic transformations in which y is an increasing function of x . A more advanced version of AVAS is implemented in the *areg.boot* function in the *HMISC* package of R (Harrell, 2010). Transformed-variable models tend to inflate R^2 and it can be difficult to get confidence limits for each transformation. This method solves both of these problems using the bootstrap with monotonic transformations.

Bonferonni Correction. A correction applied to the p value in a test for significance to take account of the expected number of false positives in a large number of tests. For example, if you test for a treatment effect on 100 plots, and set the p threshold at 0.05, then you can expect to find about 5 false positives. See Miller, 1981.

Categorical variable. A variable that takes values from a fixed, usually small, number of specific outcomes or levels. As an example, substances can be classified as liquid, solid, or gaseous. In contrast, a continuous variable can assume an infinite number of possible values, e.g. all positive real numbers.

Duan's smearing correction for retransformation bias. When predictions are made from a regression model for a transformed response such as the logarithm of concentration, they generally need to be retransformed back to the original units. A bias is introduced by the retransformation: the retransformed response is not equal to its mean value for the given set of predictors. There are three main methods for adjusting the retransformed responses to remove the



bias (Cohn et al., 1989). Two of these methods assume that the transformed responses are normally distributed. The third method, Duan's smearing correction, does not. To apply Duan's smearing correction each prediction is multiplied by the mean of the retransformed regression residuals.

Hysteresis. In the context of streamflow and water quality, hysteresis implies that the two are out of phase. Most commonly, concentration peaks before streamflow and a graph of concentration versus discharge forms a loop pattern, referred to as clockwise hysteresis, in which concentration is greater for a given discharge on the rising limb of a hydrograph than for the same discharge on the falling limb. Seasonal hysteresis can also occur, where concentration is greater for a given discharge early in the season than for the same discharge later in the season.

GRMSE. Gilroy's (Gilroy et al., 1990) estimate of root mean square error (GRMSE) for the predicted load. This criterion utilizes information in the complete predictor data set that is used to compute a sediment load.

MK Test. The Mann-Kendall trend test is a non-parametric test often used to test for the significance of a time trend in water quality and air quality data. It has some advantages over ordinary least-squares regression in that it does not assume normality of residuals, and is resistant to leveraging by outliers. The test calculates the slope of all lines between all possible pairs of points in a time series, and finds the median slope. See Helsel and Hirsch (2002).

LOESS. An abbreviation for LOcal regrESSion, otherwise known as locally-weighted scatterplot smoothing (Cleveland and Devlin, 1988). A smooth curve is generated by fitting weighted first or second degree polynomials to neighborhoods around each data point. Each local regression gives more weight to points near the point whose response is being estimated and less weight to points further away. A user-specified "smoothing parameter" determines how much of the data is used to fit each local regression. The R implementation was employed using first degree polynomials, smoothing parameter equal to 0.8, and two different options for curve-fitting: (1) "gaussian" fitting by least-squares (loess.g), and (2) "symmetric" fitting (loess.s), which uses a "re-descending M estimator with Tukey's biweight function."

MAPE. Median Absolute Percent Error. The 50th percentile error, as percent of the sample mean. This was used as a diagnostic criterion for comparing load calculation programs.

Monotonic transformation. A variable transformation that preserves the ordering of values. For example, a logarithmic transformation is monotonic because $x_2 > x_1$ guarantees that $\log(x_2) > \log(x_1)$.

Monotonic trend. A chronological series of values that never decreases (monotonically increasing series) or that never increases (a monotonically decreasing series).



Power of a test. The power of a test is its ability to detect a treatment effect or trend, that is, to detect an alternative hypothesis when it is true.

Primary Stations. The stream gaging and sampling stations located near the lake, at or slightly up-stream from tributary mouths. Secondary stations are located at higher elevations, and were installed later with the goal of sampling relatively undeveloped areas.

PWS. Period-weighted sample method of calculating total load. Each two successive concentrations are averaged, multiplied by the cumulative discharge between sampling times, and the resulting load increments summed over the water year.

Resampling. Drawing independent sample set from the same population (either with or without replacement)

RMSE. Root Mean Square Error is a frequently used measure of accuracy, i.e. the differences between values predicted by a model or an estimator and the values actually observed. It is calculated as the square root of the mean of the squared differences between observed and predicted values.

RSE. Residual standard error is the estimate of the standard error of the regression residuals



Abstract

Since 1980, the Lake Tahoe Interagency Monitoring Program (LTIMP) has measured discharge and sampled water quality at up to twenty stations in Tahoe basin streams. Measured constituents have included suspended sediment and various forms of nitrogen and phosphorus. In order to improve the usefulness of the program and the existing data base, we have 1) identified and, to the extent possible, corrected for two sources of bias in the data base; 2) generated synthetic data sets using turbidity, discharge, and time of year as explanatory variables for different forms of nitrogen, phosphorus and suspended and fine sediment; 3) resampled the synthetic data sets and part of the historic record in experiments to compare the accuracy of different load calculation models; 4) identified the best load calculation models for estimating each constituent load; 5) using the best models, recalculated total annual loads for all constituents and stations over the period of record; 6) regressed total loads against total annual and maximum daily discharge, and tested for time trends in the residuals; 7) developed a spreadsheet showing the relationships between sample size and confidence limits for estimated loads of the constituents. The time series analyses show significant long-term downward trends in some constituent loads and some streams, which we attribute to long-term recovery of watersheds from historic disturbance. The confidence-limit spreadsheet will be a useful tool for managers in modifying LTIMP to make it a streamlined and effective tool for future water quality monitoring in the Tahoe Basin.



Executive Summary

Since 1980, the Lake Tahoe Interagency Monitoring Program (LTIMP) has measured discharge and sampled water quality at up to twenty stations in Tahoe basin streams. Suspended sediment and various forms of nitrogen, phosphorus and iron have been measured. The purpose of the program has been to document long-term trends in water quality of the major tributaries to the Lake, and thus provide a basis for public policy and management decisions that may affect Lake clarity.

Several problems have limited the usefulness of LTIMP and over time, some of these problems have become more apparent. Based on our current understanding of water quality and its effect on lake clarity, these problems include 1) analysis of water quality parameters with a limited connection to lake clarity; 2) changes in the chemical methods and chemical species analyzed, which complicate efforts to measure long-term trends; 3) changes in the time of sampling for some streams, which may have introduced bias in records for flow-driven constituents such as suspended sediment and total phosphorus; 4) use of inaccurate models and lack of estimates of statistical error in calculating total constituent loads.

The purpose of this project is to review the existing program, develop and apply procedures for recalculating total constituent loads and time trends, and recommend programmatic changes that will make LTIMP a useful and cost-effective management tool. We take both a retrospective approach, looking back at the existing program and data, and a forward-looking approach, recommending changes based on calculated sample numbers and project costs for different levels of uncertainty in estimates of total constituent loads.

The Problem of Bias

Two sources of bias have crept into the LTIMP record. First, the nitrate-N record has been affected by changes in chemical methods. From 1976 to April 2003, nitrate-N was analyzed by reducing it to nitrite, and developing a color for photometric analysis. In 2003, it was discovered that addition of a catalyst--pyrophosphate with copper--gave higher yields, and this catalyst was used in subsequent analysis. In order to provide a basis for adjusting the old data, nitrate-N was measured by both the old and new methods in 2,370 pairs of samples from all LTIMP stations, between 2003 and 2008. A test for homogeneity of the regression coefficients showed significant differences between stations, possibly because the concentrations of interfering cations varied between stations. Separate regression equations for each station were thus used to adjust the old data to the value estimated for the new method. Details of the adjustment procedure and the history of the analytic methods are given in Appendix A-1.



The second source of bias is related to a change in the times of sampling throughout the day. Prior to 1989, USGS staff sampled intensively during snowmelt, with samples collected both day and night. Due to (very real) safety concerns, sampling in the dark was cut back or discontinued for streams in Nevada, as well as Trout Creek and the Upper Truckee River (UTR) in about 1989. The TRG/TERC, however, has continued night-time sampling in Ward, Blackwood and General Creeks, and the USGS has continued to sample as late as 9:00 PM around the summer solstice. On the larger watersheds, especially in the latter days of the snowmelt season, the daily snowmelt pulse (which carries most of the daily water volume and constituent loads) may arrive at the gaging station after dark. Eliminating nighttime sampling could thus create an apparent downward trend or sudden drop in total load or concentration. In small watersheds, daytime-only sampling could over-sample the rising hydrograph limb, and result in an upward bias in estimated daily load. Although there is no way to reconstruct the nighttime data that have been lost by the reduction in nighttime sampling, we were able to estimate the potential magnitude of bias that would have been introduced in Ward, Blackwood and General Creeks by calculating loads with and without nighttime samples, and for other streams by resampling simulated records. At Ward Creek, elimination of nighttime sampling would create an apparent downward trend or sudden drop in suspended sediment. The resampled simulated records showed modest introduced bias in some constituents for some stations. Because of these problems, time trends in total load estimates were calculated for daytime only samples as well as for all samples.

Testing and Choosing Load Estimation Methods

To develop a basis for selecting the best load calculation methods, we used a simulation approach. The simulations involve resampling from (1) synthetic populations of target variables or (2) worked records developed from stations and years (mid-1980s) when sample sizes were large. The synthetic data sets were constructed using regression relationships with transformed and untransformed continuous variables (discharge, lagged discharge, turbidity, conductivity, water temperature) from previous studies. Random error was added to the synthetic concentrations. For maximum relevance to historic load estimation, the data sets were resampled in a way that retains the characteristics of historic LTIMP sampling protocols, and loads were estimated using multiple methodologies on each synthesized sample. The worked records were resampled by subsampling days on which LTIMP water quality samples were collected.

To create the synthetic data sets, we obtained data sets from studies in sub-basins around the lake: Trout Creek, Homewood Creek, Angora Creek, Ward Creek Blackwood Creek Rosewood Creek and Third Creek. An essential feature of all these data sets is that most of them included near-continuous turbidity data that could be correlated with sample data to produce near-continuous concentration data. In addition to the turbidity data, several stations included near-continuous conductivity or water temperature data. All these variables, together with discharge, gave us the ability to develop models for accurately, or at least realistically, constructing



synthetic data sets that we could use for simulating sampling protocols and load estimation methods.

We then resampled the synthetic data sets 90 times each for 5 sample sizes between 10 and 80, and estimated the load using a variety of regression models, both parametric and non-parametric, and interpolating methods (Table ES-1). The variables used in the regression models included turbidity (T), instantaneous discharge (Q), mean daily discharge (MDQ), mean daily discharge lagged by 1 day (MDQ₁), and number of days since start of water year (D).

Table ES-1. Load estimation methods used in simulations. See Glossary for definitions.

Short name	Type	Time step	Description
rload.turb	simple regression	30-min	$\log(C) \sim g(T)$
rload.turb2	simple regression	30-min	$C^{0.5} \sim T^{0.5}$
rload	simple regression	30-min	$\log(C) \sim \log(Q)$
rload.mdq	simple regression	daily	$\log(C) \sim \log(Q)$
rload.mdq2	multiple regression	daily	$\log(C) \sim \log(Q) + \log(MDQ/MDQ_1)$
rload.mdq3	multiple regression	daily	$\log(C) \sim \log(Q) + \log(MDQ_1)$
rload.mdq4	multiple regression	daily	$\log(C) \sim \log(Q) + \log(MDQ/MDQ_1) + D$
rload.mdq5	multiple regression	daily	$\log(C) \sim \log(Q) + D$
rload.mdq6	simple regression	daily	$C^{0.5} \sim Q^{0.5}$
loess.g	nonparametric	daily	Loess with gaussian fitting
loess.s	nonparametric	daily	Loess with symmetric fitting
ace	nonparametric	daily	ACE transformations (see text)
avas	nonparametric	daily	AVAS transformations (see text)
areg.boot	nonparametric	daily	AVAS <i>areg.boot</i> implementation
pdmean	averaging	daily	Period-weighted sampling estimator
pdlinear	interpolating	daily	Daily interpolator
pdinstant	interpolating	30-min	“Continuous” interpolator
pdlocal2	interpolating	daily	Two-point rating curves + global curve
pdlocal2a	interpolating	daily	Two-point rating curves + interpolation
pdlocal4	interpolating	daily	Four-point rating curves + global curve
rcb1	best regression	daily	Selection by AIC without turbidity
rcb2	best regression	daily	Selection by GRMSE without turbidity
rcb3	best regression	daily	Selection by AIC, all $\log(C)$ models
rcb4	best regression	daily	Selection by GRMSE, all $\log(C)$ models

The best model was selected based on both root mean square error and median absolute error, averaged over all synthetic data sets for each sample size. Note that the last four methods in Table ES-1 are themselves programs that select the best regression model among five models (rload.mdq through rload.mdq5), using one of two selection criteria. Table ES-2 shows the final selections of best methods. “Period Weighted Sampling Estimator” or “Period Weighted Mean” (pdmean) is an averaging method that steps through the record, averaging successive pairs of concentration values and multiplying the average by the total discharge between the two



sampling times. It is sometimes called the “integration method.” Selection by GRMSE (rcb2) selects the best regression of 5 models for the logarithm of concentration using Akaike's Information Criterion (AIC).

Table ES-2. Selected best estimation methods for all constituents with and without turbidity data.

<i>Constituent</i>	<i>With turbidity</i>	<i>Without turbidity</i>
Suspended Sed. (SS)	rcload.turb2	rcb2
Fine Sed. By mass (FS)	rcload.turb2	rcb2
Fine particle number (FSP)	rcload.turb2	rcb2
Total (TP)	rcb3	rcb2
Total Kjeldahl N (TKN)	pdmean	pdmean
Nitrate-N (NO ₃ -N)	pdmean	pdmean
Soluble Reactive P (SRP)	pdmean	pdmean

Recalculating Total Loads

The selected methods (Table ES-2) were then used to recalculate annual loads for all stations, years, and constituents. Nitrate-N data were corrected for bias, as explained above. Loads were calculated when a minimum of 10 samples was available for analysis, and a stream gage was co-located with the sampling site. For each station, year, and water quality parameter, we saved the following information, which is provided with this report in electronic form as “LTIMP loads.xls”:

- Annual yield (kg/ha) computed from all samples collected
- Annual flow volume
- Annual peak daily flow
- Sample size
- Discharge weighted mean concentration
- In the case of best regression, the form of the best model and Gilroy’s estimate of root mean squared error (GRMSE)
- Annual yield computed from daytime samples only (9am-6pm)
- Daytime sample size
- Watershed area (km²)



A file of mean daily concentration is available on request, and together with MDQ can be used to calculate daily constituent loads.

Time trends in Annual Loads

Hydrology—especially annual runoff volume and the maximum daily flow—plays a major role in explaining the variance in total annual load. To examine time trends, we ran regressions of annual load vs. these two hydrologic variables, and included station as a categorical variable. We used the daytime samples only, to avoid the problem of trends induced by the time-of-sampling bias. We then tested separately for time trends in the regression residuals from each station, using the Mann-Kendall Trend Test (see Glossary). With 20 separate stations tested, we used the Bonferroni correction to limit the number of false positives, setting the threshold significance level at 0.0025 for each test. The significant trends identified were:

- SS: ED-3, IN-1, TH-1, UT-1
- TP: GC-1, IN-2, TH-1, UT-1, WC-8
- TKN: ED-3
- NO₃-N: BC-1, GC-1, IN-1, IN-3, TH-1, UT-1, WC-8
- SRP: GC-1, TC-1, TH-1

Stream names and USGS station numbers are given in Table 1-1. All significant trends are downwards, with the exception of SRP at TC-1. The significant trends at IN-2 and ED-3 are for short periods of record. Those sites have not been sampled since 2006 and 2001, respectively. Figure ES-1 shows the nitrate-N data for all stations. Similar figures for other constituents are in the main body of this report.

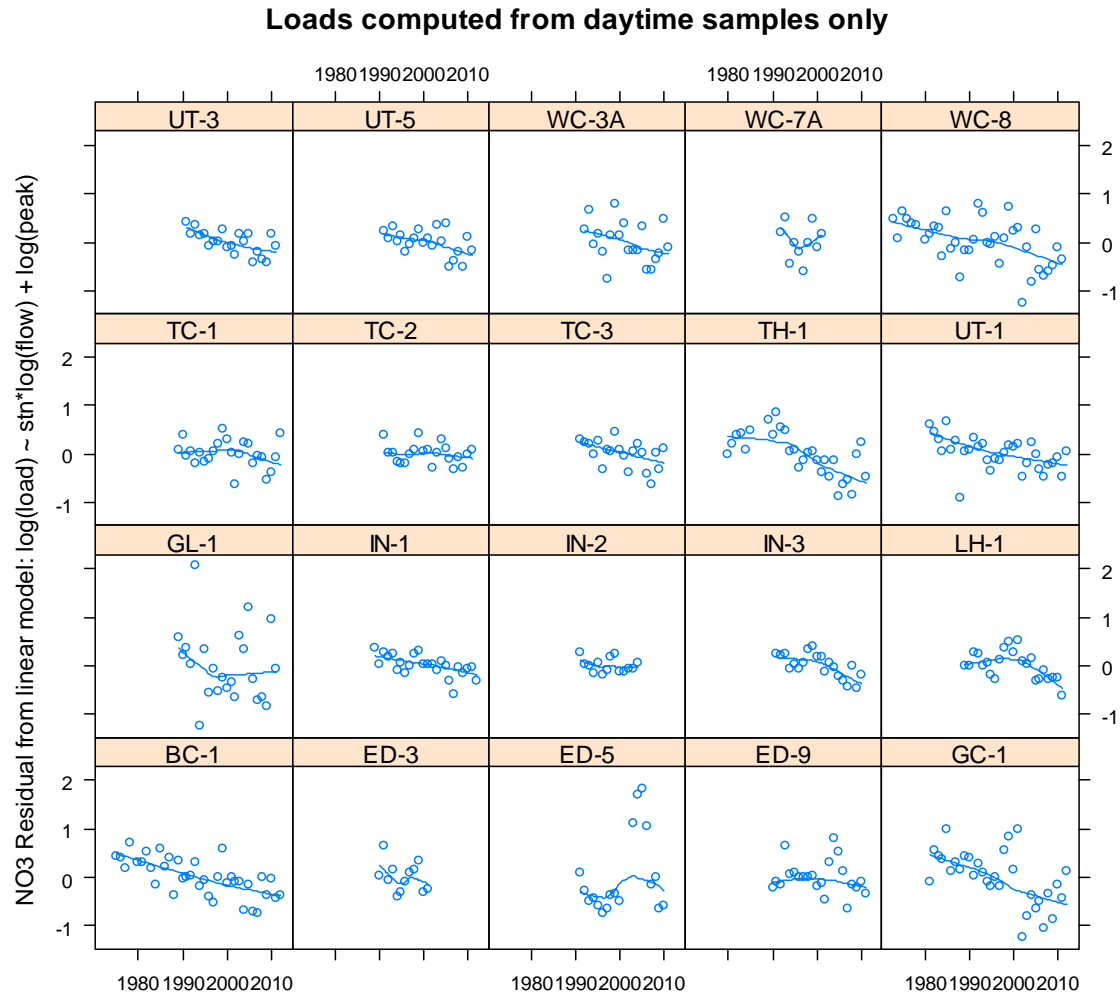


Figure ES-1. Trends in NO₃-N after accounting for inter-annual variation in total and maximum daily runoff. See Sec. 11 for more details.

The occurrence of so many downward trends in loads, especially for NO₃-N, is striking. The atmospheric deposition data for NO₃-N show no corresponding time trend. We hypothesize that the trends are caused by long-term recovery from logging and overgrazing in the 19th century and first half of the 20th century. Essentially, the forests are accumulating biomass, and becoming more effective in retaining nitrogen, phosphorus and sediment. In the case of Blackwood Canyon, recovery may involve a shift from nitrogen-fixing alder toward conifers, which produce a litter and humus layer with high carbon-nitrogen ratio (Coats et al., 1976). The long-term trend toward warmer temperatures could accelerate plant growth and contribute to closing of nutrient cycles and reductions in sediment production. Land use controls and BMPs implemented since the mid-1970s may also have played a role.



Confidence Limits and Costs for New Estimates of Total Load

The simulations of concentration and calculations of total load allowed us to examine the relationships between sample size and error in new load estimates for each constituent. We created a spreadsheet showing alternative levels of precision for each constituent as a function of sample size (Table 13-1). The sample numbers refer to the required number of samples per year at a given station. For example, with 25 samples per year, one can be 90 percent sure that the true annual load of total phosphorus is within +/- 20 percent of the value estimated using the best model selected by the GRMSE criterion. For the same level of confidence and percent error for SSC, 67 samples per year would be required. The relationship between confidence level and sample number is highly non-linear. To achieve the 90/10 level for TP and SSC would require over 100 samples per year.

Table 13-1 also shows the comparison of required sample numbers for an improved LTIMP (using new load calculation models) with a turbidity-based program, where loads of the particulate constituents are calculated by regression with continuous turbidity. For SSC at the 90/20 level, the required sample size drops from 67 to 20.

These sample size tables have been used to develop cost estimates for different levels of effort in a realigned LTIMP. The spreadsheet showing the cost alternatives is available on request.

The derived confidence limits can be used in the design of monitoring projects to calculate the sample size required to detect a given percent change in load between an upstream and downstream station. For example, without turbidity data, detecting a 30% change in total phosphorus load would require at least 40 samples along with instantaneous and mean daily discharge.

Summary and Recommendations

In this study, we have developed and compared different methods of calculating total constituent loads, and expressed the results as the number of samples (per station-year) required to achieve a given level of confidence that the true load is within a given error band around the estimated load. Using the best methods (that is, the methods that maximize precision and minimize bias), we recalculated the total annual loads of NO₃-N, NH₄-N, TKN, SRP, TP and SSC for all of the LTIMP stations over the periods of record. We then related the annual loads to annual runoff and maximum daily peak discharge, and (for all but NH₄-N) analyzed time trends in the residuals. The significant downward trends indicate some long-term improvement in water quality, which we suggest may be due to long-term recovery of terrestrial ecosystems from 19th and 20th century disturbance.

Based on our results and our experience working with the LTIMP data, we recommend the following:



- Near-continuous measurement of turbidity and temperature with automated probes should become a central part of the realigned LTIMP.
- Fine sediment is now recognized as an important factor in lake clarity and is incorporated in the TMDL targets and used in the Lake Clarity Model. Increased emphasis should be placed on its measurement as number of particles.
- The load calculation models developed in this study present an opportunity for major cost savings (or improvements in accuracy of load estimates) especially for the dissolved constituents.
- If station numbers need to be reduced for budget reasons, stations on the big contributing streams (Ward, Blackwood, Trout Creeks and the UTR) should have priority for continued discharge measurement and sampling.
- An intermediate confidence and error level—90 percent confidence that the true value lies within +/- 20% of the estimated value—is achievable with 20 samples per year per station combined with continuous turbidity, for all constituents, and 25 samples per year per station without turbidity, for the chemical constituents. Without good turbidity data, this level for SSC would require about 70 samples per year.
- The relationships between sample size, confidence and error should be used to plan monitoring of restoration and mitigation projects.
- Ammonium-N could be dropped from the list of constituents routinely measured, since about half the time its concentration is below the MDL. It is included in the measurement of TKN. It might be useful, however, for tracing event-related point-sources of contamination.
- Dissolved phosphorus (DP) can be reliably predicted by linear regression with SRP, and could be dropped from the list of constituents measured.
- The time-of-sampling bias for dissolved constituents can only be addressed by increased night-time sampling during snowmelt and storm runoff. This would require either use of automated pumping samplers, or grab sampling from stream banks.
- The realigning and improvement in LTIMP should be considered a work-in-progress. There is still room for improvement in the load calculation programs, and with simultaneous measurement of fine sediment and turbidity, confidence limits and error bands on fine sediment loads could be better estimated.
- The LTIMP needs a working director, with a strong background in hydrology, biogeochemistry and statistics along with experience in fund-raising. The director should be housed in one of the scientific research organizations active in the basin and have decision-making authority on operational matters. Overall policy direction would continue to be the responsibility of the management and funding agencies. With



continued involvement of support staff from the scientific organizations, this could perhaps be a half-time job.

- Any changes to the LTIMP must maintain or improve the program's ability to respond quickly to emerging water quality issues and crises. The program's contribution to addressing water quality problems could be improved by periodic (at least annual) inspection of the concentration data as they become available. Unusual spikes in concentration could provide a basis for targeted synoptic sampling designed to identify problems for remediation or enforcement action.



1 Introduction and Background

The Lake Tahoe Interagency Monitoring Program (LTIMP) was established in 1979 in response to declining water quality and clarity of Lake Tahoe. Its original purpose was to provide data for estimating annual streamflow and loads of nutrients and sediments from basin watersheds to the Lake. It is currently funded by the US Geological Survey (USGS), the University of California Davis Tahoe Environmental Research Center (TERC), the Tahoe Regional Planning Agency (TRPA) and the US Forest Service Lake Tahoe Basin Management Unit (LTBMU), Nevada Division of State Lands, and the Lake Tahoe License Plate Program. The TRPA and LTBMU, along with the Lahontan Regional Water Quality Control Board (LRWQCB, or “the Board”), and the Nevada Division of Environmental Protection (NDEP) have statutory responsibility for maintaining and improving water quality in the Tahoe basin. To fulfill their responsibilities, they need accurate and precise information on the loading rates and sources of sediment and nutrients that enter the Lake, along with assessment of the status and long-term trends in basin water quality. In addition, the data provided by LTIMP are of considerable interest to scientists, and to engineers, planners and consultants in the private sector. The LTIMP data base has proven to be especially important in the development of the TMDL (Total Maximum Daily Load) Program (Lahontan and NDEP, 2010), the assessment of climate change impacts on the Lake (Sahoo et al., 2013) and in a number of scientific journal articles.

Annual funding levels for the LTIMP have varied over the years, reaching a high (in 1992 dollars) of \$0.55 million in WY 2007 and declining substantially since then. The allocation for 2014 (in current dollars) is \$0.383 million. Since 1988, the USGS and TRPA have spent over \$9.1 million on the program (Alvarez, et al, 2007). Given the present fiscal environment, however, it is likely that future funding levels will not be generous. In order to maintain a program that will provide the information needed by managers and scientists in the basin, it will be important to establish the relationships between costs and the quality of data, including the accuracy and precision of loading estimates, and to choose the most cost-effective methods for data acquisition. Figure 1-1 (from the USGS) shows the history of funding levels for the LTIMP.

The purpose of this project is to develop and analyze alternatives for realigning LTIMP to provide useful data for the agencies and research scientists. We first take a retrospective approach. This includes (1) cleaning up and removing (where possible) identifiable sources of bias in the data; (2) using a Monte Carlo method to find the optimum methods for calculating total loads; (3) recalculating loads for all years, constituents and stations; (4) using the recalculated loads to test for time trends in water quality. Second, we evaluate alternative sampling protocols for both cost and confidence limits of loading estimates, in order to inform future decisions about funding and project design. Our approach is to outline the costs and



benefits of various levels of effort for the future program, recognizing that the agencies themselves must choose how much to spend and what level of accuracy is acceptable. We do, however, make some recommendations of our own.

The early phase of the LTIMP was an outgrowth of stream sampling on Ward and Blackwood Creeks by the UC Davis Tahoe Research Group (TRG) and USGS (Leonard et al., 1979). Early data from that effort have been incorporated into the LTIMP data base, although instantaneous discharge values are not available. In 1978-79 the sampling was funded, formalized, and extended to four more streams on the California side and Third Creek, with USGS gaging stations installed at the stream mouths near the lake. In 1988-82 upper watershed stations were added in five tributaries to provide (in some cases) better data for catchment areas not directly affected by development. Table 1-1 lists the stations that have been included in the LTIMP, and indicates span of years of sampling. Table 1-2 shows the full USGS site names and site numbers corresponding the numbers in Table 1-1. Figure 1-2 shows the locations of the primary and secondary stations that are listed in Tables 1-1. Note the significant cutback in the number of stations starting in 2011.

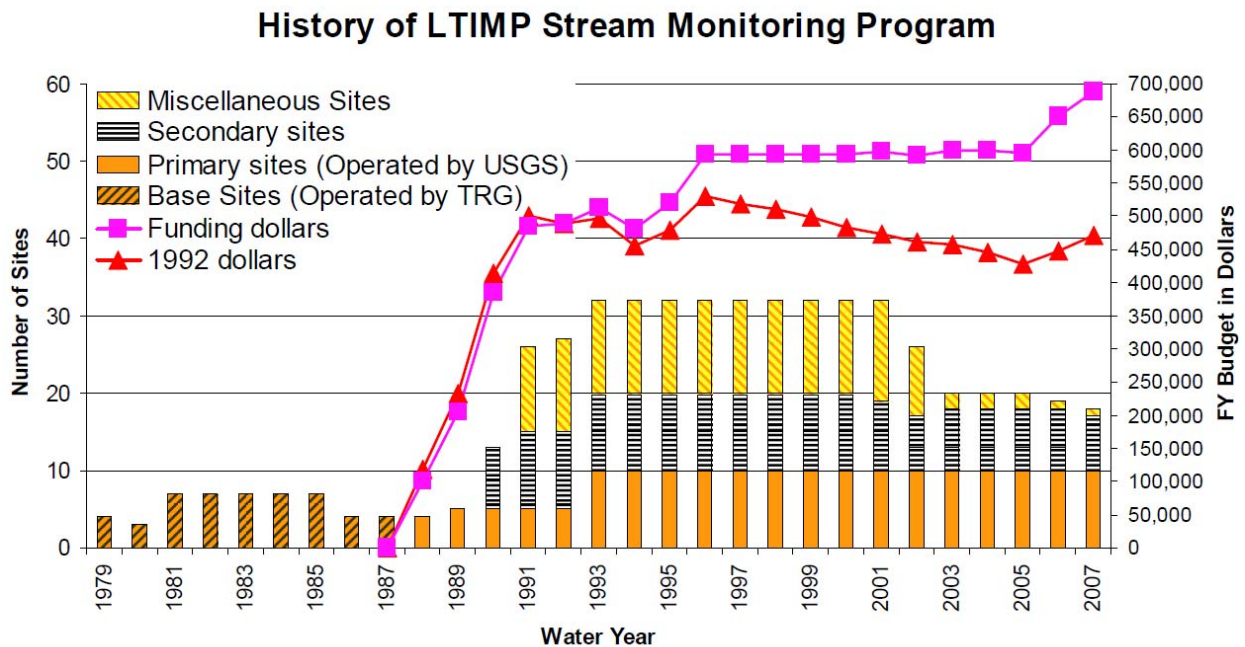


Figure 1-1. LTIMP history of funding levels and station numbers. From U.S. Geological Survey



Table 1-1. List of LTIMP stations with USGS code, LTIMP code and range of years sampled. A few stations are missing some years, not shown. Stations for which annual load was calculated in this study are shown in bold typeface; primary station names are in italics. Others are miscellaneous or secondary stations, some with incomplete records. TH-1 is used for sampling; corresponding discharge measurements are from TH-4.

Tributary Name	LTIMP Sta. Name	USGS Sta. ID No.	Water Year		Length of Record
			Begin Record	End Record	
Angora	AC-1	1033660958	2007	2008	2
Angora	AC-2	103366097	2008	2010	3
<i>Blackwood</i>	BC-1	10336660	1974	2012	39
<i>Edgewood</i>	ED-1	10336765	1984	2002	19
Edgewood	ED-2	10336761	1984	1992	9
Edgewood	ED-3	103367585	1989	2002	14
Edgewood	ED-4	10336750	1989	2002	14
Edgewood	ED-5	103367592	1990	2011	22
Edgewood	ED-6	10336756	1981	2001	21
<i>Edgewood</i>	ED-9	10336760	1992	2011	20
First	FI-1	10336688	1970	2002	33
<i>General</i>	GC-1	10336645	1980	2012	33
<i>Glenbrook</i>	GL-1	10336730	1972	2011	40
Glenbrook	GL-2	10336725	1989	2000	12
<i>Incline</i>	IN-1	10336700	1970	2012	43
Incline	IN-2	103366995	1989	2006	18
Incline	IN-3	103366993	1989	2011	23
Incline	IN-4	12336700	1989	1990	2
Incline	IN-5	103366997	1989	2002	14
<i>Logan House</i>	LH-1	10336740	1984	2011	28



Logan House	LH-3	10336735	1991	2002	12
Rosewood	RC-2	103366974	2001	2003	3
Second	SE-1	10336691	1991	2001	11
Second	SE-2	103366905	1995	2000	6
Snow	SN-1	10336689	1980	1985	6
Taylor	TA-1	10336628	1998	1999	2
Trout	TC-1	10336790	1972	2012	41
Trout	TC-2	10336775	1989	2011	23
Trout	TC-3	10336770	1990	2011	22
Trout	TC-4	10336780	1974	2002	29
Third	TH-1	10336698	1970	2012	43
Third	TH-4	103366965	1989	2000	12
Third	TH-5	103366958	1989	2001	13
Upper Truckee	UT-1	10336610	1970	2012	43
Upper Truckee	UT-2	103366098	1989	2002	14
Upper Truckee	UT-3	103366092	1989	2011	23
Upper Truckee	UT-4	103366094	1989	2002	14
Upper Truckee	UT-5	10336580	1989	2011	23
Ward	WC-3A	10336674	1991	2011	21
Ward	WC-7A	10336675	1989	2003	15
Ward	WC-8	10336676	1972	2012	41
Wood	WO-1	10336694	1970	2002	33
Wood	WO-2	10336692	1991	2001	11



Table 1-2. Site numbers and names of USGS gaging stations used in the LTIMP. Numbers correspond with those of Table 1-1

USGS Site No.	Name
10336580	UPPER TRUCKEE RV AT S UPPER TRUCKEE RD NR MEYERS
103366092	UPPER TRUCKEE RV AT HWY 50 ABV MEYERS, CA
103366097	ANGORA CK NR MOUTH AT LAKE TAHOE GOLF COURSE
103366610	UPPER TRUCKEE RV AT SOUTH LAKE TAHOE, CA
103366645	GENERAL C NR MEEKS BAY CA
103366660	BLACKWOOD C NR TAHOE CITY CA
103366674	WARD C BL CONFLUENCE NR TAHOE CITY CA
103366675	WARD C A STANFORD ROCK TRAIL XING NR TAHOE CITY CA
103366676	WARD C AT HWY 89 NR TAHOE PINES CA
103366689	SNOW C A TAHOE VISTA CA
103366698	THIRD CK NR CRYSTAL BAY, NV
103366993	INCLINE CK ABV TYROL VILLAGE NR INCLINE VILLAGE NV
103366995	INCLINE CK AT HWY 28 AT INCLINE VILLAGE, NV
10336700	INCLINE CK NR CRYSTAL BAY, NV
10336730	GLENBROOK CK AT GLENBROOK, NV
10336740	LOGAN HOUSE CK NR GLENBROOK, NV
10336750	EDGEWOOD CREEK BELOW SOUTH BENJAMIN DR. NR DAGGETT PASS, NV
10336756	EDGEWOOD CK TRIB NR DAGGETT PASS, NV
103367585	EDGEWOOD CK AT PALISADE DRIVE NR KINGSBURY, NV
103367592	EAGLE ROCK CK NR STATELINE, NV
10336760	EDGEWOOD CK AT STATELINE, NV
10336765	EDGEWOOD CK AT LAKE TAHOE NR STATELINE, NV
10336770	TROUT CK AT USFS RD 12N01 NR MEYERS, CA
10336775	TROUT CK AT PIONEER TRAIL NR SOUTH LAKE TAHOE, CA
10336780	TROUT CK NR TAHOE VALLEY, CA
10336790	TROUT C A SOUTH LAKE TAHOE CA
10337500	TRUCKEE R A TAHOE CITY CA

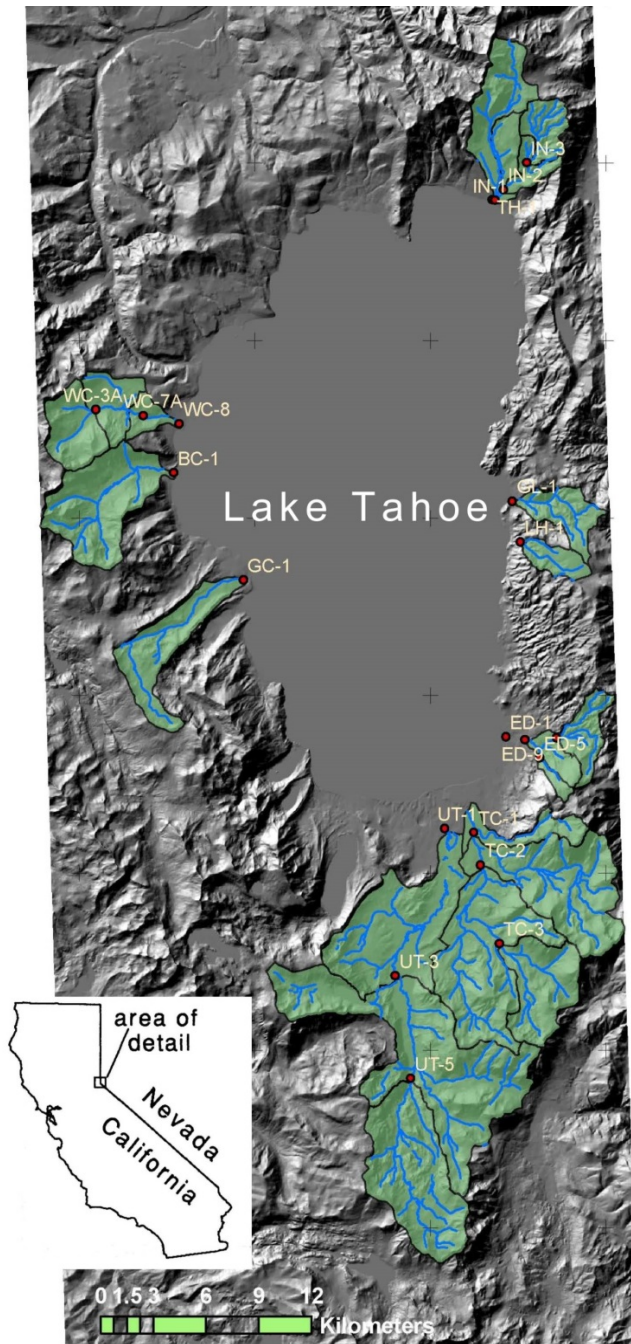


Figure 1-2. Map of the Tahoe Basin, showing locations of the LTMP watersheds and sampling sites for which load calculations were completed.



The water quality constituents measured in stream-water samples have focused on suspended sediment and different forms of nitrogen, phosphorus and iron. Table 1.3 lists the specific forms analyzed. For details on the analytic methods used, see Liston et al., 2013. Note that different methods have been used for nitrate-N, total phosphorus and iron. These changes in chemical methods may have introduced bias that could affect apparent time trends in loads and concentrations. The problem of bias introduced by a change in the method for nitrate-N is discussed in Appendix A-1.

Table 1-3. Water quality constituents analyzed at some time during the LTIMP. Constituents currently analyzed are indicated in bold typeface.

ASSAY CODE	ASSAY DESCRIPTION
DBAFE/DFE	Iron, biologically available, diss. (ug/l as Fe)
DHP	Phosphorus, hydrolyzable+ortho, diss. (ug/l as P)
DKN	Nitrogen, ammonia plus organic, diss. (ug/l as N)
NH₄-N	Nitrogen, ammonia, dissolved (ug/l as N)
NO₃-N	Nitrogen, NO ₂ + NO ₃ , dissolved (ug/l as N)
DP	Phosphorus, dissolved (ug/l as P)
FSP	Fine Sediment Particle Number
DRFE	Iron, dissolved (ug/l as Fe)
Sol.Fe	Soluble Iron (ug/l)
SRP	Phosphorus, orthophosphate, diss. (ug/l as P)
TBAFE/BAFE	Iron, biologically available, total (ug/l as Fe)
THP	Phosphorus, hydrolyzable+ortho, total (ug/l as P)
TKN	Nitrogen, ammonia + organic, total (ug/l as N)
TNH ₄ -N	Nitrogen, ammonia, total (ug/l as N)
TNO ₃ -N	Nitrogen, NO ₂ + NO ₃ , total (ug/l as N)
TP	Phosphorus, total (ug/l as P)
TRFE	Iron, total (ug/l as Fe)
TRP	Phosphorus, orthophosphate, total (ug/l as P)
SSC	Suspended Sediment Concentration, mg/l
TSS	Total Suspended Sediment, mg/l



Changes in the regulatory environment have imposed changes in demands for information on the LTIMP. Under Sec. 303(d) of the Clean Water Act, the LRWQCB found eight basin streams out of compliance with the standards of the Basin Plan, and the Nevada Division of Environmental Protection added three more. Table 1-4 lists the streams and the constituents for which the streams are listed.

In 1995, the LRWQCB in its revised Basin Plan defined the water quality of objective for Tahoe basin streams such that the 90th percentile value (exceeded by 10 percent of the samples) should not exceed 60 mg/l. The 90th percentile cannot be defined without a set of samples, and what the samples should represent is not defined. For Blackwood Creek, using all of the available samples in the data base, the 90th percentile concentration is 169 mg/l. But the sampling times were concentrated during high flows, when sediment loads were highest. If the 90th percentile is based on estimated values for all days in the record (available for 1976-87), the 90th percentile concentration is 20 mg/l. A change in the sampling regime for sediment might require a revision of the Basin Plan objective.

In 2010, the LRWQCB formally adopted a TMDL, which identified four major source types for pollutant loads, and set reduction targets aimed ultimately at improving lake clarity. The source types include urban runoff, channel erosion, atmospheric deposition, and upland forested areas. The LTIMP stations, due to their locations, sample the contributions primarily from upland forested areas and stream channels, with contribution in some watersheds from urban sources. The contribution from the latter is targeted more directly by the urban runoff monitoring program using automated sampling methods.



Table 1-4. 303(d) listed streams, and parameters named as impairing water quality. Lists from LRWQCB (1995) and NDEP (2013).

	Parameter					Pathogens
	Total N	Total P	Sediment	Total Fe	Zn*	
Ward	X	X	X	X		
Blackwood	X	X	X	X		
General		X		X		
UTR						
Trout	X	X		X		X
Edgewood		X		X		
Glenbrook		X				
Incline				X		
First					X	
Second					X	
Third					X	

*May be due to contamination; reevaluation pending.

Since its inception in 1978, the administration and funding sources of LTIMP have varied. In its first five years eleven state and federal agencies contributed funds or made in-kind contributions of labor or facilities. During that period, the State Water Resources Control Board (SWRCB) provided the chairmanship, but actual implementation was the responsibility of the UCD Tahoe Research Group. In WY 1988, the Carson City office of USGS Water Resources Division took over the federal role from the Sacramento office and data reporting was incorporated into the USGS/STORET system (now called the National Water Information System, or NWIS). In 1992 additional stations were installed in upper watershed locations.

2 Current Understanding of Water Quality Issues in the Tahoe Basin

Our current understanding of basin water quality issues and their relationship to the clarity of Lake Tahoe is somewhat different from our understanding at the time the LTIMP was established. This is due in part to the monitoring program itself and in part to related research projects over the last 34 years. Realignment and redesign of the LTIMP must be informed by our



current understanding of the water quality issues. Here we highlight the important issues that relate to the design of the monitoring program. For a deeper look into these issues, the reader is referred to Rowe et al., 2002.

2.1 Limiting Nutrients

Nutrient addition experiments during the 1960s indicated that primary productivity in the lake was limited by nitrogen. Additions of phosphorus had little stimulatory effect (Goldman and Armstrong, 1969). By 1980, however, phosphorus limitation was noted, with some additional role played by iron and zinc (Goldman, 1981). Subsequent work confirmed the increasing importance of phosphorus as a limiting nutrient, with a shift from co-limitation by N and P to consistent P limitation (Goldman et al, 1993). Chang et al. (1992) also found a strong limitation of primary productivity by phosphorus as well as a possible role for iron. They noted, however, that the availability of the latter is strongly influenced by complexation with dissolved organic matter.

The primary cause of the shift from N to P limitation was the high rate of nitrogen loading to the lake. The most important source of nitrogen is atmospheric deposition of nitrate and ammonium. Jassby et al. (1994) found that the combined wet and dry deposition of dissolved inorganic nitrogen (DIN) on the lake (1989-1991) was 19 times that of the loading from the watersheds. This finding contributed to increased attention to the role of air pollution in modifying water quality.

More recently, however, bioassays have been showing a return to co-limitation by both nitrogen and phosphorus. Nitrogen alone seems to be increasingly stimulatory in summer and fall (when the lake is stratified), while phosphorus continues to be more important as the limiting nutrient in winter and spring (Hackley et al., 2013).

Since WY 1989, the LTIMP has monitored concentrations and fluxes of dissolved and particulate organic nitrogen from the watersheds. The results show that organic nitrogen typically accounts for about 85 percent of the total nitrogen delivered to the lake from the watersheds (Coats and Goldman, 2001; Coats et al., 2008). Between 40 and 80 percent of the Total Organic Nitrogen (TON) load is dissolved (DON). If only a fraction of the DON is biologically available, its importance as a nitrogen source for algae growth would outweigh that of dissolved inorganic nitrogen (DIN). In a study of the bioavailability of DON to bacteria and phytoplankton, Seitzinger et al. (2002) found that 30-45 percent of the DON in streamwater from a pine forest was biologically available. The availability of DON from urban runoff varied from 48 to 70 percent. The bioavailability of even humic-associated nitrogen in a river draining coniferous forest (generally thought to be refractory) may be as high as 37 percent (Carlsson et al. 1999). Although primary productivity in the lake is now P-limited at times, the warming of the lake may (by the end of this century) increase the internal supply of phosphorus, and thus



shift the lake back to a condition of N-limitation (see Sec. 2.5, below). Although the bioavailability of DON has not yet been measured in the Lake Tahoe or basin streams, TKN and DON are clearly important parts of the lake's nutrient budget.

2.2 The Importance of Fine Sediment

At its inception, LTIMP was focused primarily on nutrients known to be limiting to primary productivity in the lake. In recent years, however, modeling, field and laboratory work have shown the importance of fine (0.5-16 μm) sediment (FS). According to Swift, et al. (2006), about 60 percent of the loss of clarity (measured by Secchi depth) is caused by fine sediment. Four streams—Ward, Blackwood, Trout Creeks, and the UTR account for about half of the stream contributions to the Lake (Nover, 2012). Fine sediment is doubly important, in that it not only reduces lake clarity directly, but also carries adsorbed phosphorus that may be liberated to support algal growth (Froelich, 1988; Hatch et al., 1999). Methods for sampling, measuring and reporting fine sediment loads and concentrations are discussed below in Section 4.1.

2.3 Channel Erosion as a Source of Sediment

The Tahoe TMDL (Lahontan and NDEP, 2010; Simon et al., 2003; Simon, 2006) modeled the contribution of stream channel erosion to the lake's sediment load. They found that channel erosion accounted for 17 percent of fine sediment particles (< 16 μm). The models assumed, however, that the flood frequency distribution is stationary, that is, historic flood frequency can be used to estimate future flood frequency. With climate change such an assumption may be unreliable.

2.4 Land Use Influences: Urban Runoff, Fire and Dirt Roads

The Lake Tahoe TMDL (Lahontan and NDEP, 2010; Coats et al., 2008; Sahoo et al., 2013) showed that the nutrient and fine sediment contribution per unit area of urbanized lands far outweighs that of forested lands. Although urbanized areas account for only 6 percent of the surface runoff to the lake, they contribute 18, 7 and 67 percent respectively of the TP and TN loads and FS numbers. These estimates, reported by Sahoo et al. (2013) are based on extensive automated sampling and modeling of urbanized areas, sampling of atmospheric deposition, modeling of channel erosion, and previous LTIMP load estimates. Previous studies (Coats et al., 2008) identified unimproved dirt roads as a contributing factor in sediment production. This is consistent with a large body of work on impacts of timber harvest activities on sediment yields.

Two major fires in the last eleven years have provided information on the potential water quality impacts of wildland fire. The 600 ac Gondola fire of 2002 burned on steep slopes southeast of the lake. In order to document the water quality effects the USGS reactivated a retired stream gaging station on Eagle Rock Creek in the Edgewood Creek drainage. Sampling in the post-fire period showed large spikes in the concentrations and loads of suspended sediment, nitrate-N,



ammonium-N, TKN, soluble reactive phosphorus (SRP) and TP (Allender, 2007). The results of stream sampling were corroborated by UNR study based on plot sampling in the burned and unburned area (Johnson et al. 2007).

In 2007, the 3,100 ac Angora fire burned in mixed conifers, lodgepole pine and residential homes southwest of the lake. Monitoring of water quality was initiated shortly after the fire. Maximum concentrations of nitrate-N, TKN, SRP and SS were elevated relative to baseline concentrations for at least three years, but a downstream large wet meadow area trapped much of the pollutant load, and the impacts to the UTR and lake were slight (Reuter et al., 2012). The contrast in impacts between Gondola and Angora fires illustrates the site-specific nature of fire impacts on water quality, as well as the value of rapidly deployed post-fire monitoring.

2.5 Implications of Climate Change

The reality of climate change and its likely impacts in the Tahoe basin are by now well established. Documented historic and modeled future impacts in the basin include 1) a shift from snow to rain; 2) earlier spring onset of snowmelt; 3) increased frequency of large channel-modifying floods; 4) reduced summer low-flow; 5) more frequent and severe forest fires and tree mortality from bark beetle attacks; 6) warming of the lake, with concomitant increased thermal stability, food web changes and exotic species invasions; and 7) increased summer drought, especially on the east side of the basin (Coats, 2010; Coats et al., 2013; Sahoo et al., 2013, Riverson et al., 2013; Das et al., 2013; Whittmann et al., 2013).

These impacts of climate change have important implications for lake clarity and for future monitoring efforts in the basin. Increased thermal stability increases the resistance of the lake to deep mixing, which is essential for keeping the deep water of the lake oxygenated. The combined results from the LSPC, a basin-wide hydrology model (Riverson et al., 2013) and the lake clarity model (Sahoo et al., 2013) indicate that by the end of the century the deep mixing of the lake will cease, the bottom waters will become anoxic, and phosphorus that is locked up with oxidized iron (Fe^{+3}) in the lake sediments will be released to the water column. Ammonium would also be released from the sediment. The large release of phosphorus could trigger unprecedented algae blooms, and shift the trophic status of the lake from phosphorus limitation back to nitrogen limitation. This possibility underscores the importance of reducing phosphorus loading to the lake now, since much of the phosphorus entering the lake will be stored in the sediment for future release to the water column when deep-water sediments become anoxic.

Increases in frequency of large floods, intense wildfire and bark beetle mortality may increase surface and stream-channel erosion, contributing to the input of fine sediment to the lake. It will be important to monitor these processes and their contribution to sediment loads in order to design effective mitigation strategies.



Climate change may also have important effects on watershed biogeochemical processes. Warmer summer temperatures and higher CO₂ may increase plant growth and the uptake of nitrogen and phosphorus, thus reducing the loss of these nutrients to the lake. Increased drought may reduce saturation in wetland soils and riparian zones, and thus reduce the denitrification of nitrate, and increase the immobilization of phosphorus with oxidized iron.

3 Measuring Stream Discharge

Measurement of stream discharge is an essential part of LTIMP. First, there can be no measurement of nutrient and sediment loads without discharge data. Second, discharge itself is important for water resource planning (water supply) and flood frequency analysis (flood control and land use planning).

Discharge measurement at USGS gaging stations in the Tahoe basin involves several steps. First, stage (or water surface elevation) is measured at 15-min intervals using a Sutron Accububble pressure transducer (<http://www.sutron.com/products/Accububblegauge.htm>) or similar instruments from WaterLOG (<http://www.waterlog.com/index.php>). These devices emit a stream of air bubbles into the water, and measure the back-pressure with a pressure transducer. Data are stored in a data logger in the gaging station. The stage at 15-min intervals is transmitted hourly to the GOES satellite, and is publically-available on-line (see for example http://waterdata.usgs.gov/ca/nwis/uv?site_no=10336645). Second, a rating curve is developed by measuring water velocity at selected points in a surveyed cross section, over a range of discharges. By multiplying cross sectional area by water velocity the relationship between stage and discharge is established. This curve, together with the stage record, is used to calculate both instantaneous and mean daily discharges. For calculation of instantaneous loads in the LTIMP, the instantaneous discharge data from the hydrologist must be collated with the concentration data from the laboratory. This is easiest if the date-time stamps in both records correspond exactly.

Problems in the discharge measurements sometimes arise, however, due to both short and long-term changes in the stage-discharge relationship, or problems in stage measurements. Short-term problems may occur due to ice forming at or just downstream from the cross section and creating a backwater effect, or interfering directly with the stage measurement mechanism by blocking the bubble outlet or increasing the water pressure above the outlet. Such problems can greatly increase the stage and apparent discharge. The ice effect can usually be identified by inspection of the gage record, though experience and skill are needed to remove the effect from the data. For this reason, stream gaging cannot be entirely automated. Long-term changes can occur if the surveyed cross section is scoured or filled at high discharge. Following a major flood, cross sections must be resurveyed in order to maintain a correct rating curve. For a more detailed



description of stream-gaging methods, see: Turnipseed & Sauer, (2010) and Sauer & Turnipseed, (2010).

4 Water Quality Constituents: Sampling and Analytic Methods

Since its inception the LTIMP has made a number of changes in sampling methods, the constituents sampled, and the analytical methods used to measure them. Such changes are necessary in order to take advantage of changes in technology and in our understanding of the processes that influence lake clarity. The changes, however, create problems for analyzing long-term trends in water quality since detection limits, precision and accuracy may change with a change in methods. The following summarizes the constituents that have been included in the program, and discusses the rationale for including them.

4.1 Suspended Sediment

Suspended sediment samples in most of the streams are collected using the “equal-width increment” method at cross sections near the USGS gaging stations (Edwards and Glysson, 1999). Since November 1989, samples from Ward, Blackwood and General Creeks have been collected as a single depth-integrated vertical sample at the center of flow (Scott Hackley, *Pers. Comm.* 7/30/2014).

The preferred analytic method used by the USGS is to measure Suspended Sediment Concentration (SSC). In this method, samples are filtered onto tared filter paper, and the dried sample is weighed to determine mass of sediment from sample of known volume. In some in the Basin studies (not part of LTIMP) the Total Suspended Sediment method has been used. In this method a sub-sample is drawn from the sample bottle by pipette and the concentration determined gravimetrically. This method works well when most of the sediment is silt or clay, but sand does not stay in suspension long enough to be adequately sampled by the pipette. In 1988, the USGS “Total Sediment Concentration” method was used for samples at Incline Creek.

Fine (FS) sediment has been measured at the 10 LTIMP primary stations in since WY 2006. The “fine” fraction is generally defined as particles < 16 or $20 \mu\text{m}$, though the term is also applied to the fraction $< 63 \mu\text{m}$. Concentrations are sometimes reported as mass per unit volume, but reporting particle number per unit volume is preferable, since that variable is more closely related to light extinction and lake clarity, and is used in the lake clarity model (Sahoo et al., 2013). FS particle number data are currently processed using a complex and cumbersome spreadsheet to reduce the data and calculate loads by regression with discharge.

At least three instruments are in use in the Tahoe basin for measuring the volumetric percentage of fine sediment or counting individual particles. The Micromeritics DigiSizer, the Beckman



Coulter ls-13320, and the Particle Measuring Systems LiQuilaz instrument. The latter is the only particle counter of the three, it is the most sensitive, and is best suited for very low concentrations, such as those typical of Lake Tahoe water. It was used in the LTIMP sampling from 2005-2011. The other two are best suited for stream and stormwater samples. Because of its sensitivity, the LiQuilaz is considered by some to be unsuitable for measuring fine sediment particle numbers at the high concentrations typical of stormwater runoff. Samples may require dilution, which can introduce an additional source of error (Heyvaert, et al., 2011; Nover, 2012; Rabidoux, 2005). Holding time of samples is an important issue, since flocculation after sampling may reduce the particle concentrations. Samples are sometimes “sonicated” with high-frequency sound to reduce flocculation (Nover 2012). Additional research on methods for measuring fine sediment and counting fine sediment particles in basin streams is urgently needed.

4.2 Turbidity

Turbidity is closely related to the concentration of fine sediment particles. It is not routinely measured in the LTIMP, but since it can be measured at short intervals (5-10 min) by a probe installed in the stream, it offers the possibility of developing virtually continuous records of some water quality constituents by regression. (Stubblefield et al., 2007; Heyvaert et al., 2011; Reuter et al., 2012). This approach shows most promise with constituents (FS, SSC, TP) that are physically related to turbidity. The available probes rely either on backscatter of light by suspended particles or on absorbance of light over a short path through the water column.

Successful use of turbidity probes, however, requires careful installation and frequent field maintenance (at 1-2 week intervals). Modern probes are equipped with small wipers to keep the light sensor free of biofouling by algae and bacterial slime, but these are not always effective. The probe must be installed so that sunlight will not cause erroneous readings (Lewis and Eads, 2009; Anderson, 2005). Even with frequent maintenance, the probe data must be carefully inspected for problems. The program TTS Adjuster (available on request as part of this report) allows the user to inspect turbidity data along with discharge data, and provides a useful tool for finding and correcting problems. As a backup, turbidity should always be read in the laboratory sample collected for chemical analysis, and compared with the simultaneous field value, although the laboratory instrument may use a different technology than the field probe, and thus give different values. Also, the collected stream sample will represent a different water volume than that sampled by the in-stream probe.

4.3 Nitrogen

Three forms of nitrogen are measured in the LTIMP: nitrate+nitrite-N, ammonium-N and Total Kjeldahl N. The latter includes ammonium-N; reported as Total Organic Nitrogen (TON), the ammonium fraction has been subtracted from TKN. Dissolved Organic Nitrogen (DON) is



calculated by subtracting ammonium-N from TKN of a filtered sample. From WY 1989 to 2010, about 3340 LTIMP samples have been analyzed for DON. Dissolved Inorganic Nitrogen (DIN) is mostly nitrate since ammonium-N is rapidly oxidized to nitrite and then to nitrate by nitrifying bacteria. Nitrate is measured by reducing it to nitrite, so values reported as nitrate are actually nitrate+nitrite.

4.3.1 Nitrate-nitrogen

Nitrate-N ($\text{NO}_3\text{-N}$) is readily available for plant uptake, and is relatively easy to measure. Sources in streamwater include atmospheric deposition, urban runoff, and decomposition of organic matter, especially from alder, which is an important nitrogen-fixer. Nitrate-N (or more correctly, nitrate + nitrite-N) has been measured routinely in Tahoe basin streams since 1972, but the analytic methods have changed twice over the years. From WY 1972 through WY 1976, it was measured by reducing the nitrate to nitrite in columns packed with cadmium, and developing a color the intensity of which was read photometrically. In the fall of 1976, reduction by hydrazine replaced the use of the cadmium columns. It was later discovered that in streamwater (but not lake water) samples, divalent cations (Ca and Mg) interfered in the determination, and values were being under-reported. The problem was corrected by use of a pyrophosphate catalyst, and samples from each station (2002-2008) were run with and without the catalyst to allow the earlier data to be corrected. Appendix A-1 describes the problem and shows the equations used to correct the old data. The corrected data were (based on data available at the time) used in the TMDL project (Lahontan and NDEP, 2010; Coats et al., 2008) and more recent data are used in this project. The confidence limits on estimates of the individual corrected values are relatively wide, but the estimates should be unbiased and can be used to calculate total load.

Recent improvements in an optical probe for nitrate concentration offer the possibility of virtually continuous measurement of nitrate-N in basin streams (Pellerin, et al, 2013). Such a probe was used in a study of patterns of nitrate and dissolved organic matter in a stream in the Sleepers River watershed of Vermont (Pellerin et al., 2012). The minimum detection limit (MDL) is about 5 $\mu\text{g/l}$, only a little higher than the MDL of the currently-used nitrate method. By increasing the path of length of the light beam, an even lower MDL might be achievable. The probe, however, may be cost-prohibitive.

4.3.2 Ammonium-N

Ammonium-N ($\text{NH}_4\text{-N}$) has also been routinely measured since 1972, but about half the time the concentration is at or below the minimum detection level of about 2-3 $\mu\text{g/l}$. The main exception is Edgewood Creek, where concentrations have exceeded 200 $\mu\text{g/l}$ in some years. Ammonium-N is routinely measured with TKN so it is included in the TMDL variable “Total Nitrogen”. To reduce costs it could be dropped from the list of constituents sampled without much loss of



information, but continued sampling at Edgewood Creek may be needed to identify the persistent source.

4.3.3 Total Kjeldahl Nitrogen

TKN is measured by a micro-Kjeldahl method. Samples are digested in concentrated sulfuric acid, neutralized with NaOH, and the resulting ammonia distilled and captured for photometric analysis. Nitrate present in the original sample is not measured, but ammonium is. The MDL is about 40 µg/l. Most of the dissolved nitrogen in both the lake and streams is organic. From this relatively large pool, inorganic N is slowly mineralized and made available for plant growth. The rate of mineralization in basin streams and the lake is not known, but measurement of TKN will continue to be important in understanding the biogeochemical cycle of nitrogen in the lake.

4.4 Phosphorus

Phosphorus has been measured since the earliest days of the LTIMP and since it is the primary limiting nutrient for primary productivity in the lake its continued measurement will be important. Several forms have been measured and reported over the years; these include Dissolved Hydrolyzable Phosphorus (DHP), Dissolved Phosphorus (DP), Total Hydrolyzable Phosphorus (THP), Soluble Reactive Phosphorus (SRP), Total Reactive Phosphorus (TRP) and Total Phosphorus (TP). The measured concentration of these forms reflects the choice of filter size and method of digestion (if any). The different forms vary in their availability to algae. Of the various forms, TP and SRP have the longest and most complete records.

4.4.1 Soluble Reactive and Dissolved Phosphorus

SRP is virtually all orthophosphate (PO_4). It is readily available to algae and bacteria, and in the stream environment, its concentration is strongly controlled by chemical equilibrium reactions with iron and aluminum hydroxyoxides and calcium minerals (Froelich, 1988). For this reason, its concentration varies within a fairly narrow band, and is not closely tied to stream discharge. Hatch et al., (1999) found that dissolved inorganic P (SRP) best represents the short-term stream bioavailable P. Dissolved phosphorus (DP) has been measured since 1972, with measurable concentrations in over 5200 samples. It can be reliably predicted by linear regression from SRP ($R^2 = 0.92$).

4.4.2 Total Phosphorus

TP includes both soluble and insoluble forms. The latter include minerals weathered from bedrock such as calcium apatite and both dissolved and particulate organic matter. The rate at which P is released from mineral particles and organic matter is highly variable, but any form of TP may eventually be released and become available. Ferguson and Qualls (2005) found that about 20 percent of the TP associated with suspended sediment in selected Lake Tahoe



tributaries was bioavailable, and about 35 percent of the TP in sediment from urban runoff was bioavailable.

From 1980-1988, Total Hydrolyzable P (THP) rather than TP was measured. THP involved digestion of samples with sulfuric acid and spectrophotometric analysis of the resulting orthophosphate. The TP digestion uses acid persulfate, and breaks down compounds that are not dissolved in the sulfuric acid digestion. The LTIMP THP data have been converted to TP by linear regression (Hatch, 1997).

4.5 Iron

Since the inception of the LTIMP, iron has been measured and reported in five different forms: Dissolved Biologically-available Iron (DBAFe/DFe), Dissolved Iron (DRFe), Soluble Iron (SolFe), Biologically-available Total Iron ((TBAFe/BAFe), and Total Iron (TRFe). The sources of iron in basin streams include weathered mineral particles and groundwater discharge. Iron has been identified as a limiting nutrient in Lake Tahoe, and six streams are 303(d)-listed for Total Iron. Data for Total Iron, however, are only available for the water years 1981-91, with most of the 765 samples concentrated in 1988-90. Data for biologically-available iron are reported by LTIMP for WY 1992-2002. The Water Quality Objective for Total Iron in Tahoe basin streams is 30 µg/l, but in the entire record, virtually no samples met this objective. The data indicate that Total Iron is strongly influenced by discharge. The natural sources of iron (suspended sediment) overwhelm the anthropogenic sources and the availability of iron is controlled by chelation with organic matter rather than by the supply of Total Iron. A possible mechanism for the role of biological-available iron as a limiting nutrient is its importance in nitrate reduction (Chang et al. 1992). Since the lake is no longer N-limited, iron would seem to be of lesser importance now than in previous years. Total iron is not targeted for control in the Lake Tahoe TMDL plan (Lahontan and NDEP 2010).

4.6 Temperature

Water temperature is routinely measured by USGS and TERC when water samples are collected. In recent years it has been measured at short intervals *in situ* along with pH, conductivity and turbidity as digital recording thermographs have come down in price. Temperature is very important biologically, for its influence on metabolic rate of organisms and on dissolved oxygen concentration. With the coming climatic changes that are anticipated for the Tahoe basin (Coats et al., 2013; Sahoo et al., 2013), good records of stream temperature will become increasingly important.

4.7 Conductivity, pH and Dissolved Oxygen

Conductivity, like temperature, is routinely measured by USGS at the LTIMP gaging stations. It is closely related to Total Dissolved Solids and, while not by itself an important water quality



parameter in basin streams, it may be a valuable ancillary variable for use in modeling concentrations of other constituents. Dissolved Oxygen (DO) and pH are measured quarterly by USGS. Both are highly responsive to photosynthesis and respiration by stream organisms, and these fluctuate between day and night, so the data are difficult to interpret. They could, however, become useful in the event of a major sewage spill.

5 Sampling Strategy and Methodology

LTIMP sampling frequency and protocols have shifted over the years with changes in program management and budgets. There are general guidelines but no formal specification of a protocol. The current sampling program uses three sampling schedules: systematic monthly sampling, intensive storm and intensive snowmelt sampling. Some samples are collected at low, medium and high flows, but the emphasis is on sampling during high flows (Alvarez, 2006). The average number of samples per year was generally between 60 and 100 from 1973 to 1989, then dropped sharply (after the USGS took over station operations) in 1990, to between 20 and 30 samples per year, where it has remained until today (see Figure 5.1). The primary stations (at or near tributary mouths) have always been considered a higher priority for sampling than the secondary (upper-watershed) stations. Since 1990 the west-side stations (WC-8, BC-1, and GC-1) have been sampled the most frequently, averaging 33 to 36 samples per station per year. The west-side stations are maintained by USGS; samples are collected by Scott Hackley of TERC and include some nighttime samples. Currently, only 7 stations are being operated: WC-8, BC-1, GC-1, IN-1, TC-1, TH-1, and UT-1. In 2012 (the most recent year in our data set), between 20 and 26 samples were collected at these stations.

Currently, monthly samples are collected during the first week of each month, all year. Spring runoff samples are taken as soon as low elevation snow starts melting – as early as March. During spring snowmelt, samples are collected weekly or more frequently when the hydrograph is changing daily. Spring runoff samples comprise about as many samples as monthly samples, but sometimes more in years of heavy runoff. An effort is made to sample on the day of peak annual runoff. In addition, up to about 5 samples per year are collected during large storms if there is enough warning and it can be done during daylight hours. At the west-side stations more storm samples are collected-- sometimes 2 or 3 during a single event. In general the frequency of sampling is greater during high flows, but is more systematic than random, i.e. not too clustered.

Changes in time of sampling may have introduced bias in calculations of total load. Prior to 1989 USGS staff sampled intensively during snowmelt with samples collected both day and night. Due to (very real) safety concerns, nighttime sampling was cut back or discontinued for streams in Nevada as well as Trout Creek and the Upper Truckee River (UTR), though samples continued to be collected as late as 9:30 PM through WY 1999. The TRG/TERC, however, has continued nighttime sampling on Ward, Blackwood and General Creeks. On the larger



watersheds, especially in the latter days of the snowmelt season, the daily snowmelt pulse (which carries most of the daily water volume and constituent loads) may arrive at the gaging station after dark. Eliminating nighttime sampling could thus create an apparent downward trend in total load or concentration (see Section 9).



Figure 5-1. Mean number of LTIMP water quality samples per station per year. Statistics include only station-years in which at least 10 samples were collected. Primary and secondary stations are included.

Robertson and Roerish (1999) simulated different sampling strategies by subsampling water quality data from eight small streams in Wisconsin. They considered sampling at semi-monthly, monthly and 6-week intervals, with and without supplemental sampling during storms, storm peaks, or on rising hydrographs using single-stage samplers (Edwards and Glysson, 1999). Although hydrographs in these agricultural environments may be quite different from those in the Tahoe basin, many of the same principles are applicable. They found that the most precise and least biased estimates resulted when multiple years of data from semi-monthly sampling were combined. There can be some loss of precision in combining data from multiple years when regression relationships vary from year to year. The high precision that they reported probably resulted from the large sample sizes that would accrue from such a strategy--large enough to include an adequate representation of high flow events. Strategies that incorporated supplemental sampling during storms were biased because (1) the supplemental samples did not properly represent all parts of the hydrograph and (2) the unbiasedness of the regression estimation



method depends on having samples of average concentration for a given discharge. Because concentrations of sediment and associated chemical constituents in the Tahoe basin and elsewhere tend to be greater for a given discharge when the stream is rising, samples should not be preferentially collected during particular parts of the hydrograph. If too many samples are collected during rising hydrographs they will positively bias the estimates, and if they are collected exclusively during falling hydrographs they will negatively bias the estimates. This is particularly a problem in snowmelt environments where hydrographs have a 24-hour period and sampling is only done during the day. It also can be a concern during storm chasing, where crews usually arrive after the peak of the event. It is important to ensure that high flows are sampled, particularly when sample sizes are small, but the best strategies seem to be systematic or random sampling if estimates will be based on regression of concentration versus discharge. Such an approach generally results in the majority of samples on the falling limb of the hydrograph and that is appropriate because the falling limbs are longer in duration than rising limbs. Robertson and Roerish reported that the bias from storm chasing was less than that from peak or single-stage sampling precisely because crews tended to arrive after the peak. In validation of the LTIMP protocols they found that fixed-period monthly sampling supplemented by storm chasing was the most effective strategy. In some cases, however, traversing stations in a particular order during each storm event is probably not the optimal approach because it will tend to result in certain locations being sampled early in the hydrograph and others being consistently sampled late. An exception may be cases where one stream consistently peaks before another, allowing hydrologist to sample both locations near the hydrograph peak.

With the use of automatic pumping samplers, possibly controlled by programmable data loggers, efficient sampling strategies can be implemented that improve precision and accuracy in load estimation. Many more samples can be collected without additional field effort, and well-studied strategies can be implemented via algorithms without regard to time of day or convenience (Thomas, 1985; Thomas and Lewis, 1993; Thomas and Lewis, 1996). These strategies have not been considered for the LTIMP program for various reasons (cost, freezing temperatures, delays in retrieving samples), but pumping samplers have been used with some success for sampling storm runoff in the Tahoe basin. Implementations in which sampling is based on turbidity (Turbidity Threshold Sampling) have greatly improved load estimates in environments where freezing temperatures are not common (Eads and Lewis, 2003). Turbidity is nearly always more closely related to sediment concentration than is discharge. Hysteresis in the relationship is usually minor or nonexistent. The main objective of sampling in a program with continuous turbidity is to cover the full range of concentrations – the time-of sampling bias becomes irrelevant or at least much less important. The same is likely to be true for sediment related chemistry parameters.

In the early years of LTIMP, chemistry samples were collected as grab samples by filling a hand-held sample bottle from the creek bank. Since 1988, suspended sediment samples have been



collected using the equal-width increment method (EWI), on all of the streams except Ward, Blackwood and General In this method, a sample bottle is inserted into the DH-48 and lowered at a uniform rate from the surface to the bottom at equally-spaced intervals across the stream. . Since Nov. 1989, sediment samples at Blackwood, Ward and General Creeks have been taken as a single depth-integrated sample from the center of flow at low to intermediate discharge, and a single sample from the bank at high discharge, when the streams are unsafe to wade. For chemistry samples the DH84 has been used since 1988, with EWI sampling at low to intermediate discharge, and a single vertical sample from the bank at high discharge.

Sampled water is placed in a churn, thoroughly mixed, and subsamples withdrawn for analysis. Separate 250 or 125 ml plastic bottles are filled for TKN and TP, and a filtered sample is obtained for dissolved constituents. Figures 5-2(a) through 5-2(f) show the steps in sample collection.

Proper sample storage and handling is very important. Changes (uptake and release) can occur in the biologically active species. Fine sediment is at risk for flocculation, which can change the particle size distribution. The current practice is to store samples in a cooler immediately after collection for same-day or next-day delivery to the lab for dissolved constituents and TP, and within a week for TKN.



Figure 5-2. Scott Hackley of TERC collecting samples at Blackwood Creek. (a) Stretching a tape across the creek for EWI sampling; (b) Collecting a chemistry sample with the DH81 sampler; (c) Pouring the sample into the churn splitter. Photos by Jim Markle (<http://jimmarkle.smugmug.com/>).

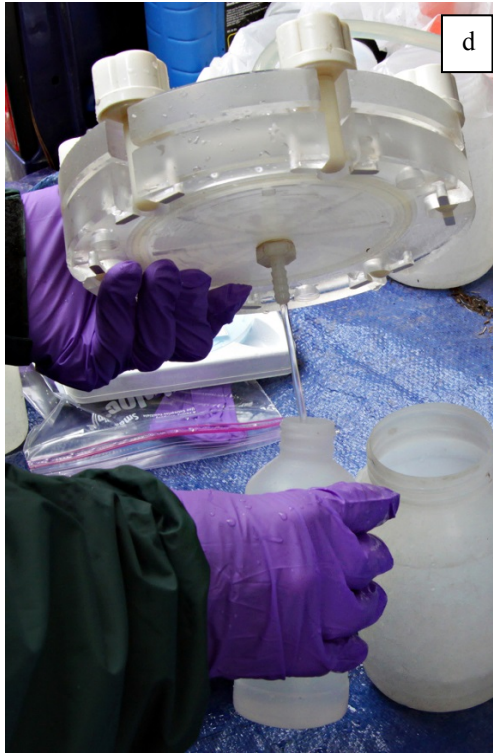


Figure 5-2. Scott Hackley of TERC collecting samples at Blackwood Creek. (d) Filtering a sample for analysis of dissolved constituents; (e) Collecting an unfiltered sample from the churn splitter for TP and TKN; (f) Labeling a sample bottle. Photos by Jim Markle (<http://jimmarkle.smugmug.com/>).

6 Calculating Total Loads

Conceptually, the calculation of tributary mass loads requires evaluating an integral. The load in a given time interval between t_1 and t_2 is given by

$$L = \int_{t_1}^{t_2} KQ_t C_t dt$$

where L is the total load in the time interval t_1 to t_2 ; K is a unit conversion factor; Q_t is the instantaneous discharge at time t ; and C_t is the instantaneous concentration at time t .

The instantaneous discharge can be measured by standard stream gaging techniques at the time of sampling, and continuous (or at least mean daily) discharge data are often readily available. The problem is that concentration of most constituents cannot be measured continuously, but must be sampled in the field and later determined in a laboratory.

A number of methods and various refinements have been developed for estimating loads. These fall into three categories: Integrating methods, model-based methods, and design-based methods. Integrating methods estimate concentration by averaging successive concentrations or interpolating between them, multiplying by the discharge between sampling times, and summing over the water year. This approach may give biased results if the sampling does not adequately characterize the extremes of flow and concentration during the entire year (Dolan *et al.*, 1981; Ferguson, 1987). The period-weighted sample method (PWS) (Dann *et al.*, 1986) is a type of averaging estimator, averaging successive concentrations rather than interpolating between them. The PWS has been used at Hubbard Brook to calculate total ion loads leaving the watersheds (Likens *et al.*, 1977).

Model-based methods use statistical relationships to predict concentration from other variables, such as discharge or turbidity. One type of model-based method is the ratio estimator, which assumes a constant ratio between two variables, usually concentration and discharge, or load and discharge (Cohn, 1995). A ratio estimator is a best linear unbiased estimator provided that: (a) samples are collected at random; (b) the relation between y_i and x_i is a straight line through the origin; and (c) the variance of y_i about this line is proportional to x_i , where y_i is the response variable and x_i is the explanatory or predictor variable. This condition is often met with instantaneous load as the response variable and instantaneous discharge as the explanatory variable (Preston *et al.*, 1989). Note that storm-chasing or snowmelt chasing (as used by LTIMP) are not random sampling strategies.

Regression estimators, another model-based method, have long been used to estimate loads of suspended sediment, usually in a log-log form, since both concentration and discharge are assumed to be log-normally distributed. Log of instantaneous concentration (C_i) is regressed against log of instantaneous discharge (Q_i), and the resulting relationship used to predict daily concentration (C_d) from daily discharge (Q_d), provided that a correction factor for retransformation bias is introduced (Ferguson, 1986; Cohn, 1995). Of course the relationship can also be applied to instantaneous discharge if available, and one would expect better results than



at the daily time step. We refer to these methods, whether applied to instantaneous or daily data, as the Rating Curve (RC) Method.

Design-based methods are applicable when samples have been collected using random sampling designs. Stratification of discharge and concentration data by flow class, month or season can appreciably improve the accuracy of load estimates (Richards and Holloway, 1987; Preston *et al.*, 1989). It can be applied to any of the main load calculation methods. Hill (1986), for example, developed separate nitrate-N rating curves for the November to April and May to October periods for Ontario streams, where nitrate-N concentrations are typically two orders of magnitude higher than in Tahoe Basin streams.

Thomas (1985) developed a variable-probability sampling method for suspended sediment load estimation in which the probability of collecting a sample is proportional to its estimated contribution to total suspended sediment discharge. This method was later compared with time-stratified sampling and flow-stratified sampling (Thomas and Lewis, 1993). Such sampling designs allow for unbiased estimates of total load, as well as estimation of sampling error; their implementation requires automated sampling equipment and programmable data loggers.

Using data for three large river basins in Ohio, Richards and Holloway (1987) simulated concentrations at six-hour intervals for nitrate, total phosphorus (TP), soluble reactive phosphorus (SRP), suspended solids (SS), and conductivity for 1,000 years. They then sampled the synthetic data sets to evaluate both sampling and load calculation methods. They found that the bias and precision of load estimates are affected by frequency and pattern of sampling, calculation approach, watershed size, and the behavior of the chemical species being monitored.

Two methods of load estimation have been used by LTIMP: the worked record and the rating curve method. The method of the worked record, used in the early days of LTIMP, may be thought of as an interpolating method. In this method, the time trace of discharge and concentration are plotted together, and the mean daily concentration is interpolated for days on which samples were not collected. This allows the technician to adjust concentrations up or down to take account of discharge variation. With a good database and relatively low intra-daily variability in concentrations, the method is accurate in the hands of a skillful technician, but the results may not be reproducible, and it does not lend itself to an estimate of sampling error (Cohn, 1995). Since mean daily concentration must be estimated from instantaneous concentration, errors may be introduced for constituents that vary widely over the course of a day.

Beginning in 1988, a variant of the rating curve method replaced the Worked record method, and has been used since by the University of California-Davis Tahoe Research Group (TRG) to calculate total nutrient loads for the Tahoe Basin (Byron *et al.*, 1989). Instead of $\log C_i$ vs. $\log Q_i$ instantaneous load (L_i) is calculated as the product $C_i Q_i$, and regressed against $\log Q_i$. The resulting relationship (with appropriate correction for retransformation bias) is used to estimate



7 Statistical Criteria for a Monitoring Program

The two most important properties of a monitoring program are bias and precision. Bias in a monitoring program is the difference between the average of measurements made on the same object (such as total annual load) and its true value. Precision refers to the degree to which repeated measurements under unchanged conditions show the same result. Figure 7-1 illustrates the two concepts.

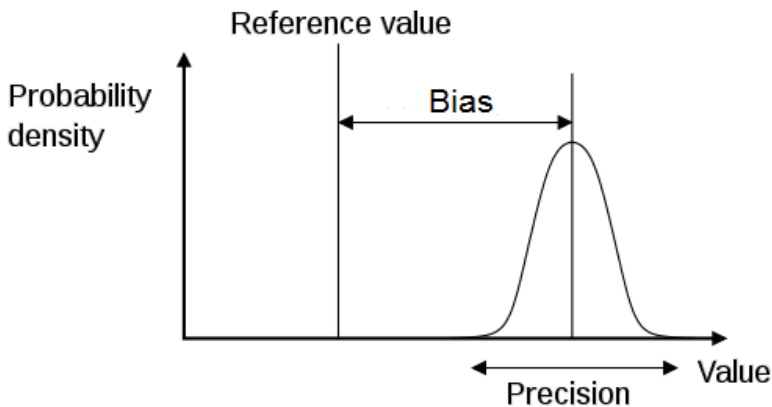


Figure 7-1. Bias and precision in a sampling program

A sampling program can produce results that are unbiased and precise, unbiased but imprecise, biased but precise, or both biased and imprecise. Random error can reduce precision without affecting bias; systematic error increases bias, but not necessarily precision. Accuracy, as we use the term, requires both low bias and high precision, though it has sometimes been used as a synonym for unbiased. Our goal in reviewing the LTIMP is to improve its accuracy by reducing bias and increasing precision, in a cost-effective manner.

In a program as complex as LTIMP, there are many sources of error. It is important that managers, as well as field, laboratory and office personnel understand these sources. Basing load estimates on automated probes (such as turbidity, nitrate, etc.) has the potential to improve both the precision and bias of estimates, but can introduce new sources of error that must be managed. For estimating sediment loads using continuous discharge or turbidity data and possibly with pumped samples, short-term sources of error may include the following:

1. Stage-discharge rating equation
 - a. Inadequate data set
 - i. Data not representative of full range of discharge



- ii. Data not representative of full time period
 - iii. Inadequate number of discharge measurements to estimate rating equation reliably
 - b. Bias in electronic stage/or and discharge
 - i. Stage measurement device not indexed accurately to staff plate
 - ii. Instrument drift (changes in calibration)
 - iii. Current meter spins too slow
 - iv. Discharge not measured at staff plate location
 - v. Errors in stage due to ice formation (see Section 3 above)
 - c. Regression model has high variance
 - i. Errors in reading staff plate and derivation of mean gage height
 - ii. Measurement errors in discharge field procedure or calculations
 - iii. Random scour and fill occurred during time period represented by regression data
 - d. Regression model is inappropriate for the data
 - i. Selected model does not fit entire range of data
 - ii. Relationship shifted but only a single model was applied
 - iii. Relationship is not linear; has wrong functional form
- 2. Sediment sampling and estimation
 - a. Inadequate data set
 - i. Data not representative of full range of SSC
 - ii. Data not representative of full time period (esp. when autosampler is out of bottles)
 - iii. Inadequate number of samples were collected to reliably estimate relation of SSC to predictor variable(s)
 - iv. Samples preferentially collected at certain times of day or on certain parts of the hydrograph, for example on falling limb or at low flows (see Section 10 below).



- b. Bias in SSC and predictor variables
 - i. Unrepresentative pump intake location if SSC not spatially uniform
 - ii. Inadequate pumping sampler line velocity for coarse particles
 - iii. Algal growth from delays in processing unrefrigerated samples
 - iv. Turbidity or stage sensor drift (calibration changes)
- c. Regression model has high variance (can be statistically estimated)
 - i. Pump sample malfunctions
 - 1. Inadequate purge cycle (residual sediment left in pump tubing leading to cross-contamination between samples)
 - 2. Overfilled bottles
 - ii. Turbidity measurement errors
 - 1. Minor biofouling, not corrected
 - 2. Interpolation and reconstruction errors
 - 3. Changes in T-probe location if turbidity not spatially uniform
 - iii. SSC (lab) measurement errors
 - 1. Spillage of sediment or sample
 - 2. Weighing errors
 - 3. Bookkeeping errors (e.g. mislabeled samples)
 - 4. Calculation errors
- d. Regression model is inappropriate for the data
 - i. Selected model does not fit entire range of the data
 - ii. Relationship shifted but only a single model was applied
 - iii. Relationship is not linear; has wrong functional form
 - iv. Model is based on external data due to lack of samples

Sources of error for chemical methods are discussed above in Section 4.



8 Statistical Tests of Sampling and Load Calculation Methods

A major objective of this project was to determine the most accurate methods for calculating historic and future loads. Based on Monte Carlo sampling of worked records from Blackwood Creek (1985-1986), Coats et al., (2002) recommended the PWS method for estimating nitrate and SRP loads. For SS and TP, the preferred method differed between 1985 and 1986. The RC method was superior for SS in 1986 (the wetter year) but was very biased for SS loads in 1985. For TP, the RC methods were recommended when regressions of concentration on discharge are statistically significant, otherwise the PWS method should be used.

We decided to run additional Monte Carlo simulations using a wider variety of populations and estimation methods. These simulations involve resampling from (1) synthetic populations of target variables or (2) worked records developed from stations and years when sample sizes were large. The synthetic data sets were constructed using regression relationships with transformed and untransformed continuous variables (discharge, lagged discharge, turbidity, conductivity, water temperature) from previous studies. Random error was added to the synthetic concentrations. For maximum relevance to historic load estimation, the data sets were resampled in a way that retains the characteristics of historic LTIMP sampling protocols, and loads are estimated using multiple methodologies on each synthesized sample. The worked records were resampled by subsampling the LTIMP water quality data.

For each simulation, we recorded the precision, bias, root mean squared error (RMSE), and the 50th, 80th, 90th, and 95th percentiles of the absolute value of the error. The 50th percentile is synonymous with median absolute percent error (MAPE). The best methods were judged using two measures of accuracy: RMSE and MAPE. The latter is less sensitive to occasional extreme errors. For each population (synthetic data set or worked record), methods were ranked for each sample size and then ordered by the sum of ranks over all sample sizes. The top 6 methods by sum of ranks were plotted for each population. To resolve differences in results among different sampled populations, RMSE or MAPE for each method and sample size was averaged across populations before ranking.

8.1 Synthetic data sets

In order to compare different sampling designs and load calculation models, we created realistic synthetic data sets of the major water quality constituents of concern: SSC, FS, TP, SRP, TKN, and NO₃-N, and resampled these sets up to 90 times in each test of a method. To create the synthetic data sets, we obtained data sets from several researchers who have conducted studies in sub-basins around the lake: Trout Creek (Conley 2013, *Pers. Comm.*), Homewood Creek (Grismer 2013; *Pers. Comm.* 2013), Angora Creek (Reuter et al., 2012; Heyvaert, *Pers. Comm.*



2013), Ward and Blackwood Creeks (Stubblefield, 2002; Stubblefield et al., 2007; *Pers. Comm.* 2013), Rosewood and Third Creeks (Susfalk et al., 2010; *Pers. Comm.*, 2013). An essential feature of all these data sets is that they included near-continuous turbidity data that could be correlated with sampled constituent data to produce near-continuous concentration data. In addition to the turbidity data, several stations included near-continuous conductivity or water temperature data. All these variables, together with discharge, gave us the ability to develop models for realistically constructing synthetic data sets that we could use for simulating sampling protocols and load estimation methods. Unfortunately, we had only one data set with fine sediment particle numbers and corresponding instream turbidity measurements (Angora Creek) but we did have data for fine sediment mass with turbidity for Homewood, Rose and Trout Creek (TC-4).

The turbidity data sets vary in quality and some of them needed extensive cleaning up to remove sunspikes, irregular intervals, gaps, timestamp errors, daylight savings changes, and other problems in the data. The discharge and turbidity data were cleaned using the TTS Adjuster graphical user interface developed at Redwood Sciences Laboratory. Data quality and incompleteness of the turbidity data limited the number and length of useable data sets. Only Homewood Creek 2010 had an entire water year of acceptable data, so partial water years were used for most of the synthetic data sets (Table 8.1-1). All regression models for SRP (Angora, Third, Trout, and Ward Creeks) and NO₃-N (Angora, Third, Trout, and Homewood Creeks) exhibited relatively high variance. We wanted to use the most realistic populations available, so we relied on the worked records rather than synthetic data for simulating SRP and NO₃.

**Table 8.1-1. Synthetic data sets used for simulations**

<i>Watershed</i>	<i>LTIMP ID</i>	<i>Year</i>	<i>Period</i>	<i># Days</i>	<i>SSC</i>	<i>FS</i>	<i>FSP</i>	<i>TP</i>	<i>TKN</i>
Angora	AC-2	2008	Mar18-Jun09	84				x	x
Angora	AC-2	2010	Apr17-Sep30	167			x		
Homewood	none	2010	Oct01-Sep30	365	x	x		x	x
Rosewood	none	2010	Oct01-May31	243		x			
Third	TH-1	2005	Feb24-Jun22	119	x				
Trout Pioneer	TC-2	2010	May13-Jul08	57	x				
Trout Pioneer	TC-2	2011	Apr05-Jul30	117	x			x	
Trout Martin	TC-4	2010	Apr16-Jul08	84		x			
Trout R1	none	2011	Apr05-Aug10	128	x				
Ward	WC-8	1999	May13-Jun24	43	x			x	x

FS – fine sediment mass concentration (mg/L <16 or <20 microns)

FSP – fine sediment particle concentration (particles/ml)

The turbidity (T) data were most useful for modeling SSC, FS, TKN, and TP. Other predictor variables entertained for modeling the various water quality parameters were instantaneous discharge (Q), discharge lagged by h (h=3,6,12,24) hours (Q_h), mean daily discharge (MDQ), mean daily discharge lagged by d (d=1,2) days (MDQ_d), number of days since start of water year (D), conductivity (C), and water temperature (WT). The lagged discharge variables were included for their potential to model hysteresis, wherein concentrations are greater for a given discharge during the rising portion of a daily or seasonal hydrograph. In some cases (e.g. Trout Creek models for SSC) data were combined from multiple locations in a watershed and/or multiple water years at the same location in order to obtain a robust model. In such cases water year was retained in the model as a categorical variable if it was a statistically significant predictor. Location was not a significant predictor in any of these models.

Regression predictors discussed above, and their logarithms, were screened in the R computing environment (R Development Core Team (2010), using all-subsets-regression in the *leaps* package (Lumley and Miller, 2009). The best models with 1, 2, and 3 predictors were identified for each response and its logarithm. The overall best generating model (Table 8.1-2) was selected through a combination of significance testing on predictors and evaluation of model diagnostics, especially linearity of predictors, normality of residuals, and homogeneity of variance.



Table 8.1-2. Models used to generate synthetic data sets

<i>Watershed</i>	<i>Year</i>	<i>Model</i>	<i>ARI</i>	<i>R²</i>	<i>RSE</i>	<i>Load</i>
Trout TC-2	2010	$SSC = 0.482T^{1.459} + 1.283\log(Q)$	0.50	0.961	6.76	310ton
Trout TC-2	2011	$SSC = 0.482T^{1.459} + 1.283\log(Q)$	0.50	0.961	6.76	310ton
Trout R1	2011	$SSC = 0.482T^{1.459} + 1.283\log(Q)$	0.50	0.961	6.76	310ton
Ward	1999	$SSC = 1.377T^{1.153}$	0.50	0.925	9.38	320ton
Homewood	2010	$SSC^{0.5} = 0.531 + 1.16T^{0.5}$	0.66	0.974	0.40	549kg
Third	2008	$SSC^{0.5} = 0.991 + 1.50T^{0.5}$	0.66	0.778	1.50	113ton
Homewood	2010	$FS = 0.239T^{1.086}$	0.50	0.997	0.32	95kg
Rosewood	2010	$FS = 119 + 0.979T$	0.98	0.864	50.0	28ton
Trout TC-4	2010	$FS^{0.5} = 0.722 + 0.107T + 0.243\log(Q)$	0.95	0.823	0.47	51ton
Angora	2010	$\log(FSP) = 4.832 + 0.648\log(MDQ) - 0.173MDQ2 + 1.658C$	0.95	0.821	0.47	3.1×10^{16} particles
Angora	2008	$TP = 1.712 + 1.943T^{0.5} + 1.021\log(Q) - 0.911\log(Q24)$	0.99	0.847	0.92	28kg
Trout TC-2	2011	$TP = 15.70 + 4.499T + 0.469Q - 0.490MDQ2$	0.95	0.814	6.06	1032kg
Ward	1999	$TP = 0.5838 + 3.995T$	0.95	0.951	6.37	628kg
Homewood	2010	$\log(TP) = 4.140 + 0.343T^{0.5} - 0.00674D$	0.95	0.894	0.28	1.4kg
Angora	2008	$\log(TKN) = 4.822 + 0.449\log(Q) + 0.383\log(T) - 0.367\log(MDQ2)$	0.999	0.691	0.45	445kg
Ward	1999	$\log(TKN) = 8.360 + 0.898\log(T) - 1.050\log(Q)$	0.98	0.767	0.38	2.20ton
Homewood	2010	$\log(TKN) = 5.926 + 0.457\log(T) - 0.00524D$	0.998	0.732	0.55	12kg

ARI – autoregressive order 1 parameter, used to generate autocorrelated random errors

R² – multiple coefficient of determination

RSE – residual standard error



Once the models were identified, they were applied to the continuous data sets at 30-minute intervals to generate synthetic traces. If one of these populations were to be sampled in a simulation, and a model of the same form as the generating model was fitted to the data, the model would fit the data perfectly with no error. Therefore it was necessary to add random error to the predicted concentrations. Because of the short 30-min measurement interval in these data sets, deviations from the modeled concentration values would almost certainly be highly autocorrelated. Sets of high-frequency measurements of concentration needed for modeling autocorrelated errors are exceedingly rare. The only such data known to the authors are 10-minute records of turbidity and SSC from several storm events at the Caspar Creek Experimental Watershed (Lewis, 1996). At 10-minute intervals, residuals from regression of SSC (or transformed SSC) on turbidity exhibited autocorrelation explainable by autoregressive (AR) models up to order 3. At 30-minute intervals, AR models of order 1 were adequate to explain the serial correlation. The exact AR coefficient varied by storm event and depended also on the SSC transformation. One of the Caspar Creek storm events had considerably more data than the others and the AR order 1 coefficients from this event (for modeling SSC, $\log(\text{SSC})$ and $\text{SSC}^{0.5}$) were used as starting points for representing the Tahoe basin errors. For each synthetic data set, autoregressive random error was generated using the appropriate coefficient and rescaled so its variance matched the variance of the generating model. Of course Caspar Creek is quite different from the Tahoe basins and, in any case, there is no reason to think these coefficients would be appropriate for parameters other than SSC. An interactive tool with a slider bar was developed to visualize the synthetic trace for any chosen AR coefficient. In many cases the traces appeared too noisy with the Caspar SSC coefficients, so the coefficients were made closer to 1 in order to smooth out the traces while keeping the overall error variance fixed. Figures 8.1-1 and 8.1-2 show the effects of increasing the AR coefficient from 0.5 to 0.98 for a portion of the record at station TC-2. In this case, synthetic TP was generated from a model involving both turbidity and discharge (Table 8.1-2).

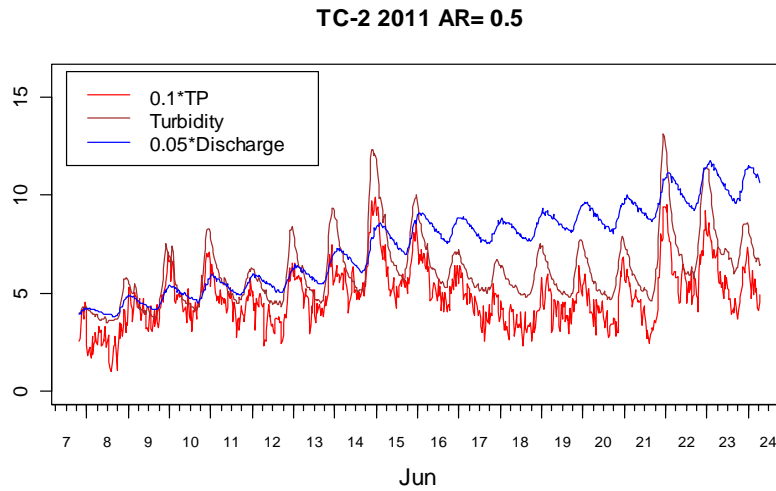


Figure 8.1-1 . Synthetic TP trace with Caspar Creek autoregressive coefficient, 0.5.

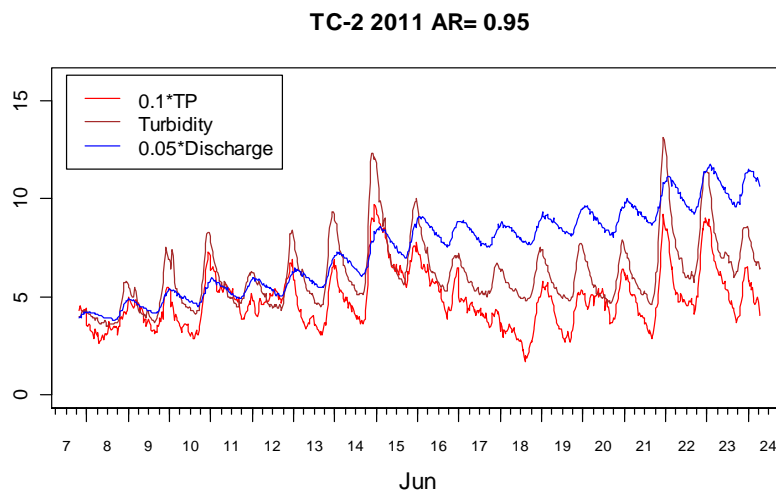


Figure 8.1-2 . Synthetic TP trace smoothed by increasing autoregressive coefficient to 0.95.

8.1.1 Sampling from the synthetic records

To create a grid of sampling times, each interval between actual LTIMP samples was subdivided into equal subintervals, preserving the relative sampling frequencies at different times of the year, e.g. least frequent during off-season, more frequent during snowmelt, and most frequent during storm-chasing. For sample sizes of 10, 20, 40, 60, and 80, an appropriately-spaced grid of



sampling times was created and all possible systematic samples of that size were sampled from the grid (Figure 8.1-3).

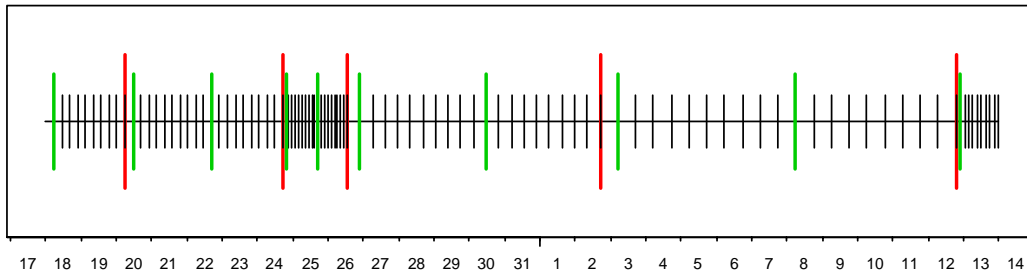


Figure 8.1-3. Illustration of algorithm for sampling synthetic data sets. Axis ticks denote days. Red segments show actual LTIMP sample times and constitute a sampling "template". Black segments delineate equal subintervals between each pair of red segments. Green segments show a systematic sample of the black segments. Simulations generate all possible systematic samples from a given set of subintervals.

Finally, to make sampling more realistic, in half the simulations selected times were mapped from a 24-hour day to a 9-6 PM workday (Figure 8.1-4). Sampling on weekends and holidays was permitted.

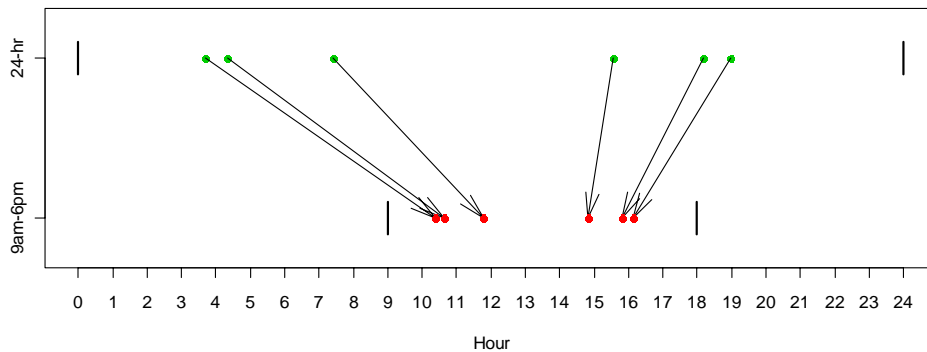


Figure 8.1-4. Illustration of mapping the 24-hour day onto a 9am-6pm work day.

The number of points (times) per subdivided interval is $n_{pi} = n_{sim} * s_{amsize} / n_0$, where n_{sim} =number of simulated samples desired, s_{amsize} =simulated sample size, and n_0 =the actual LTIMP sample size. An additional n_{pi} points are also inserted before the first LTIMP sample time and after the last LTIMP sample time, half of them before and half after. In order to get a constant sample size, points are in turn discarded in approximately equal numbers from the start and end of the sampling grid to reduce the grid size to exactly $n_{sim} * s_{amsize}$. The value of n_{sim} was kept at 30 for all simulations.



To boost the number of simulated samples we used 3 sets of actual LTIMP times for each simulation, from stations that are on substantially different sampling schedules (Figure 8.1-5). In most cases we had to insert or omit one or two sampling times to get the same $n0$ for all three stations. The result was 90 simulated samples for each combination of station and year.

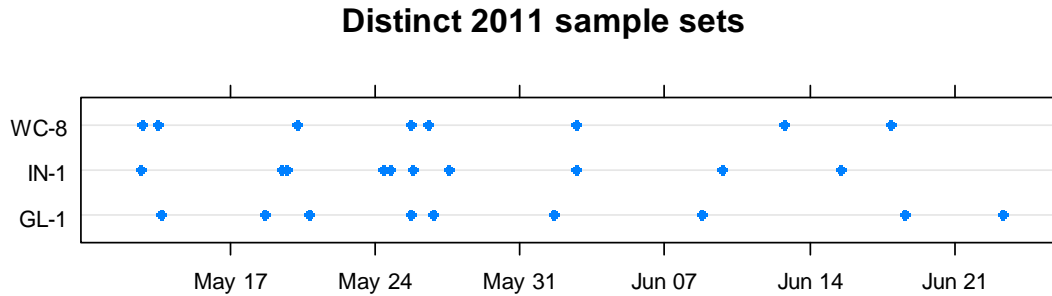


Figure 8.1-5. Three sampling templates used to sample synthetic data for WC-8 in 2011

8.2 The worked records

The method of the worked record was described earlier in section 6. The worked records consist of mean daily flows and mean daily concentrations derived from sample data and hand-drawn concentration curves. Because of the relatively large sample sizes, some of these worked records provide a fairly detailed representation of transport that is useful for Monte Carlo simulations. The worked records include 7 gaging stations: BC-1, GC-1, SN-1, TC-1, TH-1, UT-1, and WC-8. These records were compiled for years 1976-78 and 1980-1987, a total of 11 years, but the records are not complete for some combinations of constituents and years. We limited the simulations to combinations that were complete from April 15 to July 15 (Table 8.2-1), however if that period was included in a longer complete period, the entire period was used. In the majority of cases, the entire year (365 or 366 days) was used (Table 8.2-2).

Table 8.2-1. Number of worked records with complete data from Apr 15 to Jul 15

	<i>BC-1</i>	<i>GC-1</i>	<i>SN-1</i>	<i>TC-1</i>	<i>TH-1</i>	<i>UT-1</i>	<i>WC-8</i>	Total
NO3	11	7	5	6	6	7	11	53
SRP	10	7	5	6	6	7	10	51
SSC	9	7	5	6	2	7	9	45
THP	7	6	4	4	4	7	7	39



Table 8.2-2. Number of worked records with complete data from Oct 1 to Sep 30

	BC-1	GC-1	SN-1	TC-1	TH-1	UT-1	WC-8	Total
NO3	6	6	4	4	2	6	6	34
SRP	6	6	4	4	4	6	6	36
SSC	6	6	4	4	4	6	6	36
THP	6	6	4	4	4	6	6	36

Worked records are available for NO3, SRP, SSC, and THP (total hydrolyzable phosphorus). Figure 8.2-6 is an example worked record for NO3. Simulations were done on all 4 constituents, but the SSC and TP populations derived from turbidity are more realistic than the worked records and we favor the methods indicated by the continuous-data simulations.

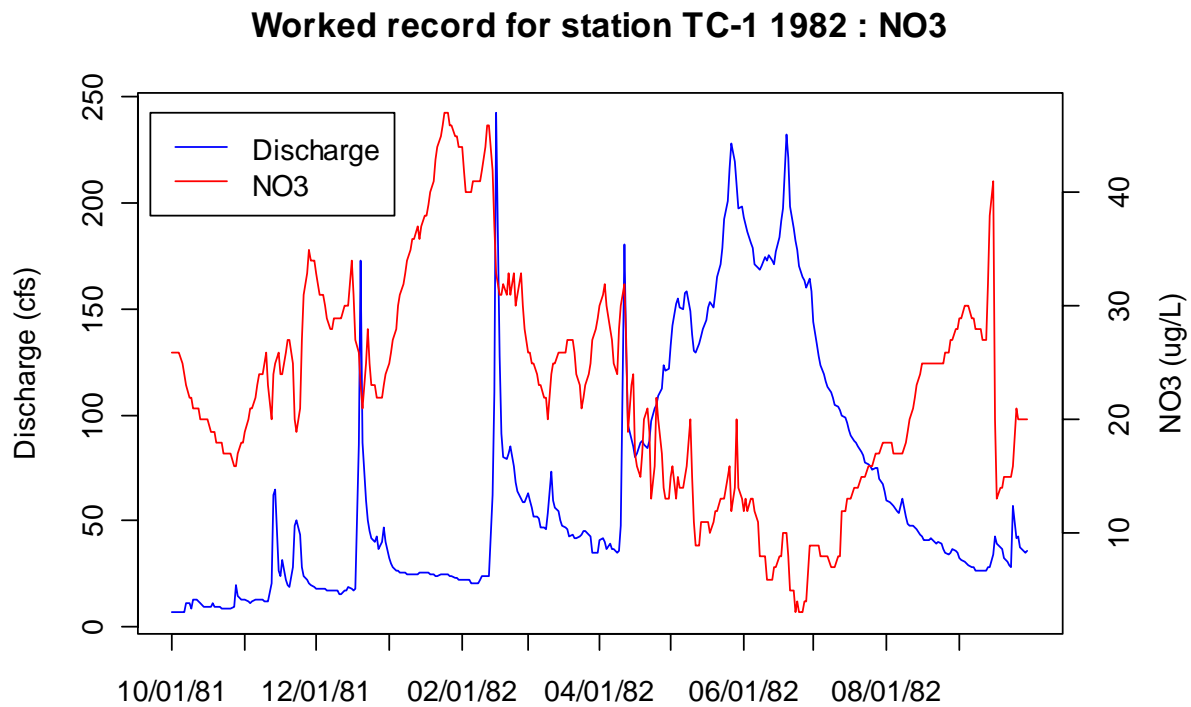


Figure 8.2-6. Example of a worked record for nitrate

8.2.1 Sampling from the worked records

The sampling algorithm used on the continuous data sets was not practical for the worked records because of their low (daily) time resolution. Days actually sampled by LTIMP were subsampled to obtain simulation sample sizes of 10, 20, 40, 60, and 80. Subsampling was not



possible when the LTIMP sample size was smaller than the desired simulation sample size (Table 8.2-3). Otherwise, subsampling was done 10 times for each simulation sample size, and results from all combinations of station and year were pooled. The simulated sample sizes were often a large fraction of the sample sizes used to develop the worked record. In these cases, primarily for simulated sample sizes of 60 or more, it is likely that (1) the worked record simulations underestimate operational errors, and (2) simulations would tend to favor the period-weighted sampling estimator, because it is similar to the interpolating methods used to derive the worked records.

Many of the worked records for SSC contain concentrations of zero (Table 8.2-4). These samples were omitted from models using logarithms of SSC concentration, since it is impossible to take the logarithm of zero. In sampling from regression-generated synthetic populations, we excluded all values of $SSC < 0.5$ to avoid extremely small values of $\log(SSC)$ that would exert too much leverage on the regression lines. This was not an issue with the worked records, which do not contain non-zero values smaller than 1 mg/L.



Table 8.2-3. LTIMP sample sizes for each worked record in Table 8.2-1

		1976	1977	1978	1980	1981	1982	1983	1984	1985	1986	1987
NO3	BC-1	78	30	80	123	91	95	91	96	79	86	68
	GC-1					50	84	86	78	73	83	58
	SN-1					96	74	80	66	51		
	TC-1				75	88	118	85	70	80		
	TH-1				102	108	92	91	101	86		
	UT-1					90	113	92	71	81	81	57
	WC-8	81	32	80	123	91	97	89	95	83	87	68
SRP	BC-1		26	80	122	95	95	91	96	79	86	68
	GC-1					50	84	86	78	73	83	58
	SN-1					96	74	80	66	51		
	TC-1				75	88	118	85	70	80		
	TH-1				102	108	92	91	101	86		
	UT-1					90	113	92	71	81	81	57
	WC-8		28	80	123	91	97	89	95	83	87	68
SSC	BC-1	78			123	95	95	91	96	79	86	68
	GC-1					50	84	86	78	73	83	58
	SN-1					96	74	80	66	51		
	TC-1				74	88	118	85	70	80		
	TH-1								101	86		
	UT-1					90	113	92	71	81	81	57
	WC-8	81			123	91	97	89	95	83	87	68
THP	BC-1					82	95	91	96	79	86	68
	GC-1						84	86	78	73	83	58
	SN-1						74	80	66	51		
	TC-1						118	85	70	80		
	TH-1						92	91	101	86		
	UT-1					74	113	92	71	81	81	57
	WC-8					82	97	89	95	83	87	68



Table 8.2-4. Percentages of zeroes in each worked record in Table 8.2-1

	<i>BC-1</i>	<i>GC-1</i>	<i>SN-1</i>	<i>TC-1</i>	<i>TH-1</i>	<i>UT-1</i>	WC-8
NO3	0	0	0	0	0	0	0
SRP	0.8	0	0	0	0	0	0
SSC	7.2	27.2	1.4	0	0	1.3	17.8
THP	0	0	0	0	0	0	0

8.3 Load estimation methods

For the Monte Carlo simulations the load was estimated using a variety of regression, both parametric and non-parametric, and interpolating methods (Table 8.3-1). The variables used in the regression models are a subset of those introduced in section 8.1.3 including turbidity (T), instantaneous discharge (Q), discharge lagged by 24 hours (Q_{24}), mean daily discharge (MDQ), mean daily discharge lagged by 1 day (MDQ_1), and number of days since start of water year (D). Most of the regression models used a log-transformed response and log-transformations for all the predictor variables except D. Two of the regression models used square root transformations for the response and predictor T or Q. A few of the models utilized turbidity or discharge at 30-minute intervals to predict a high resolution time series of concentration; however, since neither turbidity nor continuous discharge are available historically, most of the models utilized daily mean discharge in the predictions. Simulations from the worked records (i.e. those for SRP and NO3) used only models that did not require turbidity and that could be applied at a daily time step.

In addition to the specific parametric regression models, procedures were developed to select the best regression model among those that used a log-transformed response. Four model selection methods (rcb1, rcb2, rcb3, and rcb4) were compared, using (see Glossary) Akaike’s Information Criterion (AIC) and Gilroy’s (Gilroy et al., 1990) estimate of root mean square error (GRMSE) for the predicted load. Each of the model selection criteria, AIC_c and GRMSE were used to select among (1) those models for $\log(C)$ that do not depend on turbidity as a predictor (rcb1 and rcb2), or (2) the full set of $\log(C)$ models (rcb3 and rcb4); see Table 8.3-1.



Several non-parametric methods were implemented that model and predict concentration from discharge. These methods create best-fit curves of arbitrary shape using statistical algorithms, and include (see Glossary):

- LOcally-wEighted Scatterplot Smoothing (Cleveland and Devlin, 1988) also known as a LOESS smoothing
- Alternating Conditional Expectations (ACE)
- Additivity and VAriance Stabilization for regression (AVAS)

Table 8.3-1. Load estimation methods used in simulations

Short name	Type	Time step	Description
rcload.turb	simple regression	30-min	$\log(C) \sim \log(T)$
rcload.turb2	simple regression	30-min	$C^{0.5} \sim T^{0.5}$
rcload	simple regression	30-min	$\log(C) \sim \log(Q)$
rcload.mdq	simple regression	daily	$\log(C) \sim \log(Q)$
rcload.mdq2	multiple regression	daily	$\log(C) \sim \log(Q) + \log(\text{MDQ}/\text{MDQ}_1)$
rcload.mdq3	multiple regression	daily	$\log(C) \sim \log(Q) + \log(\text{MDQ}_1)$
rcload.mdq4	multiple regression	daily	$\log(C) \sim \log(Q) + \log(\text{MDQ}/\text{MDQ}_1) + D$
rcload.mdq5	multiple regression	daily	$\log(C) \sim \log(Q) + D$
rcload.mdq6	simple regression	daily	$C^{0.5} \sim Q^{0.5}$
loess.g	nonparametric	daily	Loess with gaussian fitting
loess.s	nonparametric	daily	Loess with symmetric fitting
ace	nonparametric	daily	ACE transformations (see text)
avas	nonparametric	daily	AVAS transformations (see text)
areg.boot	nonparametric	daily	AVAS <i>areg.boot</i> implementation
pdmean	averaging	daily	Period-weighted sampling estimator
pdlinear	interpolating	daily	Daily interpolator
pdinstant	interpolating	30-min	“Continuous” interpolator
pdlocal2	interpolating	daily	Two-point rating curves + global curve
pdlocal2a	interpolating	daily	Two-point rating curves + interpolation
pdlocal4	interpolating	daily	Four-point rating curves + global curve
rcb1	best regression	daily	Selection by AIC without turbidity
rcb2	best regression	daily	Selection by GRMSE without turbidity
rcb3	best regression	daily	Selection by AIC, all $\log(C)$ models
rcb4	best regression	daily	Selection by GRMSE, all $\log(C)$ models



The averaging and interpolating methods that we implemented include

- The period-weighted sampling estimator (pdmean) was described in Section 6. In this method, each two successive concentrations are averaged, multiplied by the cumulative discharge between sampling times, and the resulting load increments summed over the water year. When multiple samples were collected on the same day, the discharge applied to each average concentration was derived by multiplying the MDQ by the fraction of the day between sampling times.
- The daily interpolator (pdlinear) is similar to pdmean, but concentration is interpolated at a daily time step. The load is computed as the sum of the products of daily mean discharge and daily concentration.
- The continuous interpolator (pdinstant) is like pdlinear but operates at the time-step of the original measurements. For our synthetic data sets, the time-step is 30 minutes.
- Two-point rating curves utilize 2-point discharge rating curves in place of linear interpolation to interpolate daily concentrations. The rating curve for the segment between each pair of samples was computed from the concentrations and discharges of just those two samples. Because these rating curves are often ill-conditioned, they are only utilized for segments in which the exponent lies within a specified positive range. For other segments, one of two methods was employed: (1) a global rating curve is utilized (pdlocal2), or (2) linear interpolation as in the pdlinear method (pdlocal2a).
- Four-point rating curves (pdlocal4) work very similarly to the two-point methods but the sample size is boosted from 2 to 4 by including the adjacent samples before and after the segment being estimated. For ill-conditioned segments a global rating curve was utilized; the linear interpolation method was not implemented for pdlocal4.

While the list of load estimation methods we have tested may seem extensive, it is by no means complete. There are many more models that have potential; limited resources prevented us from testing them all. Classes of models that deserve further exploration are:

- Power models. These models appear to be equivalent algebraically to logarithmic models but they are solved in original units without taking logarithms, using non-linear least squares. Computations can be carried out without eliminating zeroes from the data set and the solutions give less weight to the typically abundant small values that become highly dispersed when transformed by logarithms.
- Mixed turbidity/discharge models. Regression models employing both turbidity and discharge were useful in creating some of the synthetic data sets, and presumably could be useful in an operational mode.



- More functional forms for turbidity models. We only considered two forms of turbidity models: linear and square-root. Other forms, such as logarithmic, power, and loess models have proven very useful in estimating sediment loads at gaging stations where turbidity is measured continuously.

8.4 Evaluation of optimal handling of low SSC values

When the logarithm of concentration is computed for log-regression models, small values less than 1 become widely dispersed (Figure 8.4-1) even though the practical differences among them are insignificant. This is particularly a problem with suspended sediment, whose concentration is often very low or below detection limits. Regression variance is typically very high in the lower ranges of discharge or concentration, and the overall relationships may be non-linear. Because they are so numerous and widely spread in logarithmic space, measurements at low concentrations and discharges can exert a great deal of influence (i.e. leverage) on the regression line, causing underestimation or overestimation of concentrations at the upper end of the range. We evaluated two options for handling low SSC values below specified limits of 0.10, 0.25, 0.50, and 1.00 mg/L: (1) discarding and (2) setting to half the limit. For stations and years in which worked records existed and LTIMP data contained sample concentrations less than 1.0 mg/L, we compared regression estimates using method rcb2 based on the LTIMP samples to the loads that had been computed from the worked records. Estimates closer to that from the worked record are considered more accurate.

Discarding low values nearly always produced more accurate estimates than setting these values to half the detection limit. Setting the MDL to either 0.5 or 1.0 and discarding lower values was the best method in 11 of 15 tests, with MDL=1.0 winning in 6 of those cases. All the exceptions were years with very small sediment loads. Since the data set did not contain values between 0.5 and 1.0, discarding values less than 1.0 was equivalent to discarding values of 0.5 or less, and the latter is the method we settled upon for the simulations.

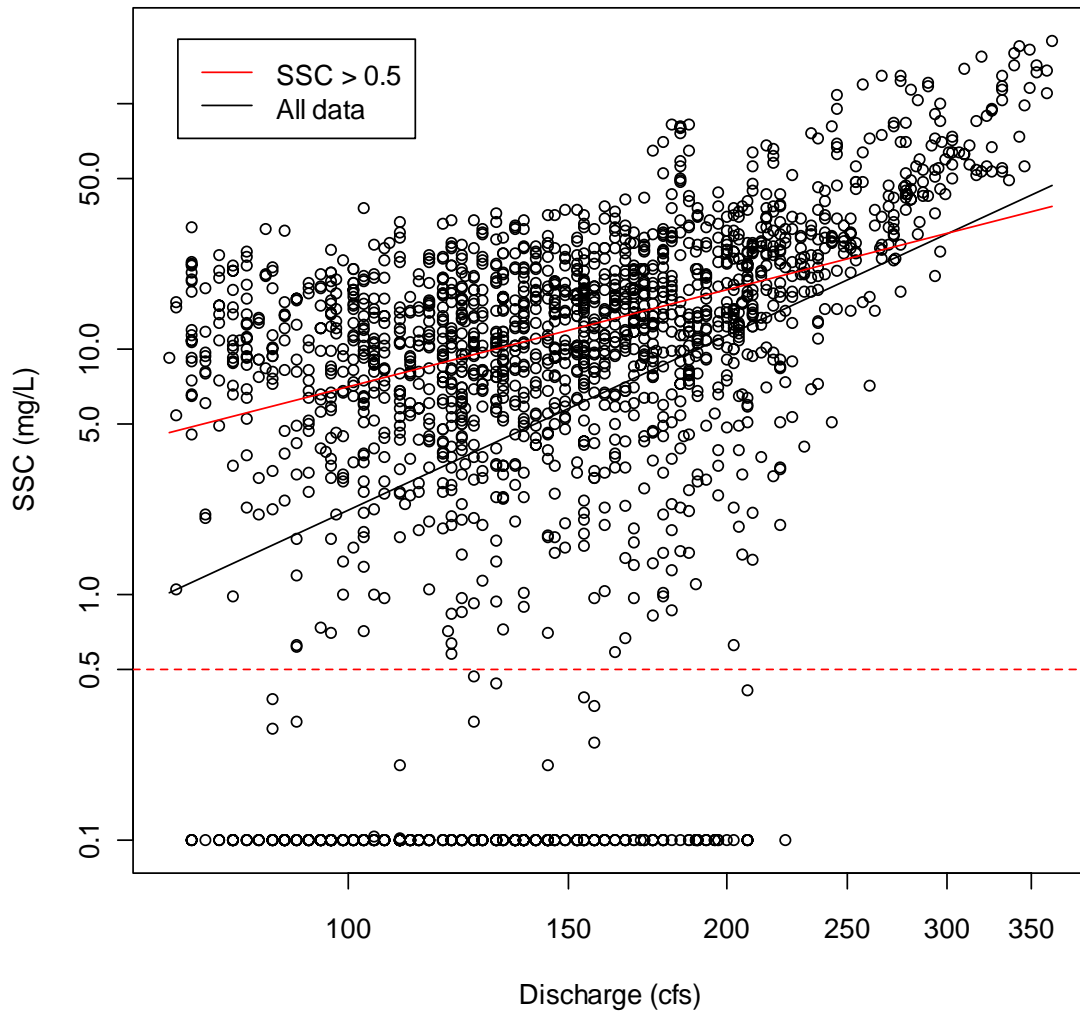


Figure 8.4-1. Synthetic data for WC-8 WY1999. Values less than 0.1 mg/L were set to 0.1 to allow computation of logarithms from samples. Relationships between SSC and discharge are shown for (1) data pairs with SSC > 0.5, and (2) all data.



Table 8.4-1. Sediment loads computed from worked records and estimated from LTIMP samples using regression method rcb2 with various rules for handling small values of SSC. Highlighted cells show the regression estimate closest to the worked record.

Site	Year	Worked Record	Sample Size	Discard values less than				Set to half if less than			
				1.00	0.50	0.25	0.10	1.00	0.50	0.25	0.10
GC-1	1982	57.98	114	78.42	76.62	83.76	82.49	93.36	92.71	85.46	81.58
GC-1	1983	12.05	107	13.90	13.07	13.39	13.61	14.69	14.57	13.78	13.61
GC-1	1984	7.37	100	7.08	6.93	6.85	6.87	7.17	7.17	7.05	6.90
GC-1	1985	2.34	85	2.64	2.52	2.51	2.51	2.58	2.58	2.51	2.51
GC-1	1986	27.81	128	27.81	24.82	25.28	25.55	28.73	28.16	26.68	26.07
GC-1	1987	0.88	70	1.34	1.05	1.05	1.04	1.13	1.11	1.07	1.06
WC-8	1982	269.97	129	307.81	298.13	321.14	321.14	347.55	335.39	321.14	321.14
WC-8	1983	55.84	110	59.07	59.20	59.60	60.32	61.42	60.91	60.91	60.32
WC-8	1985	4.15	102	4.13	3.98	4.01	4.04	4.24	4.22	4.09	4.04
WC-8	1986	57.85	136	53.64	53.69	48.65	49.29	54.87	52.67	49.55	49.29
WC-8	1987	2.23	92	5.82	5.16	4.53	4.52	4.68	4.68	4.56	4.52
BC-1	1982	285.23	115	494.11	541.15	651.12	651.12	774.50	766.17	705.01	680.79
BC-1	1983	81.81	111	94.54	99.11	101.54	101.54	104.43	103.79	101.54	101.54
BC-1	1984	39.06	124	48.30	48.45	48.70	48.70	49.13	49.13	48.70	48.70
BC-1	1985	11.56	94	12.62	12.50	12.64	12.88	13.40	13.29	13.03	12.88

8.5 Simulation results for daytime sampling

Figure 8.5-1 shows the 6 top-ranking methods by RMSE in the simulation of suspended sediment load estimation using the synthetic data for station WC-8 in WY 1999. At all sample sizes the best (most accurate) method is rload.turb2, the square root regression model for turbidity. The result is expected because that was the model used to generate the synthetic data set. The next best model selection methods with turbidity were rcb3 and rcb4; recall that these methods are restricted to searching models for log(C), which was not optimal for this population. Turbidity is not available for load estimation with historic data. The best method without turbidity was LOESS with gaussian fitting (loess.g), although it was tied with some other methods at sample sizes of 10, 60 and 80.

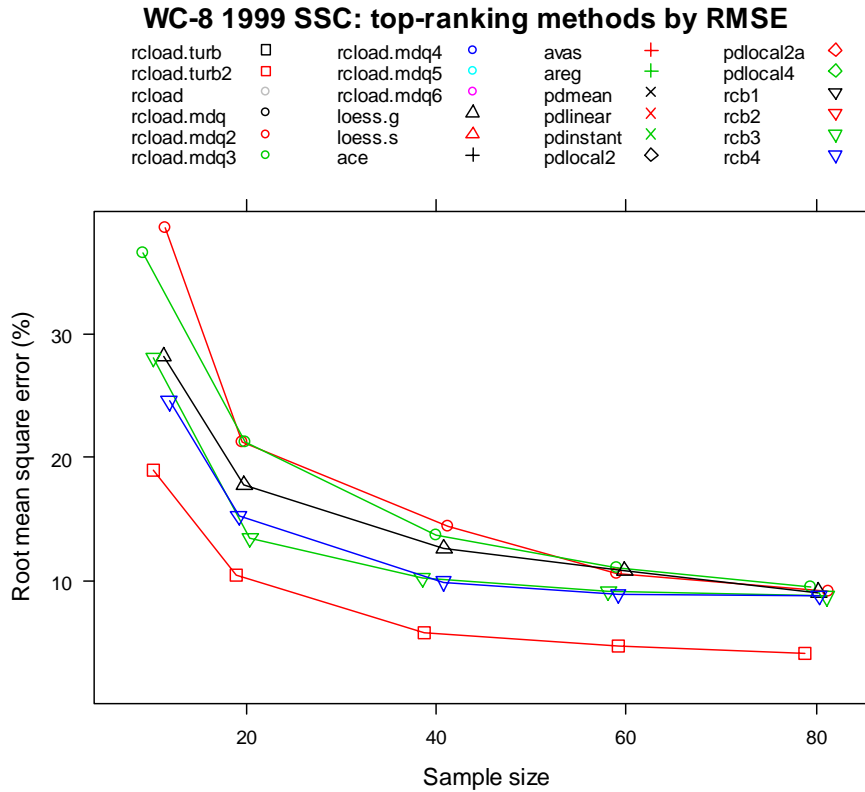


Figure 8.5-1. The 6 top-ranking methods by RMSE in the simulation of suspended sediment sampling from the synthetic data for station WC-8 in WY 1999.

Note that the simple rating curve (rload.mdq) was not among the top-ranking methods in this simulation. The most accurate method depends on both the population that is being sampled, sample size, and the selection criterion. See Tables 8.5-1 and 8.5-2. In these tables, TC-R1 refers to “Trout Creek Reach 1” (Conley, Pers. Comm., 2013) ; HWD refers to Homewood Creek, (Grismer, Pers. Comm., 2013).



Table 8.5-1. Best estimation method for suspended sediment according to either RMSE or MAPE from simulated sampling of synthetic data sets. Methods requiring turbidity are included. Last two rows show method with lowest mean rank for given sample size.

Station	year	Criterion	n=10	n=20	n=40	n=60	n=80
WC-8	1999	RMSE	rload.turb2	rload.turb2	rload.turb2	rload.turb2	rload.turb2
		MAPE	rload.turb2	rload.turb2	rload.turb2	rload.turb2	rload.turb2
TC-R1	2011	RMSE	pdlocal4	pdlocal4	rload.mdq6	rload.mdq6	rload.mdq6
		MAPE	pdlocal4	pdlocal2a	pdlocal2	rload.mdq6	rload.mdq6
HWD	2010	RMSE	rload.turb2	rload.turb2	rload.turb2	rload.turb2	rload.turb2
		MAPE	rload.turb2	rcb3	rload.turb2	rload.turb2	rload.turb2
TC-2	2011	RMSE	rload.mdq	rload.mdq	rload.mdq	rload.turb2	rload.mdq3
		MAPE	pdlocal2a	rload.turb2	rcb3	rload.mdq3	rload.mdq3
TC-2	2010	RMSE	rload.mdq	rload.turb	rload.mdq3	rload.mdq3	rload.mdq3
		MAPE	ace	rload.mdq3	rload.mdq3	rcb3	rload.mdq3
TH-1	2005	RMSE	rload.turb2	rload.turb2	rload.turb2	rload.turb2	rload.turb2
		MAPE	rload.turb2	rload.turb2	rload.turb2	rcb3/4	rcb3/4
Combined		RMSE	rcb4	rload.turb2	rload.turb2	rload.turb2	rload.turb2
		MAPE	rload.turb2	rload.turb2	rcb3	rload.turb2	rload.turb2



Table 8.5-2. Best estimation method for suspended sediment according to either RMSE or MAPE from simulated sampling of synthetic data sets. Methods requiring turbidity are omitted. Last two rows show method with lowest mean rank for given sample size.

Station	year	Criterion	n=10	n=20	n=40	n=60	n=80
WC-8	1999	RMSE	loess.g	loess.g	loess.g	rcload.mdq2	pdmean
		MAPE	rcb1	loess.g	loess.g	areg	pdlinear
TC-R1	2011	RMSE	pdlocal4	pdlocal4	rcload.mdq6	rcload.mdq6	rcload.mdq6
		MAPE	pdlocal4	pdlocal2a	pdlocal2	rcload.mdq6	rcload.mdq6
HWD	2010	RMSE	rcb2	rcb2	rcb2	rcb2	rcb2
		MAPE	rcb2	rcb2	rcload.mdq3	rcload.mdq2	rcload.mdq3
TC-2	2011	RMSE	rcload.mdq	rcload.mdq	rcload.mdq	rcload.mdq3	rcload.mdq3
		MAPE	pdlocal2a	pdlocal2a	rcload.mdq2	rcload.mdq3	rcload.mdq3
TC-2	2010	RMSE	rcload.mdq	rcload.mdq	rcload.mdq	rcload.mdq3	rcload.mdq3
		MAPE	ace	rcload.mdq3	rcload.mdq3	rcload.mdq3	rcload.mdq3
TH-1	2005	RMSE	pdlocal2a	pdmean	pdlocal2a	pdlocal4	loess.s
		MAPE	pdlocal4	pdlocal2a	pdlocal4	pdlocal4	pdlocal4
Combined		RMSE	pdlocal2a	rcload.mdq2	rcb2	rcload.mdq2	rcload.mdq2
		MAPE	rcload.mdq	pdlocal2a	rcload.mdq2	rcload.mdq2	rcload.mdq3

The turbidity models performed better and there was more consistency of results when turbidity was available, but the latter may be partly due to the fact that the number of methods simulated for turbidity was fewer. Figure 8.5-2 shows the 6 top-ranking methods for suspended sediment based on the mean RMSE across populations and sample sizes. We see that, as for WC-8, rload.turb2 and other turbidity methods excel, but when turbidity is excluded, the best method is rcb2, the best model selection method based on GRMSE. For suspended sediment, selection by MAPE produced similar rankings as by RMSE.

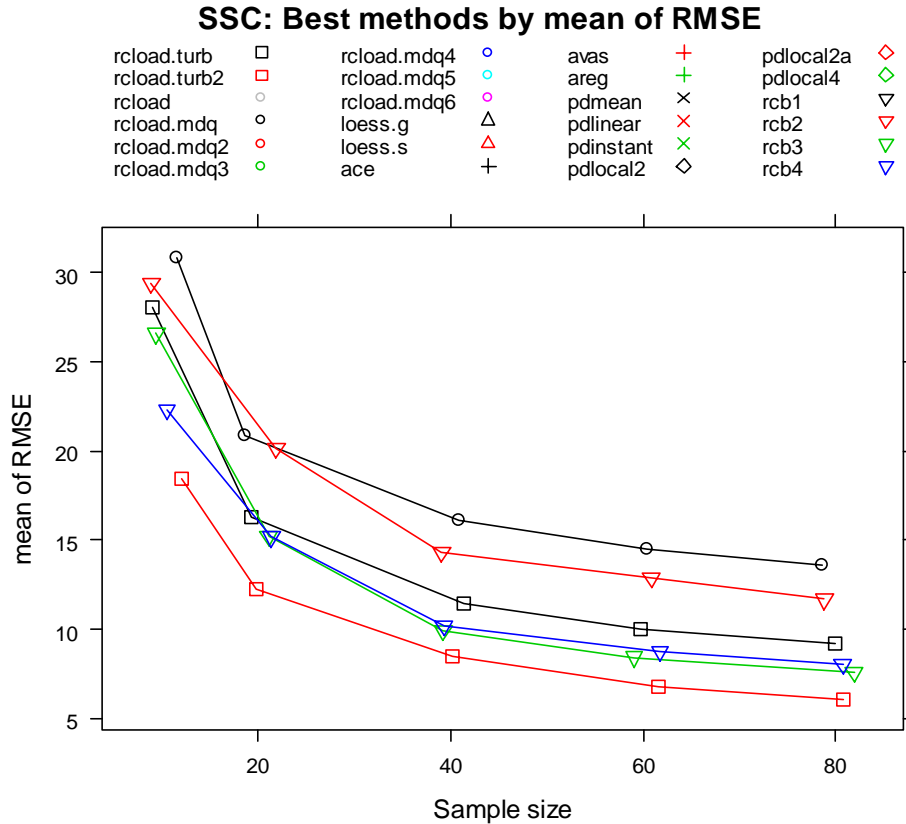


Figure 8.5-2. The 6 top-ranking methods by RMSE in the simulation of suspended sediment sampling from the synthetic data. Rankings are determined by the mean of RMSE (%), first across populations and then across sample sizes.

The dependency of methods on population, sample size, and selection criteria was general across all constituents. Appendix A-2 shows detailed results for all simulations. There is no method that is consistently more accurate than all the rest. The best approach to estimating sediment loads is to have a statistician look carefully at alternative models and make case-by-case decisions that consider goodness-of-fit and adherence to model assumptions. However, for estimating historic loads that will be impractical because we have 5 water quality constituents at 20 gaging stations over a 43 year period. In the future a case-by-case approach might be possible, but if estimation must be done by a technician without a strong background in statistics, we have selected a few methods based on the overall rankings by mean of RMSE and mean of MAPE (Table 8.5-3). We did not want to recommend a hodgepodge of methods with no logical pattern. Therefore, in a few cases based on other considerations, we selected a method that was nearly the best.



Table 8.5-3. Selected best estimation methods for all constituents with and without turbidity data.

<i>Constituent</i>	<i>With turbidity</i>	<i>Without turbidity</i>
SSC	reload.turb2	rcb2
FS	reload.turb2	rcb2
FSP	reload.turb2	rcb2
TP	rcb3	rcb2
TKN	pdmean	pdmean
NO3	pdmean	pdmean
SRP	pdmean	pdmean

For example, for estimating TP without turbidity, the best method in the overall rankings was usually reload.mdq3 or reload.mdq5, depending on sample size. However the best model varied by synthetic population and we have no assurance that our synthetic populations represent the full range of situations that might be encountered in the Tahoe Basin. Best regression model selection using GRMSE (rcb2) was the method we selected for SS and FS when turbidity was unavailable and the method should do reasonably well with unknown populations because of its flexibility. The method was also one of the three top-ranking methods for TP, so we are recommending rcb2 for TP as well as SSC and FS when turbidity is unavailable. When turbidity is available the best method for TP seems to be rcb3; it slightly outperformed reload.turb at larger sample sizes and, for unexplained reasons, it did considerably better than rcb4 at all sample sizes.

For fine sediment by mass, reload.turb2 was the overall best performing method. For fine sediment by particle count, the best method was a standard rating curve (reload.mdq). However, owing to the paucity of particle count data in the basin we had only one synthetic population of counts (TC-2 2010) and, while turbidity data were available, they were of very poor quality. Theoretically, the count data should be well-correlated to turbidity, and we have assumed for Table 8.5-3 that the most accurate methods for fine sediment mass will also be optimal for fine sediment particle counts.

For TKN, the turbidity methods were best for the Ward Creek and Homewood Creek synthetic data, but were inaccurate for Angora Creek. Averaging/interpolating methods pdmean and pdlocal2a performed well (and similarly to each other) in the overall rankings. In general, the period-weighted sampling method (pdmean, aka PWS) performed very competitively with all of its sister methods (pdlinear, pdinstant, pdlocal2, pdlocal2a, pdlocal4) in all the simulations. While it was not always the best, it was probably the most consistently accurate. Therefore,



pdmean was selected as the generally preferred method for estimating TKN load, with or without turbidity. In some specific cases, however, one of the turbidity methods is likely to be more accurate.

For both NO₃ and SRP, the worked record simulations indicated that pdmean, pdlinear, and pdlocal2a were the overall most accurate estimation methods. We recommend pdmean for its overall consistency.

The worked record simulations for SS and THP also favored the averaging and interpolating methods. Because the worked records were created using an interpolating process they tend to favor these methods. However, this process may not be the best representation of reality so we believe the results from sampling the synthetic data sets are a better indication of likely performance.

8.6 Recalculated annual loads and total annual Q

The selected methods (Table 8.5-3) were then used to recalculate annual loads for all stations, years, and constituents. Loads were only calculated when a minimum of 10 samples was available for analysis. For each station, year, and water quality parameter, we saved the following information, which is provided with this report in electronic form as “LTIMP loads.xls”.

- Annual yield (load per unit area) computed from all samples collected
- Watershed area
- Annual flow volume
- Annual peak daily flow
- Sample size
- Discharge weighted mean concentration
- In the case of best regression, the form of the best model
- Gilroy’s estimate of root mean squared error (GRMSE)
- Annual yield computed from daytime samples only (9am-6pm)
- Daytime sample size

9 Time-of-Sampling bias—methods and results

Because snowmelt occurs preferentially during the day, there is a diurnal periodicity to spring runoff in the Tahoe basin. Daytime sampling therefore systematically oversamples certain parts

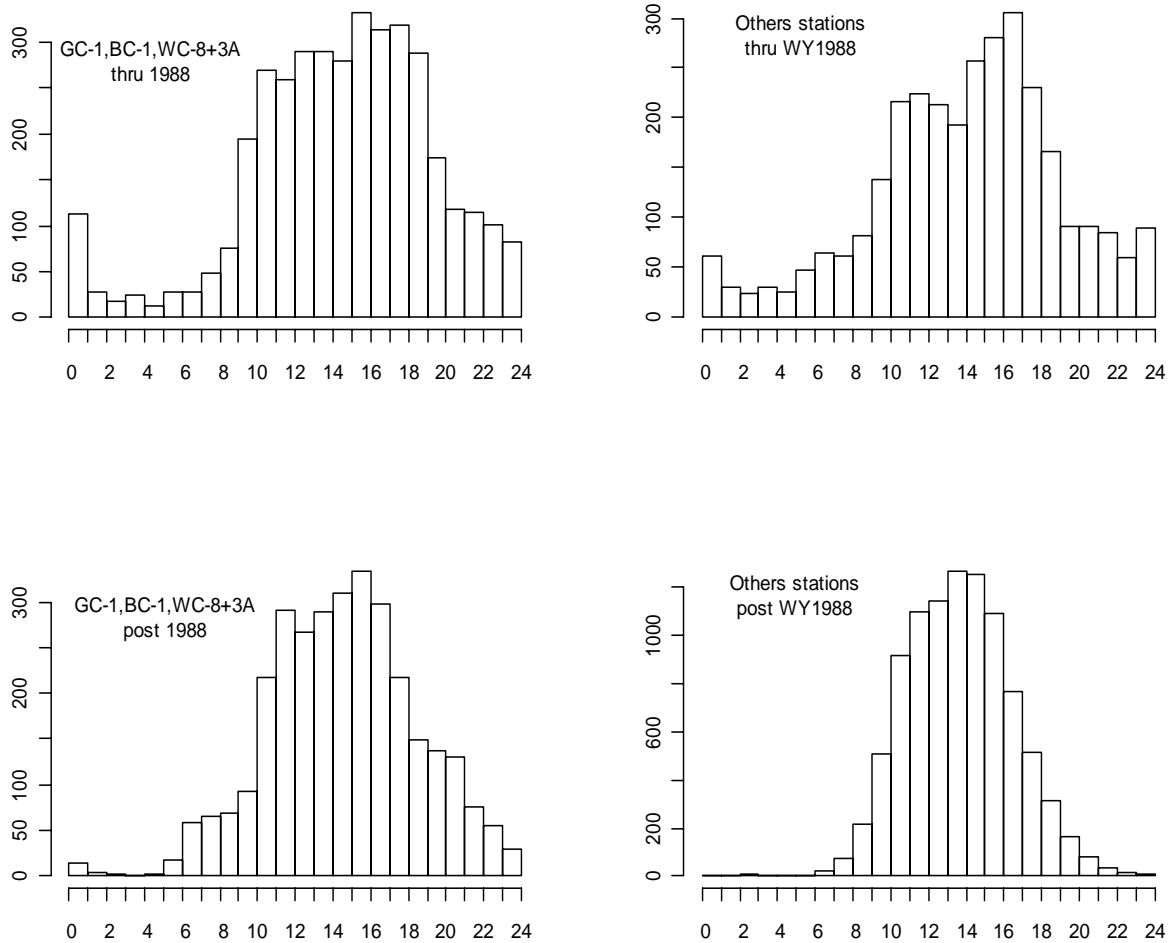


Figure 9-1. Histograms of the distribution of sampling times for the three west-side streams and other streams, for two time periods

of the hydrograph and neglects others, introducing a bias in estimating the loads of constituents whose concentration depends on flow. The phasing of diurnal hydrographs depends on factors such as the distribution of elevation and aspect in a basin, size of the basin, and time of year.

In 1988, the USGS cut back on nighttime sampling for safety reasons, but TERC continued with some nighttime sampling in Ward, Blackwood and General Creeks. Figure 9-1 shows the distributions of sampling times for west-side streams and all others, for the pre-1989 and subsequent time periods. The histograms show that there has been some reduction in nighttime sampling in Ward, Blackwood and General Creeks, but a severe reduction for the other streams. The problem of introduced bias due to the change in sampling regimes must be addressed.



Figure 9-2 shows the distribution of simulated SS load estimates based on a standard log-log sediment:discharge rating curve applied to mean daily discharge, and using the actual LTIMP sample size of n=28. The true synthetic load is shown in both plots as the red bar at 549 kg. The bias in the simulation for 24-hr sampling is -8.1% of the true load (RMSE=23.7%) and that for workday sampling is 11.8% (RMSE=26.5%). The hydrograph generally peaks between 6 and 7pm at Homewood Creek, so daytime sampling essentially restricts samples to the rising limb of the hydrograph when discharge is on a daily snowmelt cycle. Clockwise hysteresis is common in these sediment:discharge relationships (Stubblefield, 2007), explaining why daytime sampling would produce higher estimates than 24-hour sampling.

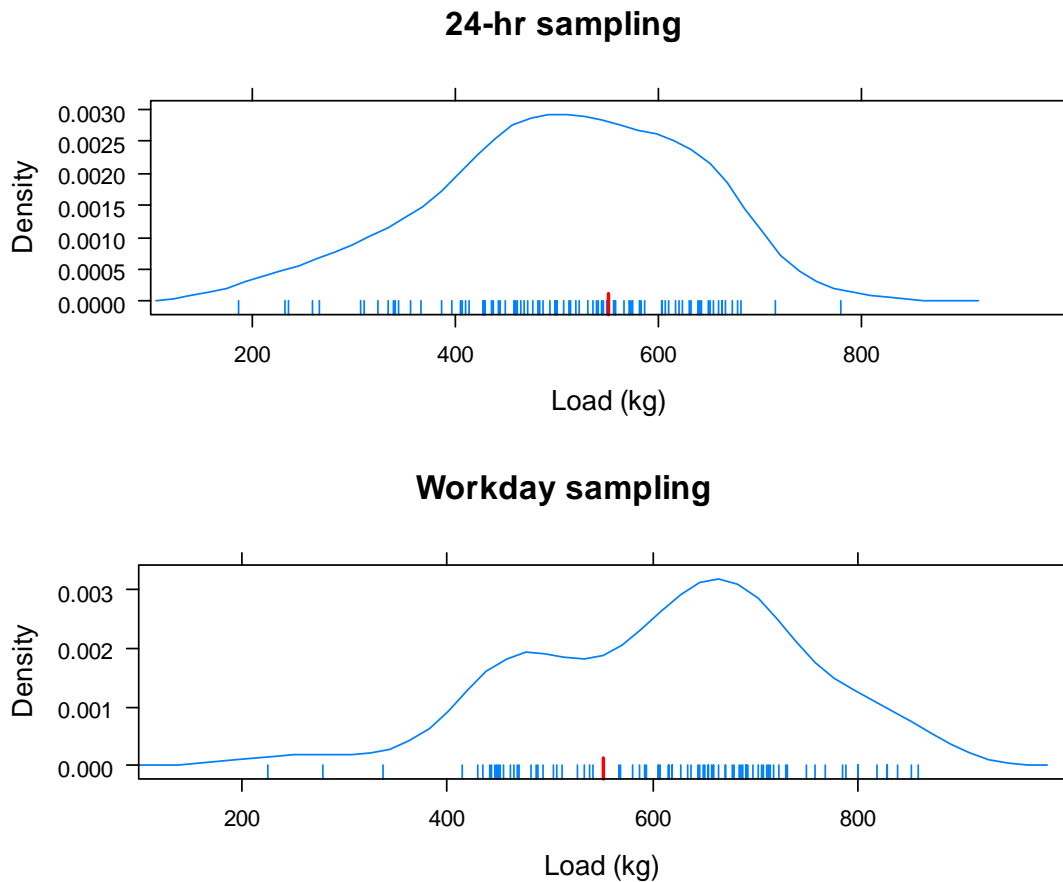


Figure 9-2. Results of 90 simulations at Homewood Creek WY2010 for sediment rating curve load estimates (n=28). Top: 24-hour sampling. Bottom: sampling is limited to a 9am to 6pm workday.

We investigated the time-of-sampling bias using 3 different approaches:

1. We simulated sampling from our synthetic data sets first on a 24-hour basis, and then on a workday (9am-6pm) basis. Since sampling continued in early evening (as late as 9:30),



the “workday sampling” assumption is conservative, and may slightly over-state the bias. Both sets of loads were compared with the known loads of these synthetic data sets to determine the bias of both sampling schedules.

2. We calculated historic LTIMP loads first using all samples, and then using only samples collected between 9am and 6pm. We then plotted the relative difference between the loads as a function of number of samples omitted.
3. We tried to induce trends at the west-side stations (GC-1, BC-1, and WC-8) by eliminating night samples from 1992-2012. These are the stations that have the most night-time samples. This approach was intended to reveal the potential importance of the time-of-sampling bias in relation to trend detection; the methods for this analysis are presented later, in Section 10.

9.1 Simulations

We ran simulations of our selected estimation methods for 24-hour sampling and workday (9am-6pm) sampling for sample sizes of 10 to 80 with SSC, TP, and TKN. The graphs (Figures 9.1-1 - 9.1-3) show the bias as a percentage of true load. The difference between the two curves is the time-of-sampling bias. Not surprisingly, sample size doesn't seem to have much influence on the results. The time of sampling bias is in the same direction for all constituents at a given station, but the direction varies by station. The only station with two synthetic populations (SSC for TC210 and TC211), has a negative time-of-sampling bias in both years but the magnitude differs. At Trout and Angora Creeks the time-of-sampling bias is negative for all constituents (but very small for SSC at TCR11). Hydrographs at all the Trout Creek stations peak after midnight; workday sampling is mostly on the recession limb with a little on the very early rising limb. Hydrograph timing at Angora Creek was very different than at Trout, with peaks in the late afternoon in March 2010 to early evening in May, so it is unexpected that daytime sampling would introduce a negative bias. Ward Creek, Homewood, and Third Creek peaked at 6-8pm and workday sampling is mostly of the rising limb. As expected, the bias was positive at Ward, Homewood, and Third Creeks (Figure 9.1-1). For TKN the time-of-sampling bias is very small for 2 of the 3 populations (Figure 9.1-3). For Homewood 2010, there is a large positive time-of-sampling bias for SSC, TP, and TKN. The time of sampling bias sometimes reduces the overall bias when its sign is opposite that of the bias of the 24-hour method; the prime example is SSC at Homewood 2010.

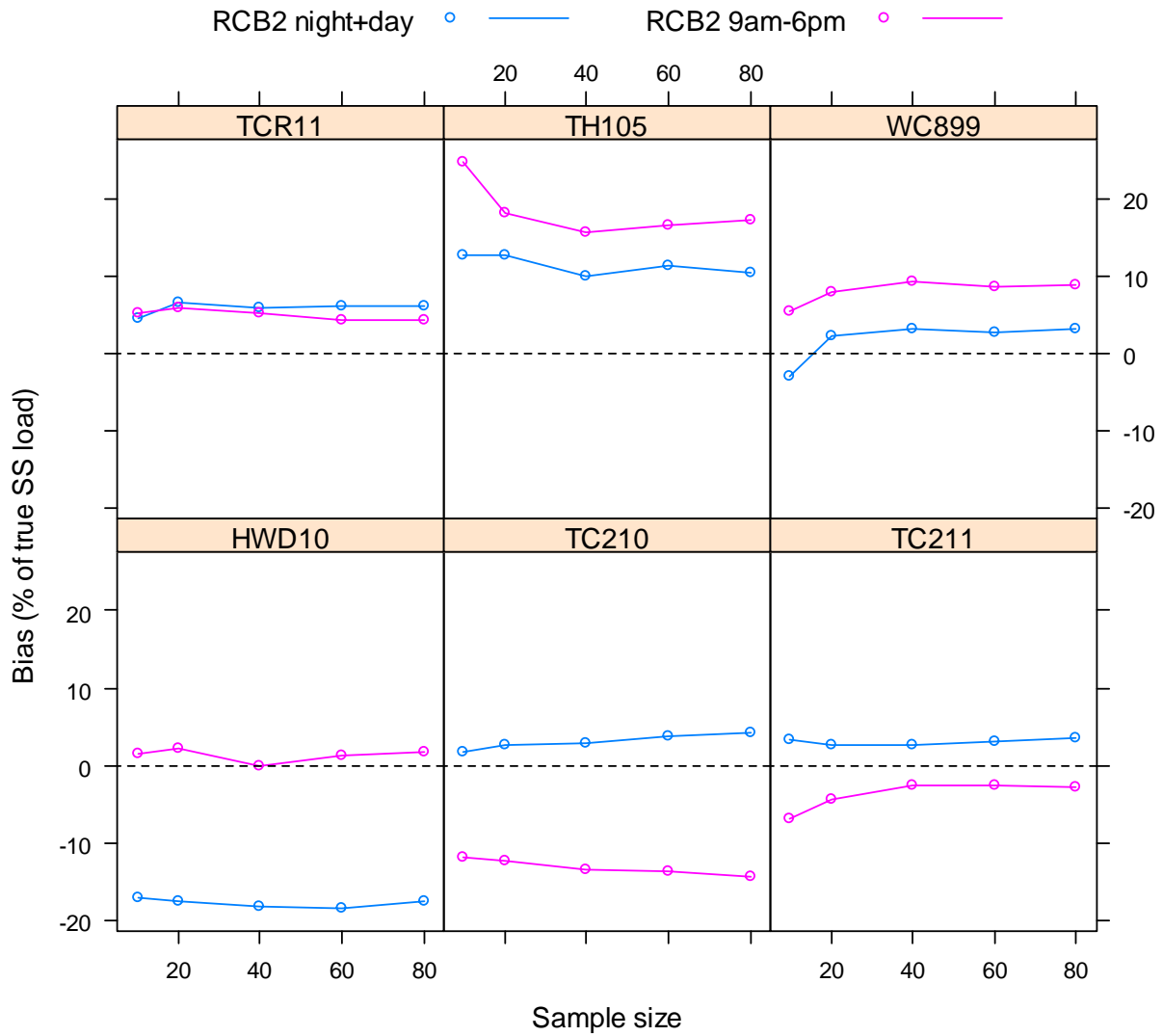


Figure 9.1-1. Bias of the estimation method rcb2 (see Table 8.3-1) for SS loads, with and without nighttime samples. TCR11 refers to Trout Creek Reach 1 (Conley, Pers. Comm. 2013), and HWD10 to Homewood Creek 2010 data (Grismer, Pers. Comm. 2013).

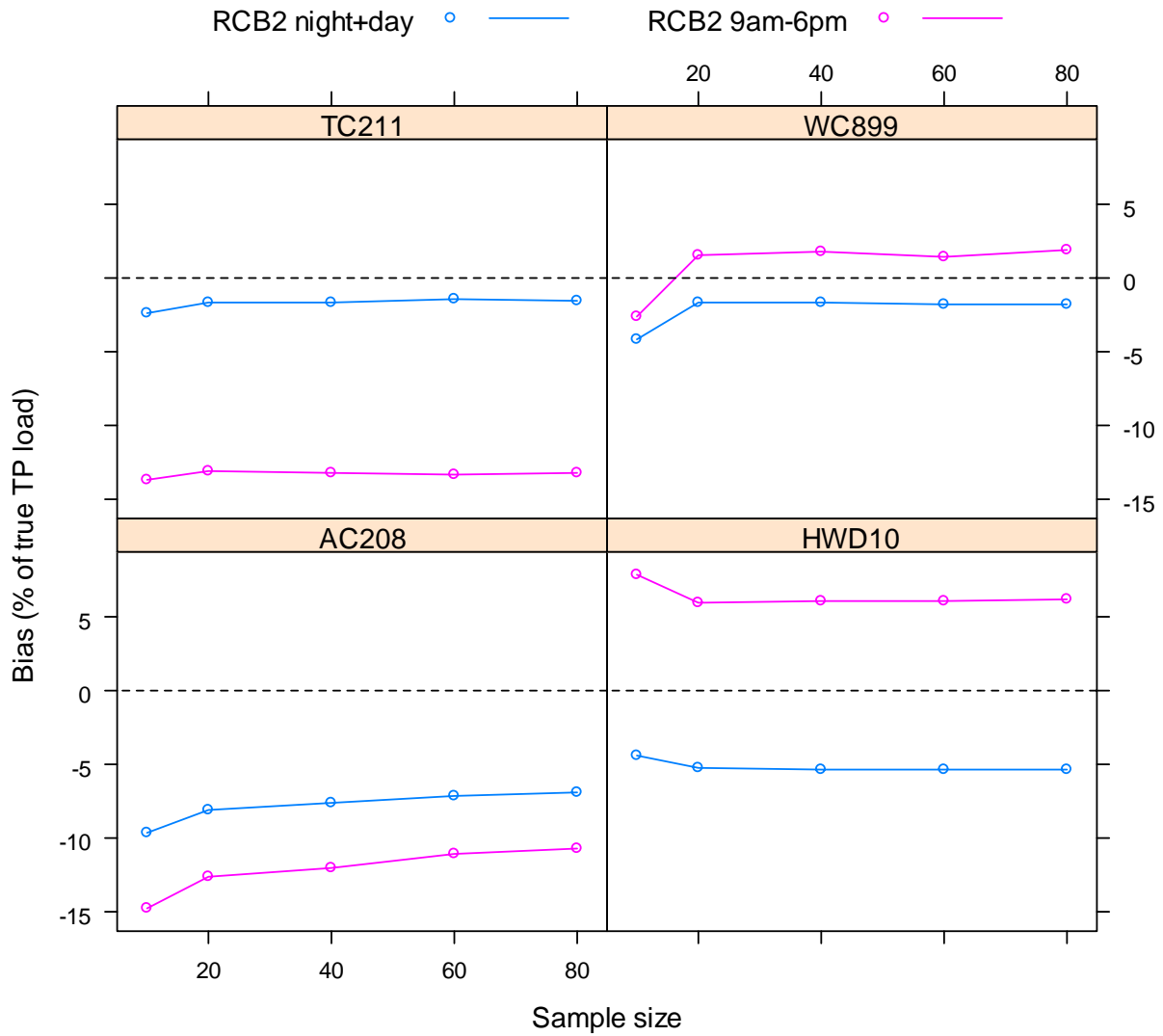


Figure 9.1-2. Bias of the estimation method rcb2 for TP loads, with and without nighttime samples

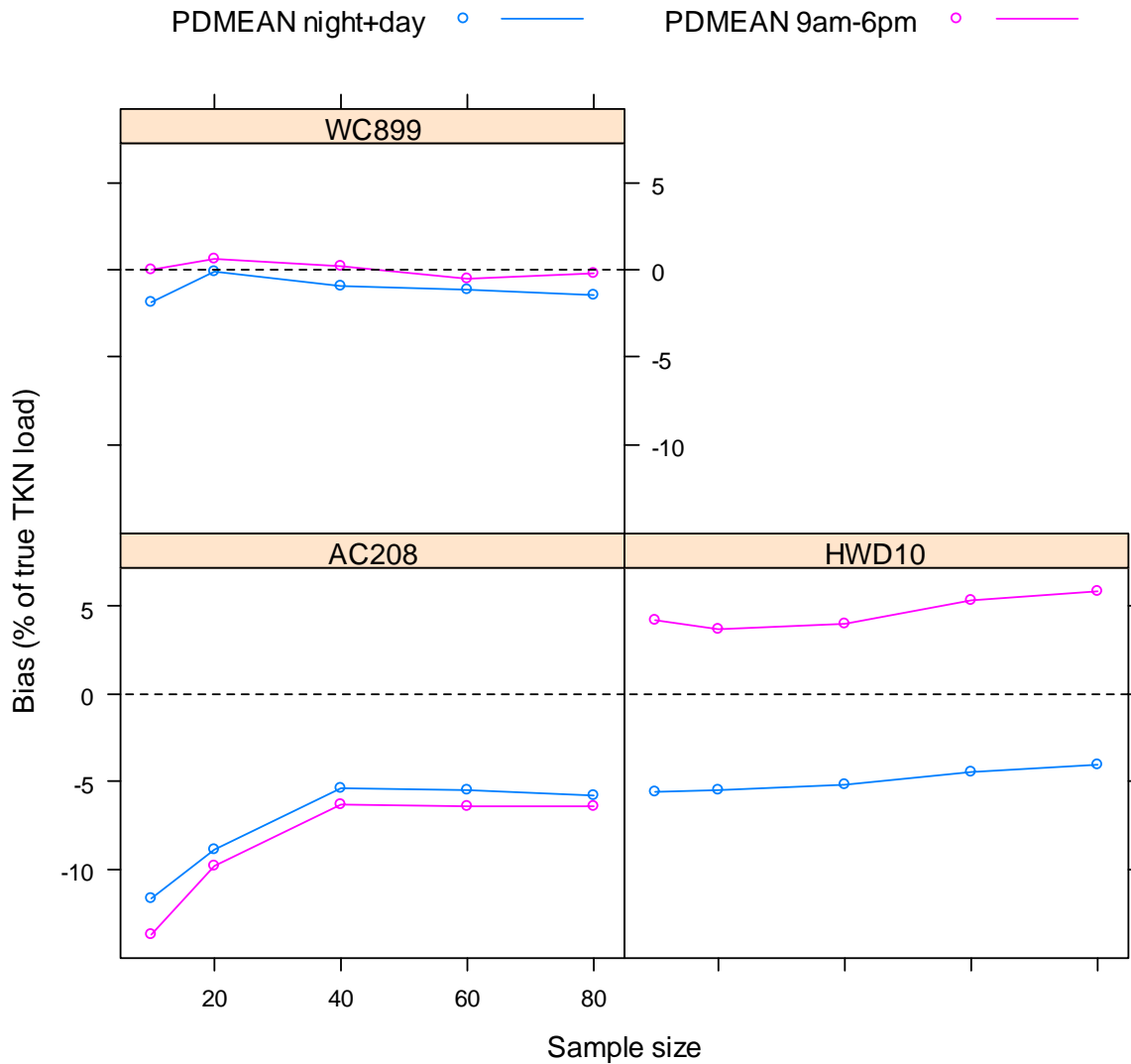


Figure 9.1-3. Bias of the estimation method pdmean for TKN loads, with and without nighttime samples

9.2 Historical load estimates

Loads were recomputed for NO₃, SRP, TKN, SSC, and TP using only samples collected between 9am and 6pm. Graphs in Appendix A-3 show the change in load as a function of the proportion of samples omitted. We screened results for stations and years where day-only sampling reduced the number of samples by 25% or more, and then averaged over years. The inter-annual variance is large and the number of cases is different for different watersheds. SSC and TP are the most affected. The bias is mostly negative, and generally not large for most



stations (Figure 9.2-1), but is probably underestimated because the baseline for comparison in each case is the actual LTIMP sample, which still under-represents nighttime conditions.

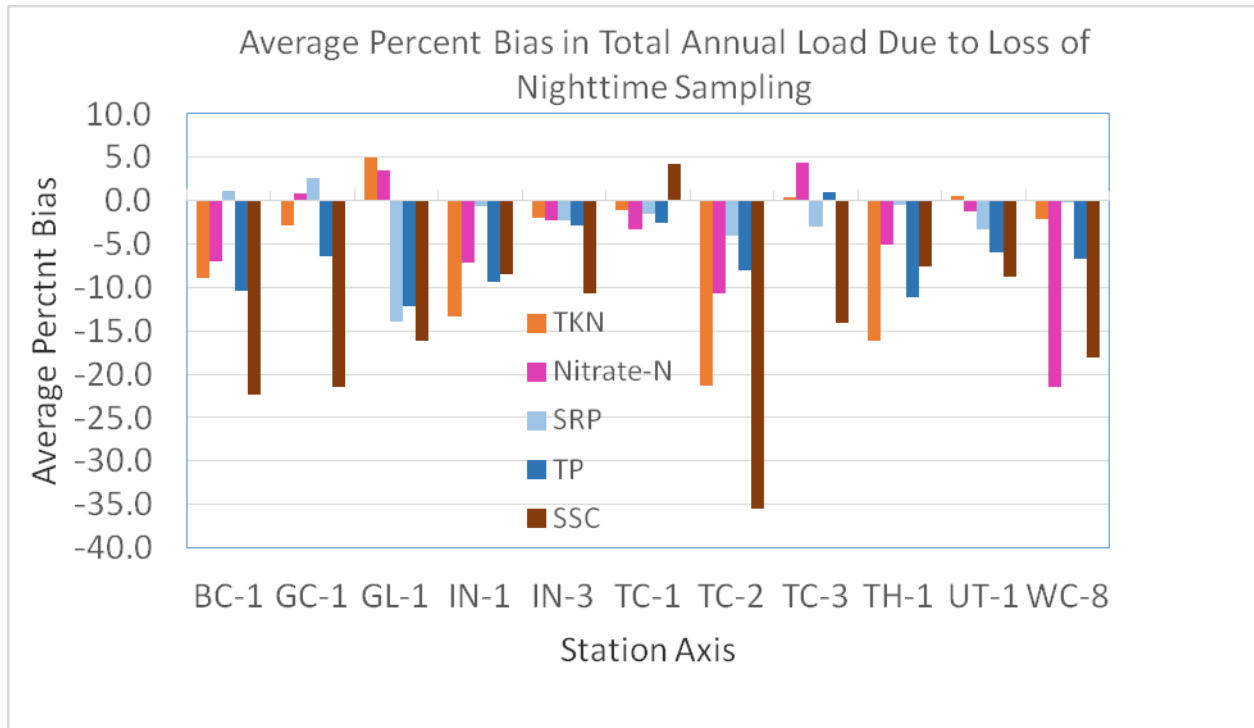


Figure 9.2-1. Average percent change in load from omitting nighttime samples, for those stations and years where this procedure reduced number of samples by 25% or more.

9.3 Induced trends from eliminating night-time samples

To test whether the time-of-sampling bias has the potential to introduce significant false trends in the data, we removed nighttime samples from the data at the west lake stations BC-1, GC-1, and WC-8 *only* for the years 1992-2012. These are stations that historically have been sampled regularly at night. We tested trends only for SSC, TKN, and SRP as trends had already been detected at NO3 and TP after eliminating *all* nighttime samples. We left significance levels for testing at 0.0025 (Bonferroni with n=20 because this was part of a 20-station experiment).

For SS, a decrease in slope is visible at all three stations and a significant trend was induced at WC-8 (Figure 9.3-1 and Table 9.3-1). For TKN, no trends or changes in trend were apparent (Table 9.3-1). For SRP, there were no consequential differences in results with and without night sampling; the SRP trend at GC-1 was highly significant in both cases (Table 9.3-1).

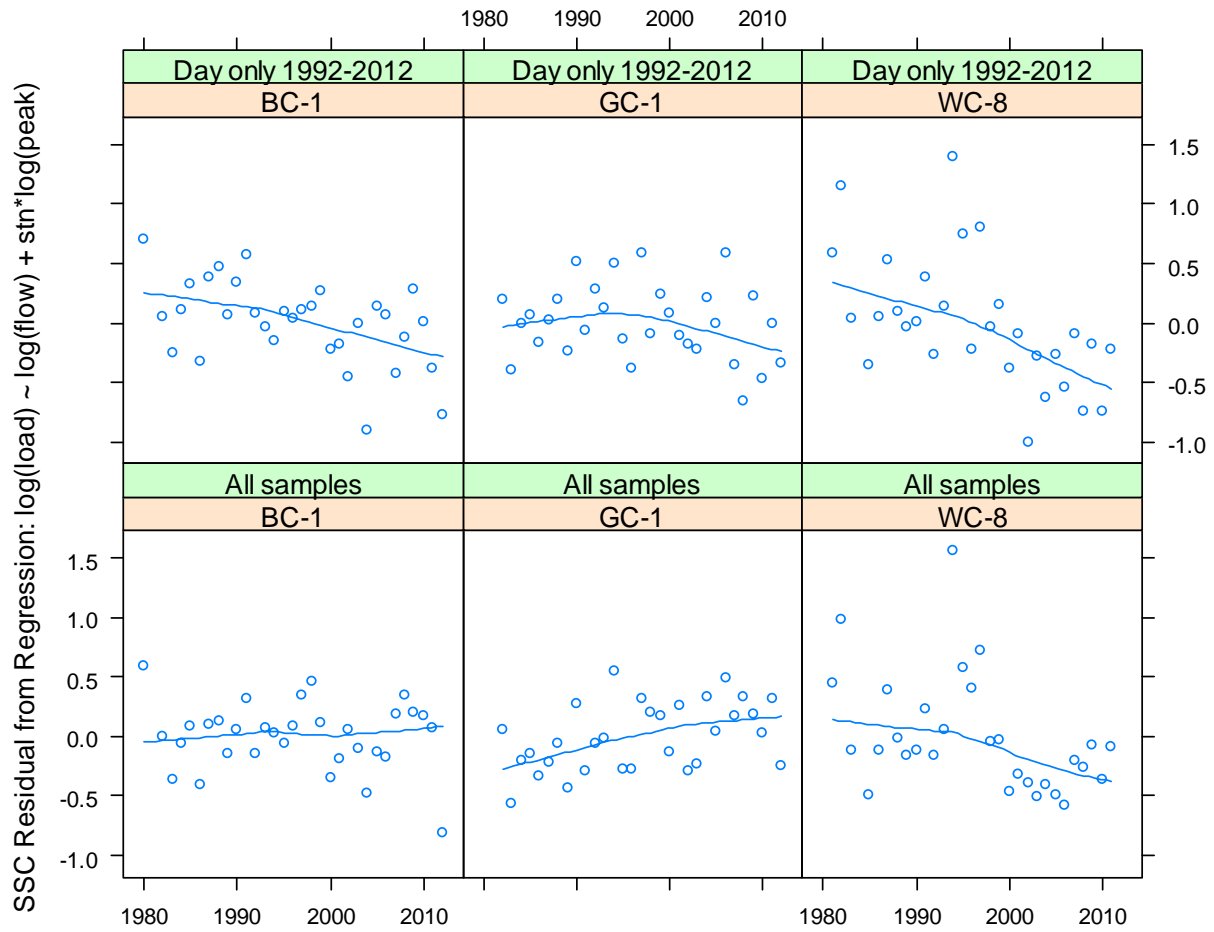


Figure 9.3-1. Trends in SS load with and without including night samples for the period 1992-2012.



Table 9.3-1. Tests of induced trend at west-side stations BC-1, GC-1, and WC-8 for selected constituents. Loads for the years 1992-2012 were computed two ways: (1) with daytime-only samples and (2) with all samples. Table shows the p-values, considered significant (*) when $p < 0.0025$.

Constituent	Night samples included	BC-1	GC-1	WC-8
SS	No	0.0135	0.3799	0.0007*
SS	Yes	1.0000	0.0199	0.0143
TKN	No	0.6410	0.9804	0.6013
TKN	Yes	0.4461	0.9024	0.5653
SRP	No	0.0176	0.0001*	0.0911
SRP	Yes	0.0233	0.0001*	0.0401

In future sampling of basin streams it will be important to eliminate the time-of-sampling bias. Short of sending crews out at night to sample flooding streams in the dark, there are two ways to get unbiased data for the flow-driven constituents (TP, SSC and FS): 1) with pumped samplers and collection of samples around-the-clock; and 2) simultaneous turbidity measurement and sample collection, with extension of the concentration records by regression to cover unsampled time periods. For the dissolved constituents, turbidity measurement will not help, and some sampling at night will be necessary.

10 Bias in standard sediment rating curves and optimal methods

The simulations permit a comparison of the bias of the standard rating curve method (rload.mdq) and the methods we have selected as "optimal". For TKN, TP, and SS, the data come from simulations of the synthetic populations that we developed. These are simulations of daytime sampling (9am-6pm). The "Best Model" by GRMSE (rcb2) method excludes models that require turbidity. For SRP, NO₃, and THP, the data come from the worked record simulations, again without the benefit of turbidity. Both rload.mdq and rcb2 employ Duan's smearing correction for retransformation bias. In all but one simulation, the mean rating curve estimates are greater than or similar to those of our selected method (Appendix A-4.1). The only



exception encountered was the simulation for TKN at AC-2 in WY 2008 (Figure 10-1). For most populations and sites we looked at, the selected optimal method is less biased than the standard rating curve, sometimes dramatically so. But there are exceptions wherein our method is more biased: 2 out of 4 for TP, 2 out of 6 for SS. This happens when the selected method is negatively biased. Three of the four cases were at one station (TC-2).

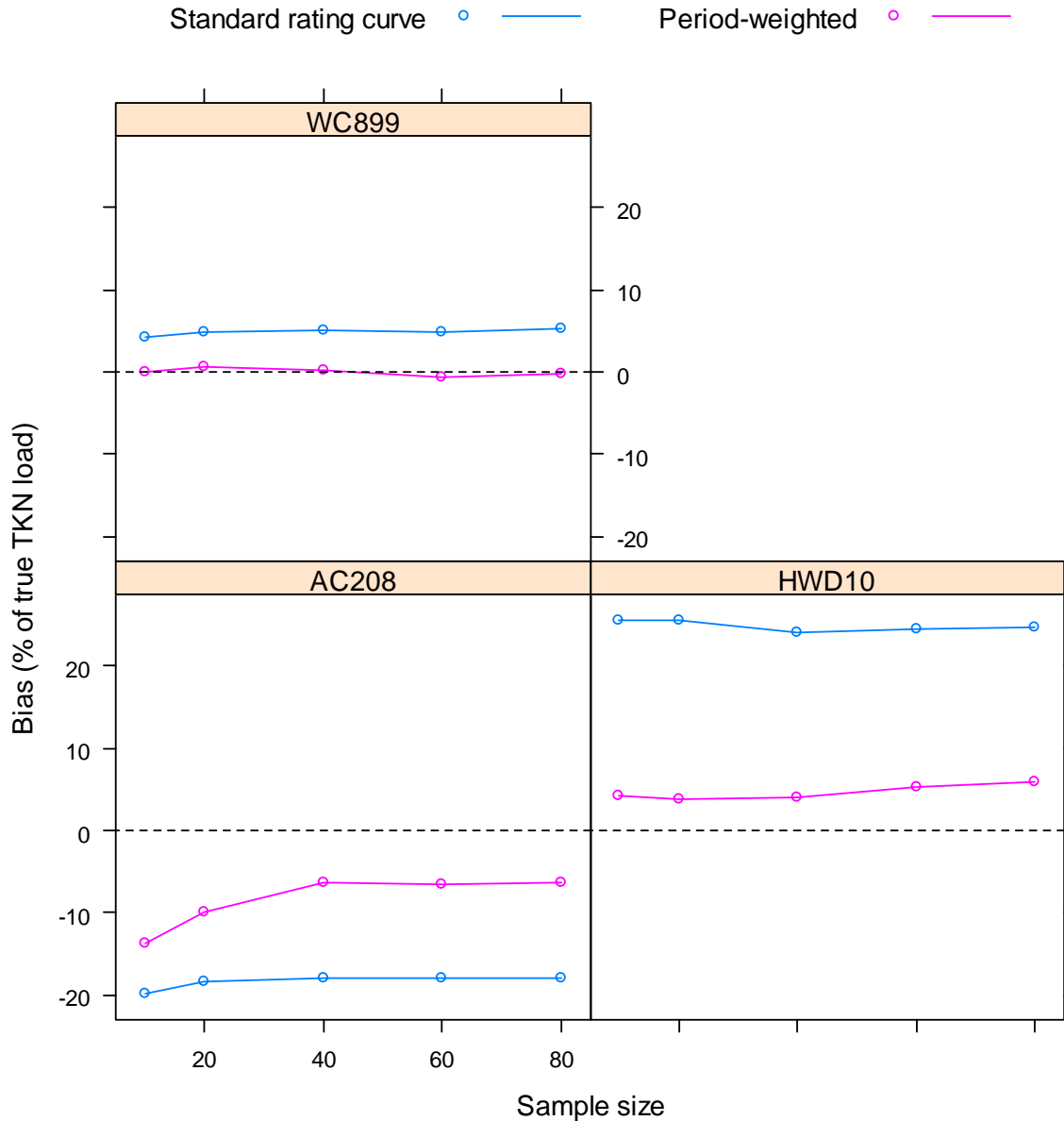


Figure 10-1. Bias in TKN load estimates for standard rating curve and period-weighted estimates, from simulations (24-hr sampling). HWD refers to Homewood Creek data, for 2010



We also looked at the differences between historic loads computed by standard rating curves and the selected methods. Loads for this analysis were computed from all LTIMP samples, not just daytime samples. Again, we find that rating curves give generally higher estimates than our selected methods (e.g. Figure 10-2 and Appendix A-4.2). For all constituents and most locations, differences are overwhelmingly positive. The only example with mostly negative differences is SRP at UT-5.

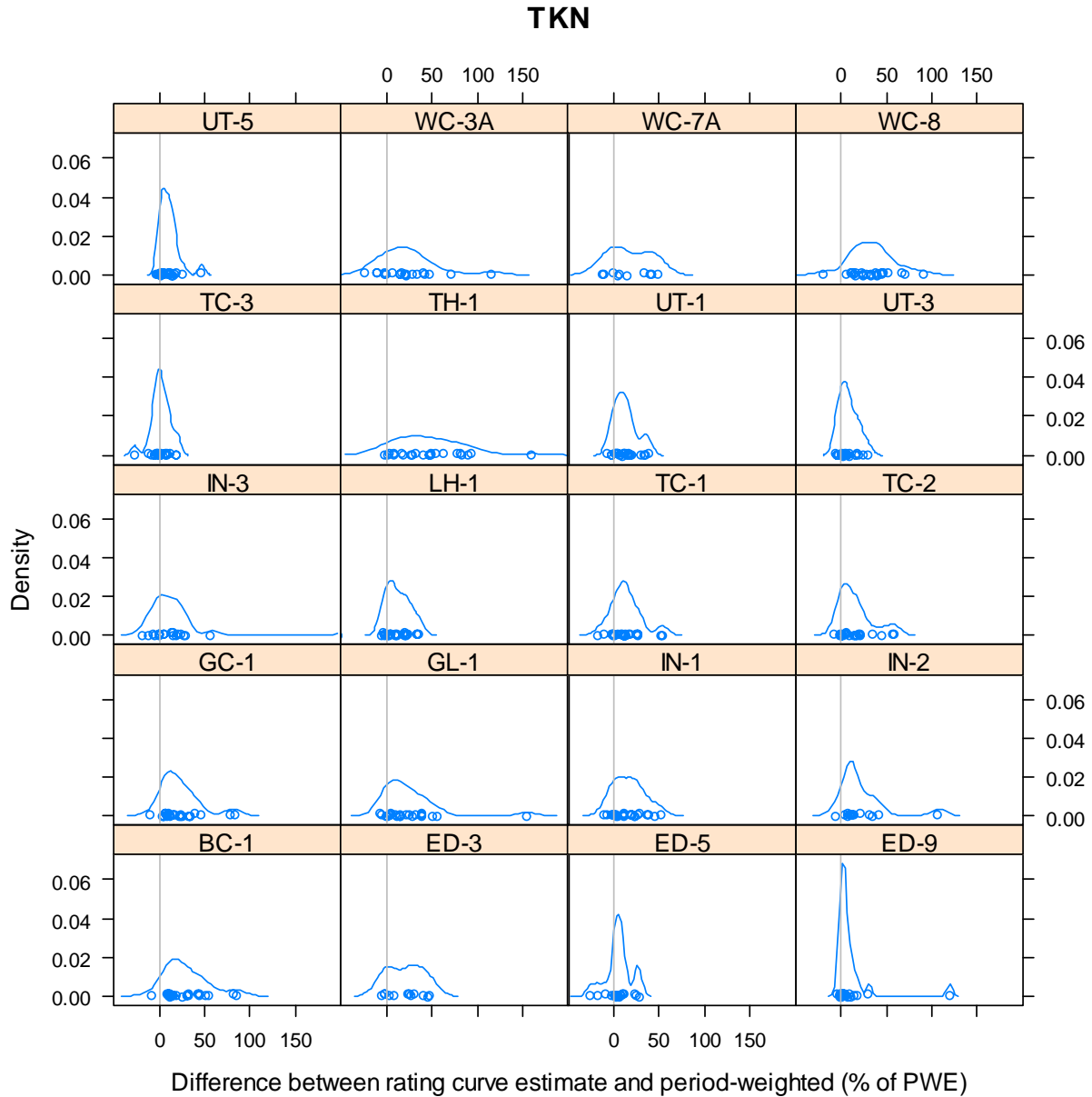


Figure 10-2. Difference between standard rating curve and period-weighted estimates of historic loads for TKN.



It is instructive to compare the sampling requirements for load calculations by the standard rating curve method and the methods developed in this study. Table 10-1 shows the comparison. For particulate constituents (SSC and TP), there are modest gains in efficiency (expressed as a reduction in the number of required samples. For the dissolved constituents, the gains are large. For nitrate-N, for example, using the period-weighted sample method instead of the simple rating curve method reduces the required sample number (at the 90/20) level from 74 to 19 samples.

Table 10-1. Number of samples required to achieve a given level of confidence in load estimates by the standard rating curve method compared with new recommended methods.

		Confidence Level, Pct	80				90				95			
		Error band, as Pct Est. Load	50	30	20	10	50	30	20	10	50	30	20	10
Constituent	Estimation Method	Required Number of Samples per year												
SS	Simple rating curve	<8	18	50	>100	9	32	85	>100	15	41	>100	>100	
Nitrate-N	Simple rating curve	<8	16	57	>100	11	45	74	>100	18	59	>100	>100	
TKN	Simple rating curve	<8	14	>100	>100	11	29	>100	>100	<8	36	>100	>100	
SRP	Simple rating curve	<8	<8	13	69	<8	15	52	91	<8	22	72	86	
Total P	Simple rating curve	<8	<8	26	>100	<8	14	38	>100	<8	20	53	>100	
SS	Best model by GRMSE	<8	15	36	>100	<8	27	67	>100	13	36	87	>100	
Nitrate-N	Period-weighted	<8	<8	14	33	<8	11	19	43	<8	16	29	51	
TKN	Period-weighted	<8	<8	15	60	<8	9	19	75	<8	12	28	85	
SRP	Period-weighted	<8	<8	<8	31	<8	8	17	43	<8	15	21	53	
Total P	Best model by GRMSE	<8	<8	16	>100	<8	10	25	>100	<8	13	34	>100	

11 Time trend analysis on Total Load residuals; Hypotheses to explain observed trends

To evaluate historic trends, we developed regression models for constituent loads to explain natural variability from variations in weather characterized by annual maximum daily flow (*max*) and annual runoff volume (*flow*). Multiple regression models were formulated to include all gaging stations. Location was treated as a categorical variable. Interactions between location and annual peaks and flows were included in these models, when significant, to permit variation in coefficients between watersheds. The model with all potential terms is represented as follows:

$$\log(\text{load}) = b_{0j} \text{stn}_j + b_1 \log(\text{flow}) + b_2 \log(\text{max}) + b_{3j} \text{stn}_j * \log(\text{flow}) + b_{4j} \text{stn}_j * \log(\text{max})$$

In the best model for each constituent one or more of these terms are zero (Table 11-1). The residuals from each of these models were tested by station for monotonic trend using the “adjusted variable” Mann-Kendall test (Alley, 1988) recommended by Helsel and Hirsch (2002). Alley's test is basically a Mann-Kendall test on the partial regression plot of log(load) versus



water year. In the partial regression plot, $\log(\text{load})$ and water year are both regressed on the same set of predictors (i.e. those in Table 11-1) and the two sets of residuals are plotted against one another and tested for monotonic trend using the usual Mann-Kendall test. Since there were 20 stations and 20 trend tests, the family-wise Type I error rate was kept to 0.05 using the Bonferroni correction, i.e. the critical p-value was set to $\alpha=0.05/20=0.0025$ for each test.

Table 11-1. Models for constituent loads to account for hydrologic variability

	Model	R ²	
		all	day
SS	$\log(\text{load}) = b_{0j} \text{stn}_j + b_1 \log(\text{flow}) + b_2 \log(\text{max}) + b_{4j} \text{stn}_j * \log(\text{max})$.894	.897
TP	$\log(\text{load}) = b_{0j} \text{stn}_j + b_1 \log(\text{flow}) + b_2 \log(\text{max}) + b_{3j} \text{stn}_j * \log(\text{flow})$.921	.928
TKN	$\log(\text{load}) = b_{0j} \text{stn}_j + b_1 \log(\text{flow}) + b_2 \log(\text{max})$.882	.882
NO3	$\log(\text{load}) = b_{0j} \text{stn}_j + b_1 \log(\text{flow}) + b_2 \log(\text{max}) + b_{3j} \text{stn}_j * \log(\text{flow})$.861	.861
SRP	$\log(\text{load}) = b_{0j} \text{stn}_j + b_1 \log(\text{flow}) + b_2 \log(\text{max}) + b_{3j} \text{stn}_j * \log(\text{flow})$.952	.954

11.1 Trend results

If runoff is changing as a result of climate change, there are probably corresponding changes in loading that these analyses would not detect. However, using the same methods as for loads, we found no systematic trends in maximum flow or flow volume. Hence, the partial regression plots (Appendix A-5) look very similar to more familiar plots (Figures 11.1-1 to 11.1-5) of residuals against water year.



Loads computed from daytime samples only

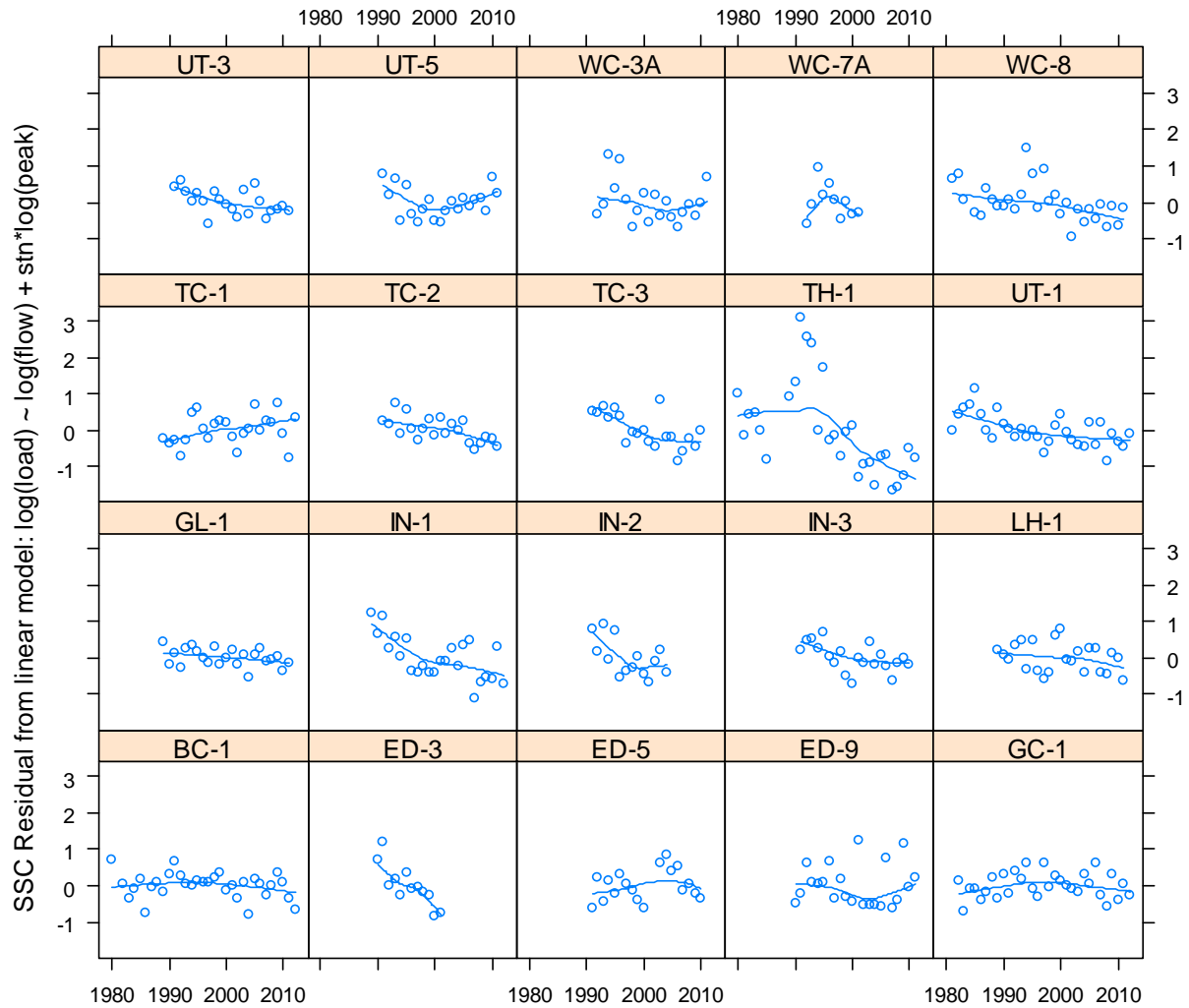


Figure 11.1-1. Trends in SSC after accounting for inter-annual variation in total and maximum daily runoff.



Loads computed from daytime samples only

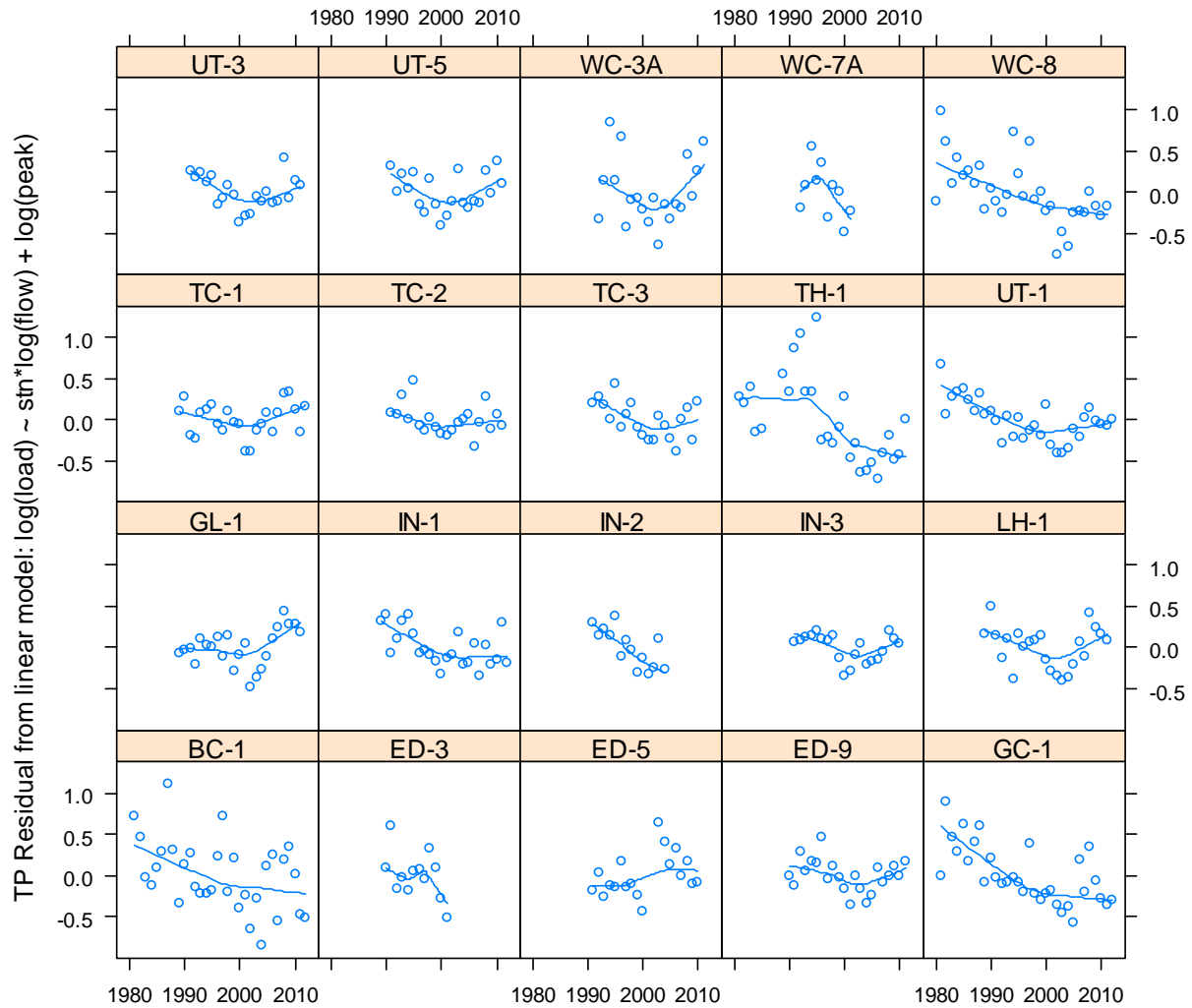


Figure 11.1-2. Trends in TP after accounting for inter-annual variation in total and maximum daily runoff.



Loads computed from daytime samples only

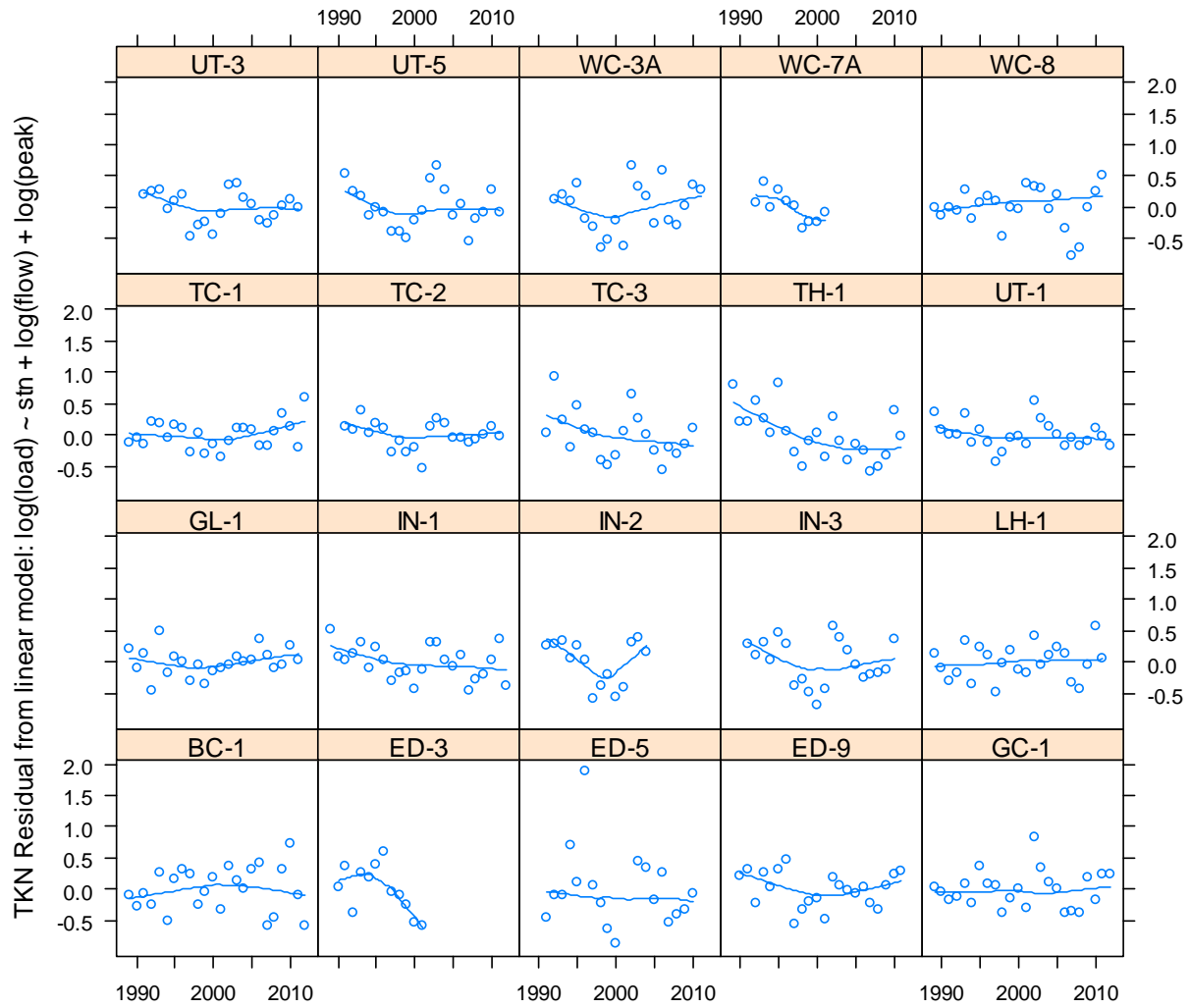


Figure 11.1-3. Trends in TKN after accounting for inter-annual variation in total and maximum daily runoff.



Loads computed from daytime samples only

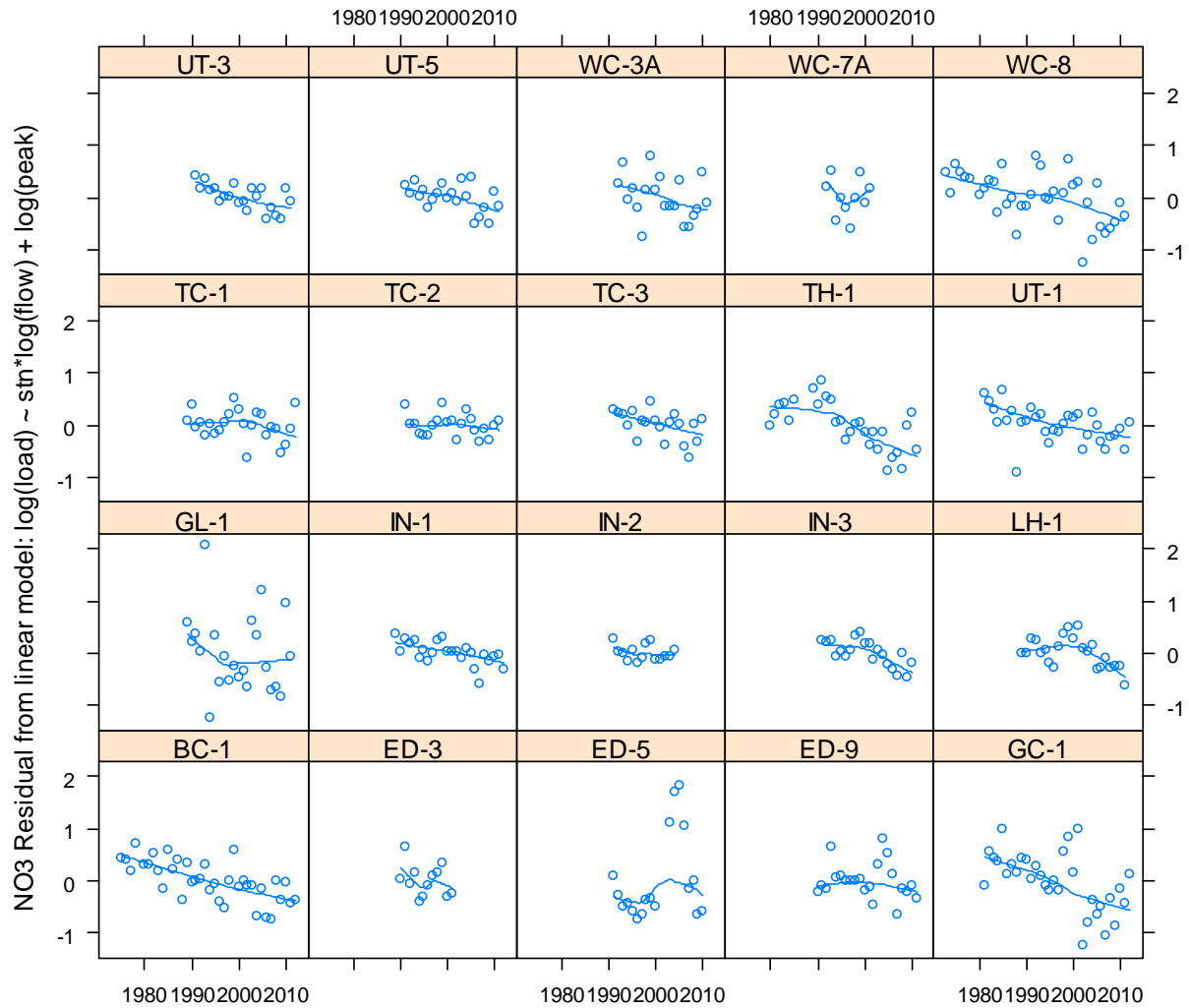


Figure 11.1-4. Trends in NO3 after accounting for inter-annual variation in total and maximum daily runoff.



Loads computed from daytime samples only

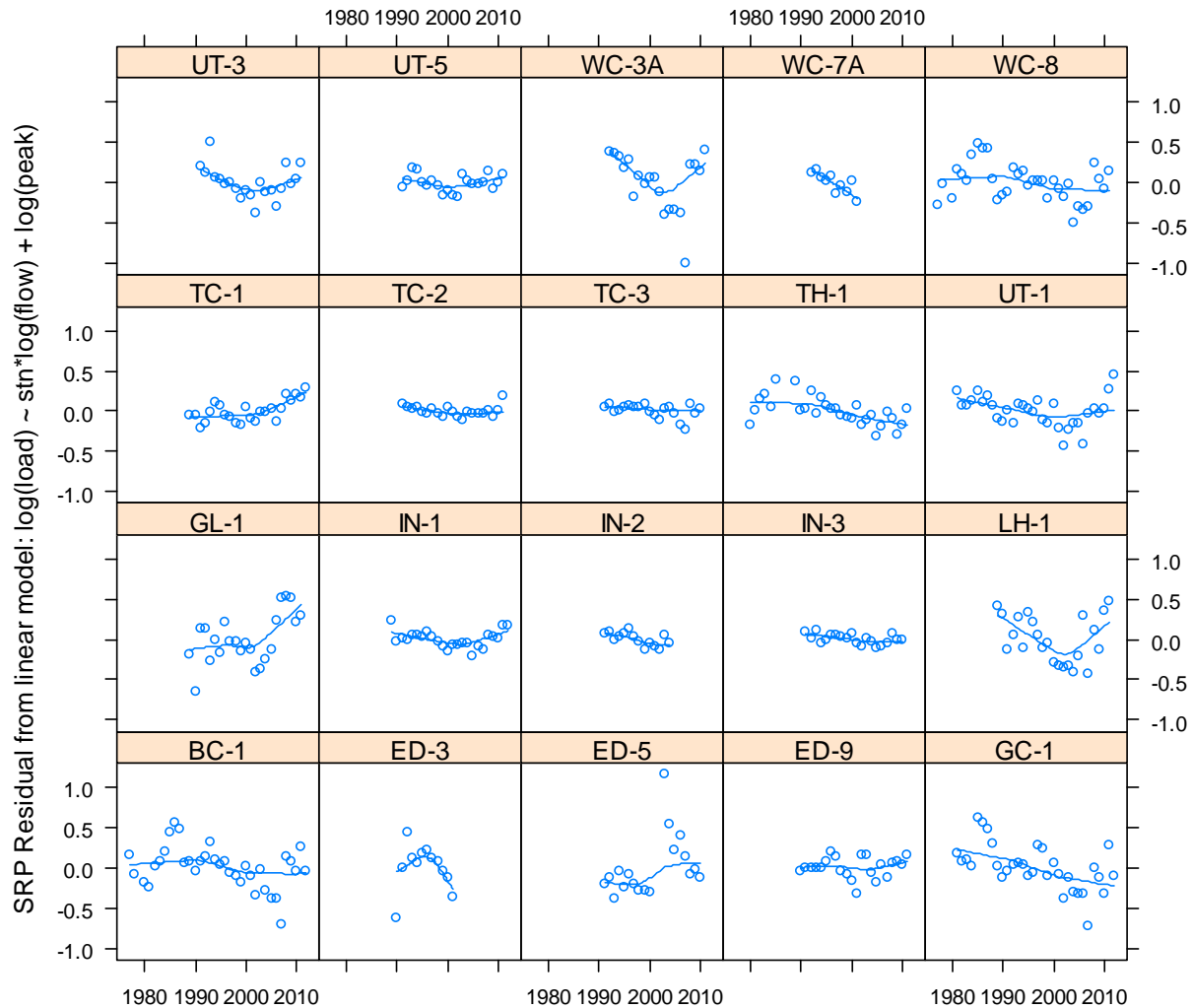


Figure 11.1-5. Trends in SRP after accounting for inter-annual variation in total and maximum daily runoff.

We have included the trend plots for loads based only on daytime samples. Tables in Appendix A-5 show p-values for loads based on all samples as well as those based on daytime samples. The significant trends for loads based on daytime samples were as follows (see Table 1-1 for full station names):

- **SS:** ED-3, IN-1, TH-1, UT-1
- **TP:** GC-1, IN-2, TH-1, UT-1, WC-8
- **TKN:** ED-3



- **NO₃-N**: BC-1, GC-1, IN-1, IN-3, TH-1, UT-1, WC-8
- **SRP**: GC-1, TC-1, TH-1

All significant trends are downwards, with the exception of SRP at TC-1. The significant trends at IN-2 and ED-3 are for short periods of record. Those sites have not been sampled since 2006 and 2001, respectively.

Apparent trends in Third Creek (TH-1) could be due to a restoration project. In summer of 2004, the confluence of Rose Creek with Third Creek was relocated from just below Highway 28 to its historic location just north of Lakeshore Blvd. (Susfalk et al., 2010). With the re-diversion, the flow of Rosewood Creek now bypasses the gage and LTIMP sampling site. According to Susfalk (2010), however, the runoff of Rosewood Creek is only about 10 percent of the runoff of Third Creek, and most of its sediment load originates during snowmelt in the upper part of the watershed. A plot of annual runoff at TH-1 vs. annual precipitation at Tahoe City showed no change in the relationship after the rediversion. Nevertheless, we tested for time trends in residuals at TH-1 for the period 1981-2004 (day-only samples), and found significant downward trends for SSC, TP, TKN, NO₃-N and SRP ($P < 0.02$ for all constituents). We conclude that the downward trends in loads at TH-1 are not an artifact of the re-diversion of Rosewood Creek.

Visually, the TP trends for BC-1 and IN-1 look compelling but they don't pass at $p \leq 0.0025$. A few stations have a concave upward pattern including UT-1 and GC-1, which seem to no longer be declining. TH-1 has the lowest p-value but the first and last 5 years don't fit the trend. A majority of stations have a concave upwards pattern for TP, declining before the year 2000 and flattening or increasing in recent years. This pattern is also evident in a plot of the pooled residuals (Figure 11.1-6).

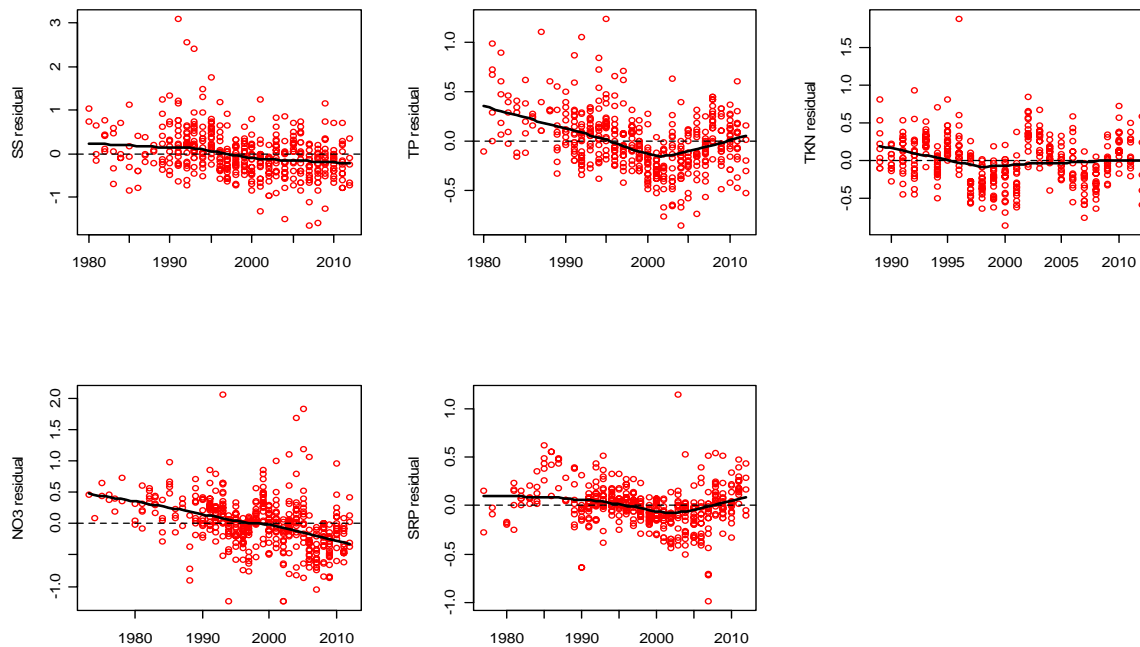


Figure 11.1-6. Trends in SS, TP, TKN, NO₃, and SRP after accounting for inter-annual variation in total and maximum daily runoff. Residuals are pooled from all gaging stations shown in Figures 10-1 to 10-5.

There are no compelling trends in TKN. The only significant trend is for the short 12-year record at ED-3.

Most stations have a decreasing pattern of NO₃-N loads, but only 7 of the trends are statistically significant at $p \leq 0.0025$. The trend for the pooled residuals (Figure 11.1-6) is linear, highly significant ($p < 2e-16$), and represents an average decrease of 2% per year since the 1970s or a total reduction of about 57%. However, small and large watersheds are equally weighted in this calculation.

While SRP had significant trends at 3 locations, one was upwards, and none are very steep. The overall pattern however starting in 1985 is similar to that of TP, with declining loads reversing around 2003.

The occurrence of so many downward trends in loads, especially for NO₃-N, is striking. We hypothesize that the trends are caused by long-term recovery from logging and overgrazing in the 19th century and first half of the 20th century. Essentially, the forests are accumulating biomass, and becoming more effective in retaining nitrogen, phosphorus and sediment. In the case of Blackwood Canyon, recovery may involve a shift from nitrogen-fixing alder toward conifers, which produce a litter and humus layer with high carbon-nitrogen ratio (Coats et al.,



1976). The long-term trend toward warmer temperatures could accelerate plant growth and contribute to closing of nutrient cycles and reductions in sediment production.

12 Statistical power analysis

Error in the estimate of a load is a type of measurement error, and it adds error to the regression model that is used in trend detection. Appendix A-6 shows specifically how this error propagates. Because measurement error inflates the regression error it erodes the statistical power to detect trends, and it will take longer to detect a trend than it would with perfect measurements. Interestingly, negative bias increases the regression variance while positive bias decreases it. This confuses interpretations, because methods like the simple rating curve often have positive bias, which makes them look better than methods with zero bias in a statistical power analysis.

12.1 Power analysis methodology

To estimate the power of the Mann-Kendall test, for sample sizes of 10 to 80 years, we randomly resampled the residuals that were tested in the adjusted Mann-Kendall tests for trend. All stations are pooled in these models. The reason for using a resampling procedure rather than generating normally distributed errors is that the residuals from the models, except those for TKN, were somewhat long in the tails (Figure 12.1-1). We also generated normally distributed measurement errors based on specified values of relative error (0.1, 0.3, or 0.5) and bias (-0.2 to +0.2). Our first analysis indicated that bias of less than 10% had very little influence on statistical power (Appendix A-6.2). Subsequently only bias factors of -0.2, 0.0, and +0.2 were used. Before adding the specified measurement error, the model residuals were shrunk by a multiplicative factor (<1) designed to approximately remove the original measurement error from the residual variance (Appendix A-6.3). Finally, a trend of a specified magnitude was added (1, 3, or 5% per year), and the Mann-Kendall test was applied to determine whether the added trend was detectable at alpha levels of 0.0025, 0.0050, and 0.05. The first two significance levels correspond to the Bonferroni rule for testing groups of 20 and 10 stations, respectively. The statistical power is estimated as the proportion of significant tests in 5000 resamplings.

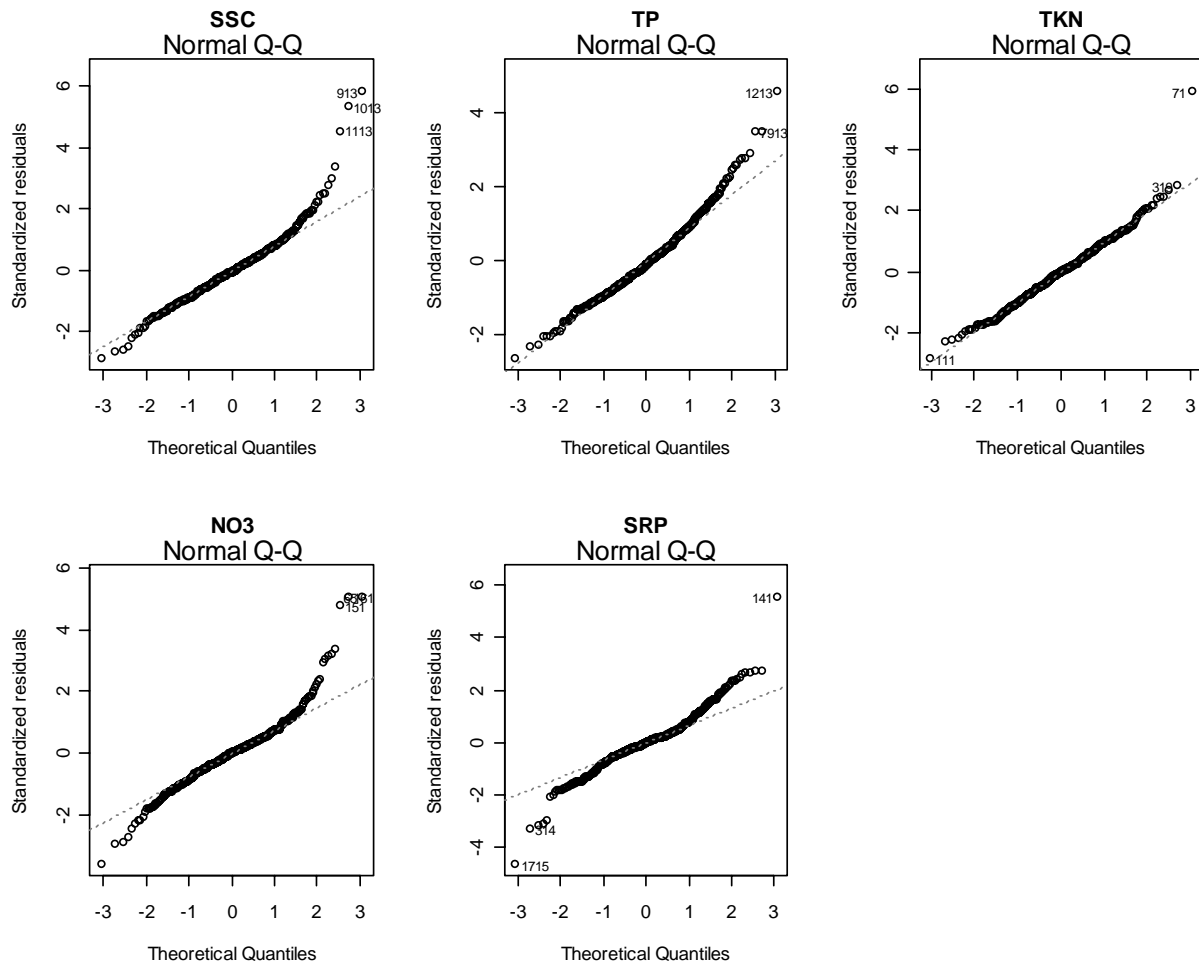


Figure 12.1-1. Quantile-quantile plots of the residuals for models used in the trend tests (Table 10-1). A linear pattern suggests a normal distribution.

12.2 Power analysis results

Figure 12.2-1 shows the power analysis for TP at the 0.005 significance level. The CV (coefficient of variation) is the measurement error as a proportion of the load. In the central frame of the figure it can be seen that to detect a trend of 3% per year with measurement errors averaging 50%, a sample size of 50 years would be needed to attain the same statistical power (close to 1) as 40 years with measurement errors of 30%, or 30 years with measurement errors of 10%. For a stronger trend (left column), statistical power is very good for sample sizes of 40 years or more, regardless of bias or measurement error. However to detect a 5% per year trend within 20 years with 80% probability requires that measurement error be limited to 10% (regardless of bias). It is virtually impossible to detect a 5% trend in 10 years, regardless of



precision and bias. To detect a more subtle trend (right column) with 80% probability or better, would require at least 50 years of measurements with 10% error. Power analysis results for the other constituents and other significance levels can be found in Appendix A-6.

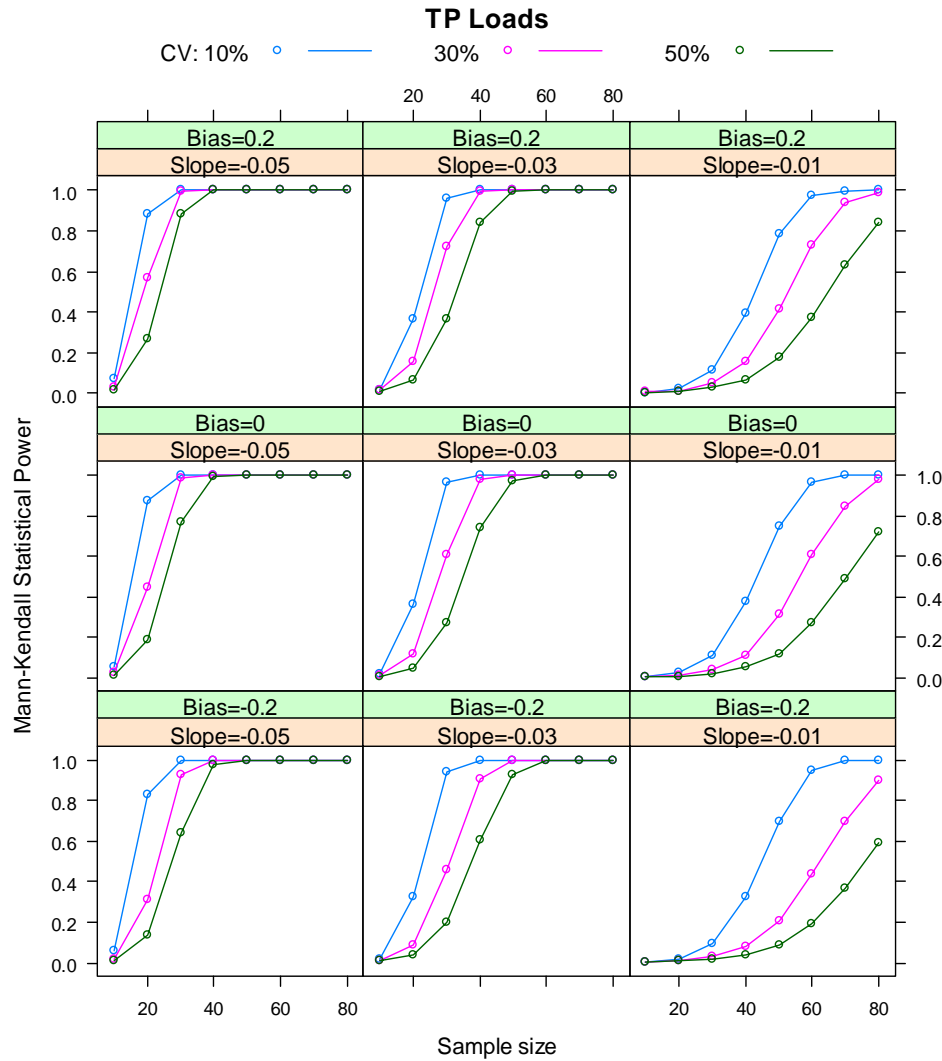


Figure 12.2-1. Power analysis for TP loads, contrasting 3 levels of relative measurement error (CV), for 3 bias levels and slopes, at 0.005 significance level.



13 Reducing Bias Through Improved Sampling

13.1 Continuous Turbidity Monitoring

In recent years, continuous turbidity monitoring has seen increasing use in the Tahoe basin for estimating sediment and total phosphorus concentrations (see Sec. 4.2). Its application in the LTIMP presents an opportunity to improve the accuracy of total load estimates and to reduce project costs. Most commercially-available probes come with the built-in capacity to measure other parameters, including temperature, pH and conductivity. The USGS has recently been investigating the possibility of retrofitting some existing gaging stations for turbidometry, and has developed cost estimates. The usefulness of continuous turbidity monitoring depends on the relationships between turbidity and the response variable (TP, SSC or FS). Figure 13.1-1 (from Figure B1, Susfalk et al., 2007) shows a set of graphs of SSC (mg/l) vs. turbidity (NTUs) for a station on Rosewood Creek at State Route 28, for five water years. The upper and lower 95 percent confidence limits on a new prediction are shown in red and blue. Regression equations Note that the data are untransformed. We found some improvement of fit by taking the square root of both variables.

Figure 13.1-2, from Stubblefield et al. (2007), shows the relationships between TP and turbidity for three years of pooled data from Ward Creek, and one year of data from Blackwood Creek. By including hydrologic variables in the regression, the precision of the estimates TP concentration can be improved.

An ancillary benefit of continuous turbidity monitoring is the ability to reliably estimate concentration with high temporal resolution and to allocate loads to specific hydrograph events. Because more load estimates are extracted from the same monitoring period, event-based statistical analyses can be much more powerful than those based on annual data. Trends and other relationships can be detectable within a few years rather than decades (e.g. Lewis et al., 2001). Applications of high resolution concentration data for understanding hydrological and ecological processes are virtually unlimited.

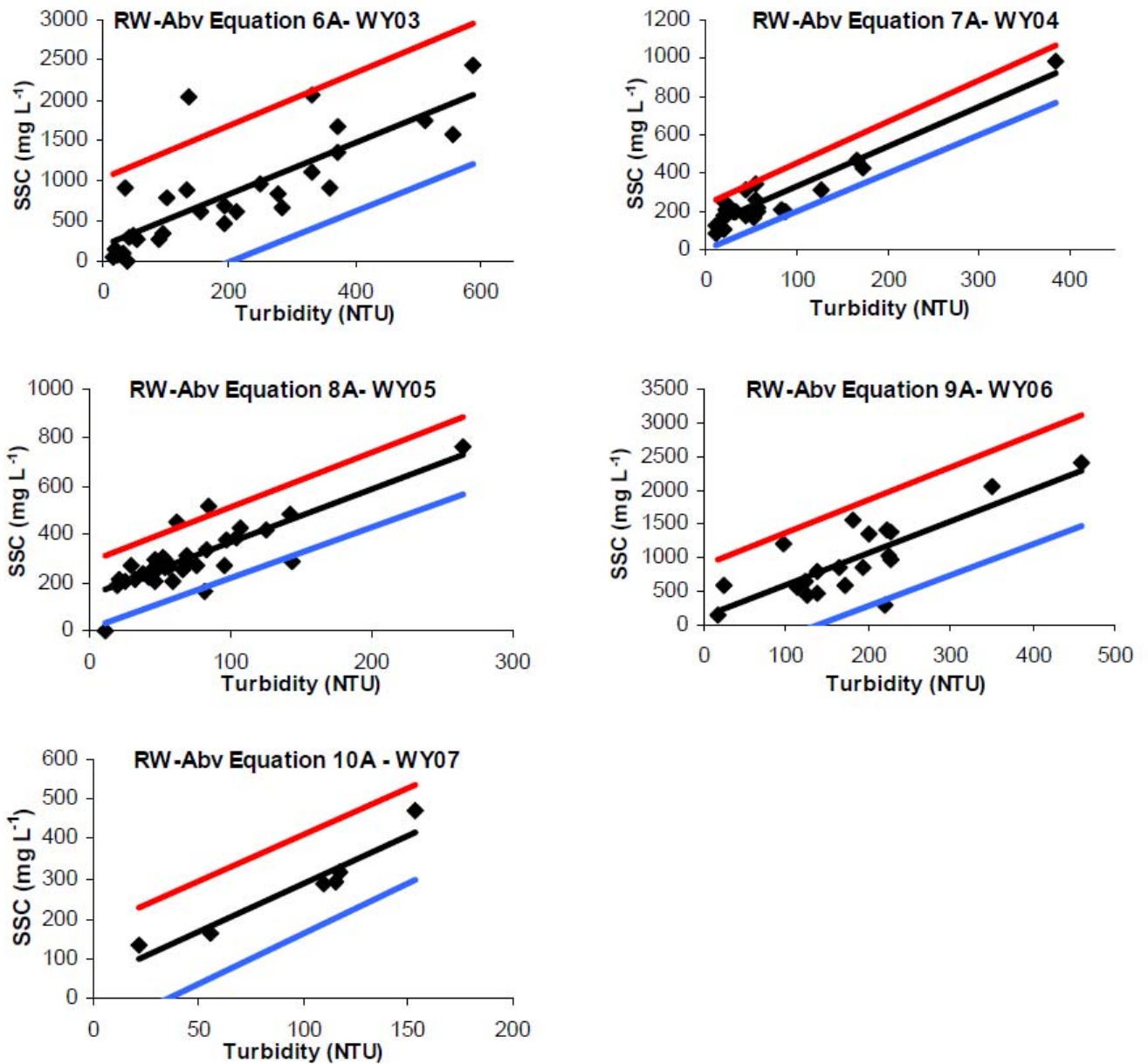


Figure 13.1-1 SSC (mg/l) vs. turbidity (NTUs) for Rosewood Creek at State Route 28, for five water years. Note that each water year's data are plotted at a different scale. From Susfalk et al., 2007

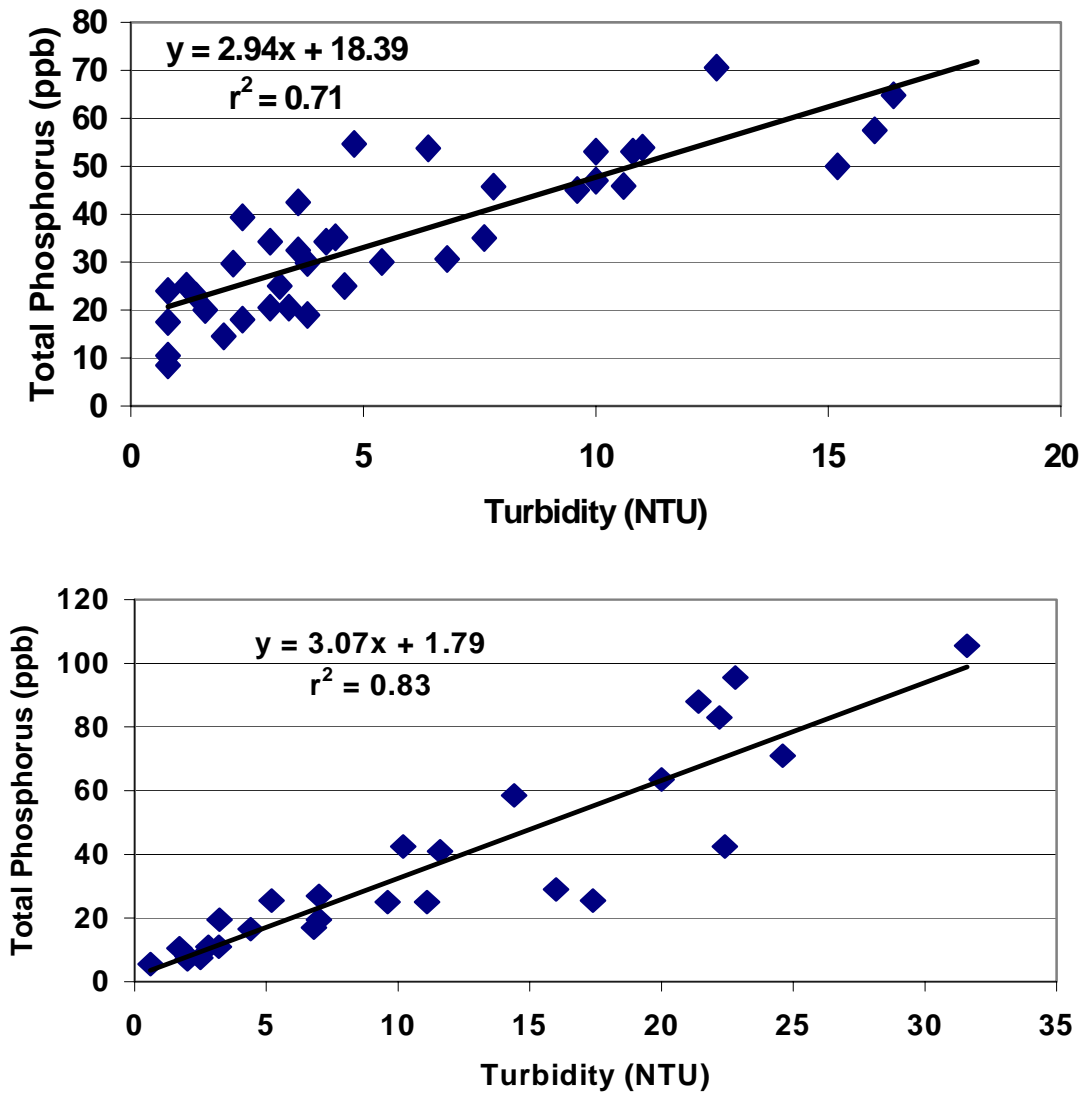


Figure 13.1-2. TP concentration vs. Turbidity during snowmelt , for Ward Creek (pooled data, 1999, 2000 and 2001), and Blackwood Creek, 2001. From Stubblefield et al., 2007

13.2 Pumping Samplers vs. Grab Sampling

Turbidity probes offer a method for addressing the problem of time-of-sampling bias for the constituents related to turbidity (SSC, FS and TP), but they offer no help for constituents for which loads will be estimated by the Period Weighted Sample method (NO₃-N, SRP and TKN). For these, there is no way around nighttime sampling. SRP is perhaps less of a problem, since its concentration is relatively independent of discharge. NO₃-N concentration varies significantly



during snowmelt over a 24-hour period. Nighttime samples can be collected by grab sampling, or by pumping samplers. The EWI method is important for particulate constituents (especially SSC), but for the dissolved constituents, it seems likely that the streams are well-mixed, and grab samples taken from the bank will be fairly representative of the flow passing the sampling point. TKN includes both dissolved and particulate nitrogen, but organic particles containing nitrogen are likely to be mostly small, buoyant and evenly distributed in a cross-section.

Pumping samplers are now in widespread use in the Basin for sampling urban runoff. During snowmelt or rainfall runoff (when the time-of-sampling bias is greatest) freezing is unlikely to be a problem. Freezing at night might be reduced by insulating the intake tubes. The machines can be programmed to sample at pre-determined times, or to collect more samples at higher flow, with a random element in the time of sampling. Samples are often composited to reduce the analysis burden, with an aliquot drawn from each sample proportional to the discharge at the time of sampling.

Regardless of the mechanics of collecting samples, it is important that a sampling scheme be devised that will minimize the time-of-sampling bias. Stratified random sampling, with strata based on discharge, is the most theoretically-defensible, but unless pumping samplers are used, this approach would require visiting stations at odd and irregular hours. An alternative approach would be to sample at fixed intervals (e.g. every six hours) during a sampling day, with samples composited for analysis. This approach would only be possible with pumping samplers.

14 Sample Size, Accuracy and Confidence Limits

In the simulations we tracked the 50th, 80th, 90th, and 95th percentiles of the absolute value of error. These percentiles represent empirical confidence levels for the error. From this information we plotted percent errors for each percentile (confidence level) as a function of sample size for each sampled population (e.g. Figure 14-1). Curves were averaged across populations (Figure 14-1) and interpolated to find the sample sizes necessary (on average) to produce an estimate of specified precision (10, 20, 30, and 50%) at confidence levels of 80, 90 and 95%. Curves for all constituents are provided in Appendix A-2.3. Sample numbers shown as 8 or 100 represent extrapolations at the low and high ends, and should be read as “<8” or “>100”.

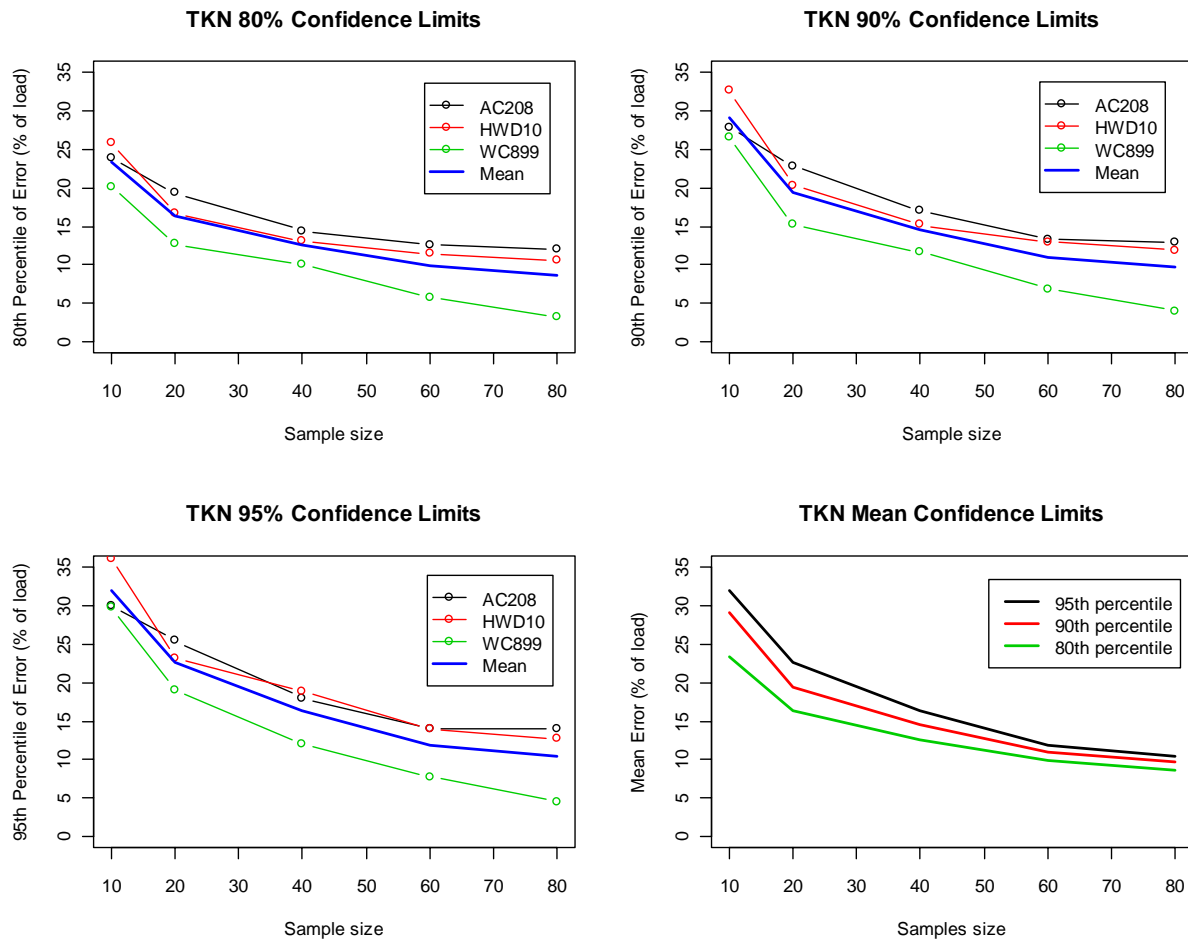


Figure 14-1. Confidence limits on errors for TKN.

14.1 Achieving specified levels of precision in total load

Using the developed relationships between error and sample size for each constituent, we created a spreadsheet showing alternative levels of precision for each constituent as a function of sample size (Table 14-1). The sample numbers refer to the required number of samples per year at a given station. For example, with 25 samples per year, one can be 90 percent sure that the true annual load of total phosphorus is within +/- 20 percent of the value estimated using the best model selected by the GRMSE criterion. For the same level of confidence and percent error for SSC, 67 samples per year would be required. Note that relationship between confidence level and sample number is highly non-linear. To achieve the 90/10 level for TP and SSC would require over 100 samples per year.



Table 14-1. Number of samples required to achieve a given level of precision at a given level of confidence in estimates of total annual load.

Confidence Level, Pct		80				90				95			
Error band (+/-), as Pct Est. Load		50	30	20	10	50	30	20	10	50	30	20	10
Constituent	Estimation Method	Required Number of Samples per year, without turbidity											
SSC	Best model by GRMSE	8	15	36	100	8	27	67	100	13	36	87	100
Fine Sed by mass	Best model by GRMSE	8	15	36	100	8	25	69	100	13	33	83	100
Fine Sed by count	log(FSP) ~ log(q)	8	11	17	60	8	15	26	85	9	19	34	86
Nitrate+nitrite-N	Period-weighted	8	8	14	33	8	11	19	43	8	16	29	51
Ammonium-N	Period-weighted	NA	NA	NA	NA	NA	NA	NA	NA	NA	NA	NA	NA
TKN	Period-weighted	8	8	15	60	8	9	19	75	8	12	28	85
SRP	Period-weighted	8	8	8	31	8	8	17	43	8	15	21	53
Total P	Best model by GRMSE	8	8	16	100	8	10	25	100	8	13	34	100
		Required Number of Samples per year with turbidity											
SS with turbidity	sqrt(SSC) ~ sqrt(turb)	8	8	13	49	8	8	20	70	8	14	27	96
FS by mass with turb	sqrt(FS) ~ sqrt(turb)	8	8	8	31	8	8	12	47	8	8	16	65
TP with turbidity	Best model by AIC	8	8	9	89	8	8	17	100	8	11	24	100
Lab NTU	Nephelometer	8	8	13	89	8	8	20	100	8	14	27	100
Max no. PWS		8	8	15	60	8	11	19	75	8	16	29	85
Max. Turb-related		8	8	13	89	8	8	20	100	8	14	27	100
Total sample no. w/turb.		8	8	15	89	8	11	20	100	8	16	29	100

Table 14-1 also shows the comparison of required sample numbers for an improved LTIMP (with new load calculation models) with a turbidity-based program, with loads of the particulate constituents calculated by regression with continuous turbidity. For SSC at the 90/20 level, the required sample size drops from 67 to 20.

We obtained estimates of project costs from TERC and USGS for station operation and maintenance and sample collection and analysis. Agency (USGS) overhead costs are included. For the chemical constituents, we multiplied the cost per sample by the maximum number of required samples for the most-variable constituent, assuming that all chemistry samples sent to the lab will be analyzed for all constituents. Aggregating the costs separately for the programs with and without continuous turbidity indicates that a turbidity-based program would be somewhat more expensive than the current program (with improved load calculation), except at the 90/20 level, where it would save over \$10,000 per station-year. The spreadsheets with formulas are available on disk.



14.2 Detecting differences of a specified magnitude

We can use our confidence limits to determine sample sizes required to detect a specified relative difference in annual load above and below a project area. Given confidence intervals for two statistics (in our case, loads) Zou and Donner (2008) present a simple method for computing a confidence interval for their difference.

$$L = \hat{\theta}_1 - \hat{\theta}_2 - \sqrt{(\hat{\theta}_1 - l_1)^2 + (u_2 - \hat{\theta}_2)^2}$$

$$U = \hat{\theta}_1 - \hat{\theta}_2 + \sqrt{(u_1 - \hat{\theta}_1)^2 + (\hat{\theta}_2 - l_2)^2}$$

where $\hat{\theta}_1$ and $\hat{\theta}_2$ are the two estimated loads, (l_1, u_1) and (l_2, u_2) are their confidence intervals and (L, U) is the confidence interval for their difference (at the same confidence level as the original intervals). If the original confidence intervals are symmetric, then the confidence interval for the difference will be symmetric around the difference in estimated loads. Thus a reasonable test of the hypothesis of no difference can be specified by the inclusion or exclusion of zero in the confidence interval for the difference.

Let's assume that the TP loading below a project is 130% of the upstream load. With sample sizes of 40 at each station, 95% mean confidence limits are +/-18.1% of the respective loads (see Appendix A-2.3.1, TP Mean Confidence Limits). Confidence intervals in percentage of the upstream load are thus (81.9, 118.1) for the upper location and (106.5, 153.5) for the lower location. Applying the formulas for L and U , the confidence interval for the difference is (0.4, 59.6), just small enough to exclude zero. Thus a sample size of 40 is required to detect the 30% difference in TP loading. Figure 14.2-1 shows the sample sizes required to detect a specified difference in loading at the 95% confidence level, for each of the major LTIMP nutrients, based on our simulations. With the benefit of continuous turbidity measurements, required sample sizes are reduced somewhat for TP and drastically for SSC (Figure 14.2-2). Reductions for fine sediment should be similar to those for total suspended sediment.

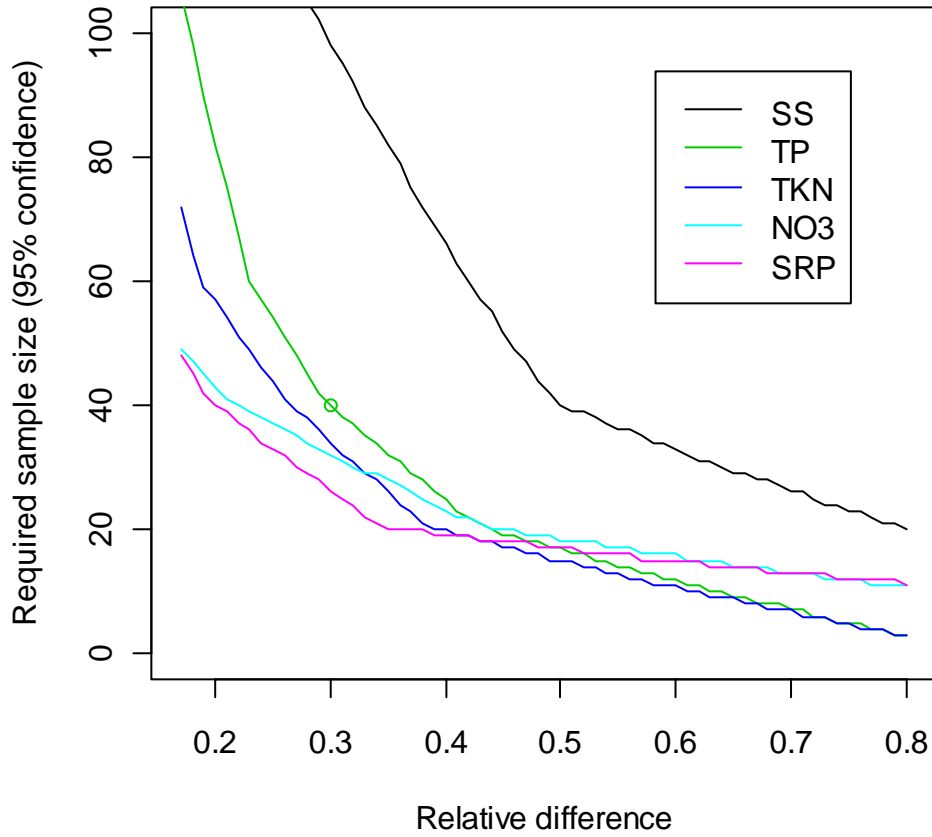


Figure 14.2-1. Sample sizes required to detect a specified difference in loading at the 95% confidence level, for each of the major LTIMP constituents.

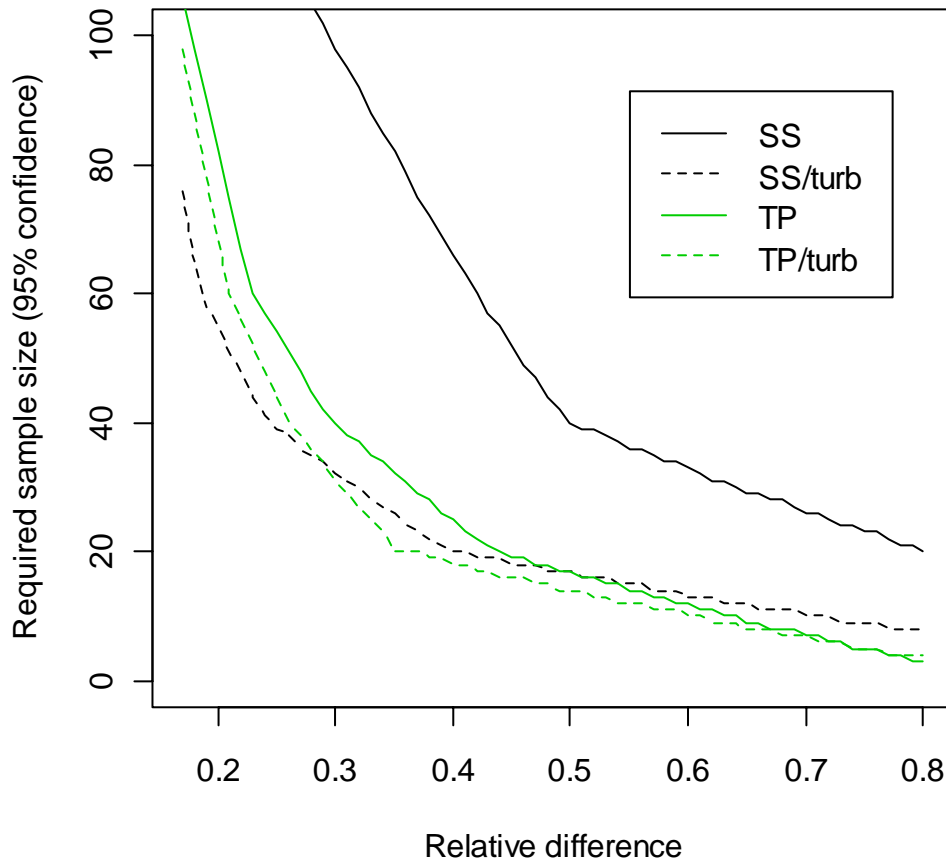


Figure 14.2-2. Sample sizes required to detect a specified difference in loading at the 95% confidence level, for SS and TP, with and without the benefit of continuous turbidity measurements.

15 Summary and Recommendations

In this study, we have developed and compared different methods of calculating total constituent loads, and expressed the results as the number of samples (per station-year) required to achieve a given level of confidence that the true load is within a given error band around the estimated load. Using the best methods (that is, the methods that maximize precision and minimize bias), we recalculated the total annual loads of NO₃-N, NH₄-N, TKN, SRP, TP and SSC for all of the LTIMP stations over the periods of record. We then related the annual loads to annual runoff and maximum daily peak discharge, and analyzed time trends in the residuals. The significant



downward trends indicate a long-term improvement in water quality, which we suggest may be due to long-term recovery of terrestrial ecosystems from 19th and 20th century disturbance.

Based on our results and our experience working with the LTIMP data, we recommend the following:

- Near-continuous measurement of turbidity and temperature with automated probes should become a central part of the realigned LTIMP. Good stream temperature data are important for the Lake Clarity Model, and will be of increasing interest as the climate warms. Turbidity, though by itself not a very important water quality parameter, could play an important role in regression-based estimates for each watershed of sediment and total phosphorus loads. Its use would address the problem of bias in load estimates of TP and SSC resulting from the lack of nighttime samples at some stations. Though at-a-station costs may be somewhat higher with the use of probes, at an intermediate confidence and error-band level (90 percent confidence that the true load lies within +/- 20 percent of its estimated value), total costs are actually reduced. Use of the probes should be phased in, with one or two gaging stations equipped in the first year, and more added in subsequent years. Turbidity should also be measured in the laboratory in splits of LTIMP samples collected for fine sediment.
- Fine sediment (FS) is now recognized as an important factor in lake clarity. It is used in the Lake Clarity Model and is incorporated in the TMDL targets for load reduction. Increased emphasis should be placed on its measurement as number of particles since the number, size and composition of particles directly affect clarity. Additional statistical research on fine sediment is needed in order to refine the error estimates for this constituent, and more work is needed to find the best methods for measuring FS at high concentrations in basin streams
- The load calculation models developed in this study present an opportunity for both improvements in accuracy of load estimates and major cost savings, especially for the dissolved constituents. These models, written in the programming language R, should be used to update the load estimates in future years for inclusion in the long-term data base of total loads. If station numbers need to be reduced for budget reasons, stations on the big contributing streams (Ward, Blackwood, Trout Creeks and the UTR) should have priority for continued discharge measurement and sampling.
- An intermediate confidence and error level—90 percent confidence that the true value lies within +/- 20% of the estimated value—is achievable for all constituents with 20 samples per year per station if continuous turbidity is measured. The number increases to 25 samples per year per station without turbidity, for the chemical constituents. Without good turbidity data, this level for SSC would require about 70 samples per year. This



intermediate level is perhaps the most realistic one for the program to adopt, since the marginal cost in sample size increases sharply above this level. Managers and planners, however, should be aware of the limitations of the adopted confidence and error level.

- The relationships between sample size, confidence and error should be used to plan monitoring of restoration and mitigation projects.
- Ammonium-N could be dropped from the list of constituents routinely measured, since about half the time its concentration is below the MDL. It is included in the measurement of TKN, but is needed to calculate TON from TKN. For special cases, such as Edgewood Creek, synoptic stream profiles of ammonium might help identify a point source. Records for all of the Edgewood Creek stations (including miscellaneous stations) suggest a point source for ammonium above ED-4, below S. Benjamin Dr.
- Dissolved phosphorus (DP) can be reliably predicted by linear regression with SRP, and could be dropped from the list of constituents measured.
- The realigning and improving of the LTIMP should be considered a work-in-progress. There is still room for improvement in the load calculation programs. For example, in cases where more than one sample per day was collected, the use of instantaneous discharge rather than subdivided MDQ in the PWS calculation would further improve the accuracy of the daily load estimate. With simultaneous measurement of fine sediment and turbidity, the RMSE, confidence limits and error bands on fine sediment loads could be estimated by resampling the continuous trace of estimated fine sediment concentration. The choice of the optimum load calculation model could then be revisited.
- The LTIMP needs a working director, with a strong background in hydrology, biogeochemistry and statistics along with experience in fund-raising. The director should be housed in one of the scientific research organizations active in the basin and have decision-making authority on operational matters. Overall policy direction would be the responsibility of the management agencies. With continued involvement of support staff from the scientific organizations, this could perhaps be a half-time job.
- Any changes to the LTIMP must maintain or improve the program's ability to respond quickly to emerging water quality issues and crises. The responses to the need for water quality monitoring after the Gondola and Angora fires were good examples of the flexibility and nimbleness the program needs to maintain. The program's contribution to addressing water quality problems could be improved, however, by periodic (at least annual) inspection of the concentration data as they become available. Unusual spikes in concentration (e.g. ammonium and nitrate in Edgewood Creek) could provide a basis for targeted synoptic sampling designed to identify problems for remediation or enforcement action.



16 References

- Allander, K. K., 2007. Update on the effect of a large uncontrolled wildfire on stream nutrient concentrations within an undisturbed watershed in the Lake Tahoe Basin. *J. Nev. Water Resour. Assoc. 2006 Lake Tahoe Special Edition*. 38 pp.
- Alley, W. M., 1988. Using exogenous variables in testing for monotonic trends in hydrologic time series. *Water Resources Research* **24**:1955-1961.
- Alvarez, N. L., A. Preissler, S. Hackley and P. Arneson, 2006. Lake Tahoe Interagency Monitoring Program--An Integral Part of Science in the Lake Tahoe Basin. *In: Science as a Tool in Tahoe Basin Management: Lake Tahoe Science Plan Workshop*. Incline, NV. Poster Abstracts, p. 53.
- Alvarez, N. L., A. Pressler, S. Hackley and P. Arneson, 2007. Lake Tahoe Interagency Monitoring Program--An integral part of science in the Lake Tahoe Basin. *Jour. Nev. Water Resour. Assoc 2006 Lake Tahoe Special Edition*. 36 pp.
- Anderson, C., 2005. Turbidity 6.7 Ver. 2.1. *In: U.S. Geological Survey Techniques of Water Resources Investigations Book 9*. Reston, VA, p. 55.
- Byron, E. R., and C. R. Goldman, 1989. Land use and water quality in tributary streams of Lake Tahoe, California-Nevada. *Jour. Environ. Qual.* **18**:84-88.
- Burnham, K. P. and D. R. Anderson, 2002. *Model Selection and Multimodel Inference: A Practical Information-theoretic Approach*. New York, USA, Springer-Verlag. 488 pp.
- Carlsson, P., E. Granell and A. Z. Segatto, 1999. Cycling of biologically available nitrogen in riverine humic substances between marine bacteria, a heterotrophic nanoflagellate and a photosynthetic dinoflagellate. *Aquat. Microb. Ecol.* **18**:23-36.
- Chang, C. C. Y., J. S. Kuwabara, and S. P. Pasilis, 1992. Phosphate and iron limitation of phytoplankton biomass in Lake Tahoe. *Can. Jour. Fish. and Aquatic Sci.* **49**:1206-1215.
- Cleveland, W. S. and S. J. Devlin, 1988. Locally-weighted regression: an approach to regression analysis by local fitting. *Journal of the American Statistical Association* **83**:596-610.
- Coats, R. N., R. L. Leonard and C. R. Goldman, 1976. Nitrogen uptake and release in a forested watershed, Lake Tahoe Basin, California. *Ecology* **57**:995-1004.
- Coats, R., 2010. Climate change in the Tahoe Basin: regional trends, impacts and drivers. *Climatic Change* **102**:435-466.



- Coats, R. N., J. Perez-Losada, G. Schladow, R. Richards, and C. R. Goldman, 2006. The Warming of Lake Tahoe. *Climatic Change* **76**:121-148.
- Coats, R. N., M. Costal-Cabral, J. Riverson, J. Reuter, G. B. Sahoo and B. Wolfe, 2013. Projected 21st trends in hydroclimatology of the Tahoe basin. *Climatic Change* **116**:51-69.
- Coats, R. N. and C. R. Goldman, 2001. Patterns of nitrogen transport in streams of the Lake Tahoe basin, California-Nevada. *Water Resour. Res.* **37**:405-415.
- Coats, R. N., F. Liu and C. R. Goldman, 2002. A Monte Carlo test of load calculation methods, Lake Tahoe Basin, California-Nevada. *Jour. Am. Water Resour. Assoc.* **38**:719-730.
- Coats, R. N., M. Larsen, A. H. J. Thomas, M. Luck and J. Reuter, 2008. Nutrient and sediment production, watershed characteristics, and land use in the Tahoe Basin, California-Nevada. *J. Am. Water Resour. Assoc.* **44**:754-770.
- Cohn, T. A., L. L. DeLong, E. J. Gilroy, R. M. Hirsch and D. K. Wells, 1989. Estimating constituent loads. *Water Resources Research* **25**:937-942.
- Cohn, T. A., 1995. Recent advances in statistical methods for the estimation of sediment and nutrient transport in rivers. *Rev. Geophys.* **33 Suppl.**
- Dann, M. S., J. A. Lynch, and E. S. Corbett, 1986. Comparison of methods for estimating sulfate export from a forested watershed. *J. Environ. Qual.* **15**:140-145.
- Das, T., E. P. Maurer, D. W. Pierce, M. D. Dettinger and D. R. Cayan, 2013. Increases in flood magnitudes in California under warming climates. *J. Hydrology* **501**:101-110.
- Dolan, D. M., A. K. Yui, and R. D. Geist., 1981. Evaluation of river load estimation methods of total phosphorus. *J. Great Lakes Res.* **7**:207-214.
- Eads, R. E. and J. Lewis, 2003. Turbidity Threshold Sampling in Watershed Research. *In: First Interagency Conference on Research in the Watersheds.*, K.G. Renard, S. A. McElroy, W.J. Gburek, H. E. Canfield and R. L. Scott (eds). USDA Agric. Res. Serv., pp. 567-571.
- Edwards, T.K., and G.D. Glysson, 1999. Field Methods for Measurement of Fluvial Sediment: U.S. Geological Survey Techniques of Water Resources Investigations, Book 3, chapter C2, 89 p.10. (available at <http://pubs.usgs.gov/twri/twri3-c2/>.)
- Ferguson, R. I., 1986. River loads underestimated by rating curves. *Water Resour. Res.* **22**:74-76.
- Ferguson, J.W. and R.G. Qualls, 2005. Biological available phosphorus loading to Lake Tahoe. Final report submitted to Lahontan Regional Water Quality Control Board, South Lake Tahoe, CA.



- Froelich, P. N., 1988. Kinetic control of dissolved phosphate in natural rivers and estuaries: A primer on the phosphate buffer mechanism. *Limnol. Oceanogr.* **33**:649-668.
- Galat, D. L., 1990. Estimating Fluvial Mass Transport to Lakes and Reservoirs: Avoiding Spurious Self-Correlations. *Lake and Reservoir Management* **6**:153-163.
- Gilroy, E. J., R. M. Hirsch and T. A. Cohn, 1990. Mean square error of regression-based constituent transport estimates. *Water Resources Research* **26**:2069-2077.
- Goldman, C. R., 1981. Lake Tahoe: Two decades of change in a nitrogen deficient oligotrophic lake. *Verh. Internat. Verein. Limnol.* **21**:45-70.
- Goldman, C. R., A. D. Jassby, and S. H. Hackley, 1993. Decadal, Interannual, and Seasonal Variability in Enrichment Bioassays at Lake Tahoe, California-Nevada, USA. *Canadian Journal of Fisheries and Aquatic Sciences* **50**:1489-1495.
- Goldman, C. R. and R. Armstrong, 1969. Primary Productivity Studies in Lake Tahoe, California. *Verh Internat Verein Limnol* **17**:49-71.
- Grismer, M. E., 2013. Stream sediment and nutrient loads in the Tahoe Basin—estimated vs monitored loads for TMDL “crediting”. *Environ Monit Assess* **185**:7883–7894.
- Hackley, S., B. Allen, D. Hunter and J. Reuter, 2013. Lake Tahoe Water Quality Investigations. Univ. Calif. Tahoe Environ. Res. Cent, Davis, CA, 107 pp.
- Harrell, F. E. et al. 2010. HMISC: Harrell miscellaneous, R package version 3.8-3.
- Hatch, L. K., 1997. The generation, transport, and fate of phosphorus in the Lake Tahoe ecosystem. Ph.D. Thesis, Univ. of Calif., Davis, 212 pp.
- Hatch, L. K., J. Reuter and C. R. Goldman, 1999. Relative importance of stream-borne particulate and dissolved phosphorus fraction to Lake Tahoe phytoplankton. *Can. J. Fish. Aquat. Sci.* **56**:2331-2330.
- Helsel, D. R. and R. M. Hirsch, 2002. Statistical methods in water resources Techniques of Water Resources Investigations. U.S. Geological Survey, 522 pp.
- Heyvaert, A., D. M. Nover, T. G. Caldwell, W. B. Trowbridge, S. G. Schladow and J. E. Reuter, 2011. Assessment of Particle Size Analysis in the Lake Tahoe Basin. Desert Res. Instit. Reno, NV and Univ. of Calif. Davis.
- Hill, A. R., 1986. Stream nitrate loads in relation to variations in annual and seasonal runoff regimes. *Water Resour. Bull.* **22**:829-839.
- Jassby, A. D., J. E. Reuter, R. P. Axler, C. R. Goldman, and S. H. Hackley, 1994. Atmospheric deposition of nitrogen and phosphorus in the annual nutrient load of Lake Tahoe (California-Nevada). *Water Resour. Res.* **30**:2207-2216.



- Johnson, D. W., W. W. Miller, E. Carroll and W. R.F., 2007. The Gondola fire: Effects on Nutrient Loss, Soil Fertility and Leaching. *Jour. Nev. Water Resour. Assoc. Lake Tahoe Special Edition 2006*. 38 pp.
- Kamphake, L. J., S. A. Hannah and J. M. Cohen, 1967. Automated analysis for nitrate by hydrazine reduction. *Water Research* **1**:205-219.
- Kempers, A. J., and G. Van Der Velde, 1992. Determination of nitrate in eutrophic coastal seawater by reduction to nitrite with hydrazine. *Jour. Environ. Anal. Chem.* **47**:1-6.
- Kempers, A. J., and A. G. Luft, 1988. Re-examination of the Determination of Environmental Nitrate as Nitrite by Reduction with Hydrazine. *Analyst* **113**:3-6.
- LRWQCB. 1995. Water Quality Standards and Control Measures for the Tahoe Basin. *In: Water Quality Control Plan for the Lahontan Region*. Lahontan Regional Water Quality Control Board State of California, South Lake Tahoe, CA.
- Lahontan and NDEP, 2010. Final Lake Tahoe Total Maximum Daily Load Report. Lahontan Regional Water Quality Control Board, and Nevada Division of Environmental Protection, South Lake Tahoe CA and Carson City NV, p. 340.
- Leonard, R. L., L. A. Kaplan, J. F. Elder, R. N. Coats and C. R. Goldman, 1979. Nutrient Transport in Surface Runoff from a Subalpine Watershed, Lake Tahoe Basin, California. *Ecological Monographs* **49**:281-310.
- Lewis, J., 1996. Turbidity-controlled suspended sediment sampling for runoff-event load estimation. *Water Resour. Res.* **32**:2299-2310.
- Lewis, J. and R. Eads, 2009. Implementation Guide for Turbidity Threshold Sampling: Principles, Procedures, and Analysis. *In: Gen. Tech. Rep. PSW-GTR-212* USDA For. Serv. Pacific SW Res. Sta., 87 pp.
- Likens, G. E., F. E. Bormann, R. S. Pierce, J. S. Eaton, and N. M. Johnson, 1977. *Biogeochemistry of a Forested Ecosystem*. New York, Springer-Verlag.
- Liston, A., V. Edirveerasingam, B. Allen, S. Hackley, J. Reuter and S. G. Schladow, 2013. *Laboratory Procedure, Field Protocol and Quality Assurance Manual*. Davis, CA, Tahoe Environmental Research Center, University of California, Davis.
- Lumley, T. and A. Miller, 2009. Leaps: regression subset selection, R package version 2.9.
- Miller, R. J., 1981, *Simultaneous Statistical Inference*. New York, Springer Verlag. 299 pp.
- NDEP, 2013. Nevada 2008-10 Water Quality Integrated Report with EPA Overlisting. Nevada Division of Environmental Protection, Carson City, NV.



- Nover, D. M., 2012. Fine particles in watersheds: measurement , watershed sources and technologies for removal. *PH.D Thesis in Civil & Environ. Eng.* University of California at Davis, 98 pp..
- Pellerin, B. A., B. A. Bergamaschi, B. D. Downing, J. F. Saraceno, J. D. Garrett and L. D. Olsen, 2013. Optical Techniques for the Determination of Nitrate in Environmental Waters: Guidelines for Instrument Selection, Operation, Deployment, Maintenance, Quality Assurance, and Data Reporting. *In: Techniques and Methods 1-D5*. U.S. Geol. Surv., Reston, VA, p. 37.
- Pellerin, B. A., J. F. Saraceno, J. B. Shanley, S. S.D., G. R. Aiken, W. M. Wolleim and B. A. Bergamaschi, 2012. Taking the pulse of snowmelt: in site sensors reveal seasonal, event and diurnal patterns of nitrate and dissolved organic matter variability in an upland forest stream. *Biogeochemistry* **108**:183-198.
- Preston, S. D., V. J. Bierman, Jr., and S. E. Silliman, 1989. An evaluation of methods for estimation of tributary mass loads. *Water Resour. Res.* **25**:1379-1389.
- R Development Core Team, 2010. R: A Language and Environment for Statistical Computing. R Foundation for Statistical Computing, Vienna, Austria.
- Rabidoux, A. A., 2005. Spatial and temporal distribution of fine particles and elemental concentrations in suspended sediments in Lake Tahoe streams, California-Nevada, University of California, Davis. M.S. Thesis, *Civil Engineering*. Univ. Calif. Davis, 154 pp.
- Reuter, J. E., A. Heyvaert, O. A., A. Parra and R. Susfalk, 2012. Water quality conditions following the 2007 Angora wildfire in the Lake Tahoe basin. Univ. of Calif. Davis and Desert Research Instit., Davis, CA, 75 pp.
- Richards, R. P., and J. Holloway, 1987. Monte Carlo studies of sampling strategies for estimating tributary loads. *Water Resour. Res.* **23**:1939-1948.
- Riverson, J., R. Coats, M. Costal-Cabral, M. D. Dettinger, J. Reuter, G. B. Sahoo and S. G. Schladow, 2013. Modeling the transport of nutrients and sediment loads into Lake Tahoe under projected climatic changes. *Climatic Change* **116**:35-50.
- Robertson, D. M. and E. D. Roerish, 1999. Influence of various water quality sampling strategies on load estimates for small streams. *Water Resour. Res.* **35**:3747-3759.
- Rowe, T. G., D. K. Saleh, S. A. Watkins and C. R. Kratzer, 2002. Streamflow and Water-Quality Data for Selected Watersheds in the Lake Tahoe Basin, California and Nevada, Through September 1998. *In: Water-Resources Investigations Rep.*, U.S. Geol. Surv. Report 02-4030, Carson City, NV, 118 pp.



- Sahoo, G. B., D. M. Nover, J. E. Reuter, A. Heyvaert, J. Riverson and S. G. Schladow, 2013. Nutrient and particle load estimates to Lake Tahoe (CA-NV, USA) for Total Maximum Daily Load establishment. *Science of the Total Environment* **444**:579-590.
- Sahoo, G. B., S. G. Schladow, J. Reuter, R. Coats, M. D. Dettinger, J. Riverson, B. Wolfe and M. Costal-Cabral, 2013. The response of Lake Tahoe to climate change. *Climatic Change* **116**:71-95.
- Sauer, V. B. and D. P. Turnipseed, 2010. Stage Measurement at Gaging Stations. *In: U.S. Geological Survey Techniques and Methods book 3, chap. A7.* p. 45.
- Seitzinger, S. P., R. W. Sanders and R. Styles, 2002. Bioavailability of DON from natural and anthropogenic sources to estuarine phytoplankton. *Limnol. Oceanogr.* **47**:353-366.
- Simon, A., 2006. Estimates of Fine-Sediment Loadings to Lake Tahoe from Channel and Watershed Sources. USDA-Agric. Res. Serv., National Sedimentation Laboratory, Oxford MS.
- Simon, A., E. Langendoen, R. Bingner, R. Wells, A. Heins, N. Jokay and I. Jaramillo, 2003. Draft Final Lake Tahoe Basin Framework Implementation Study: Sediment Loadings and Channel Erosion. USDA Agric. Res. Serv. National Sedimentation Laboratory, Oxford MS.
- Spector, P., J. Friedman, R. Tibshirani and T. Lumley, 2010. acepack: ace() and avas() for selecting regression transformations, R package version 1.3-3.0.
- Stubblefield, A. P., 2002. Spatial and Temporal Dynamics of Watershed Sediment Delivery, Lake Tahoe, California. Ph.D. Thesis. University of California Davis, Davis, CA, p. 199.
- Stubblefield, A. P., J. E. Reuter, R. A. Dahlgren and C. R. Goldman, 2007. Use of turbidometry to characterize suspended sediment and phosphorus fluxes in the Lake Tahoe basin, California, USA. *Hydrological Processes* **21**:281-291.
- Susfalk, R., B. Fitzgerald, S. Brown and D. Fellers, 2010. Rosewood Creek Monitoring Compendium 2002-2010. Desert Research Institute and Nevada Tahoe Conservation District, Reno, NV, 141 pp.
- Swift, T., J. Perez-Losada, S. G. Schladow, J. Reuter, A. Jassby, and C. R. Goldman, 2006. Water Clarity modeling in Lake Tahoe: Linking suspended sediment matter characteristics to Secchi depth. *Aquat. Sci.* **68**:1-15.
- Thomas, R. B., 1985. Estimating Total Suspended Sediment Yield with Probability Sampling. *Water Resources Research* **21**:1893-1905.
- Thomas, R. B. and J. Lewis, 1995. An evaluation of flow-stratified sampling for estimating suspended sediment loads. *Jour. Hydrology* **170**:27-45.



Turnipseed, D. P. and V. B. Sauer, 2010. Discharge Measurements at Gaging Stations. *In: U.S. Geological Survey Techniques and Methods book 3, chap. A8*. Reston, VA, p. 87.

Wittmann, M. E., C. Ngai and S. Chandra, 2013. Our New Biological Future? The Influence of Climate Change on the Vulnerability of Lakes to Invasion by Non-Native Species. *In: Climatic Change and Global Warming on Inland Waters*, C. R. Goldman, M. Kumagai and R. D. Robarts (eds.) Wiley -Blackwell, West Sussex, UK, pp. 271-294.

Zou, G. Y. and A. Donner, 2008. Construction of confidence limits about effect measures: A general approach. *Statistics in Medicine* 27:1693-1702.

17 Personal Communications

Alan Heyvaert, Desert Res. Instit., Reno NV 4/15/13 and 8/28/13

Gary Conley, 2nd Nature LLC, Santa Cruz, CA 4/10/13

Mark Grismer, Univ. Calif. Davis, CA 4/24/13

Daniel Nover, USEPA, 7/11/13

Andy Stubblefield, Humboldt State Univ., Arcata CA 4/25/13

Rick Susfalk, Desert Res. Instit., Reno NV 6/12/13